2015

Investigations into Ecogeomorphodynamics of Coastal Embryo Dunes at Padre Island National Seashore, Texas

Katherine Anne Renken
Louisiana State University and Agricultural and Mechanical College

INVESTIGATIONS INTO ECOGEOMORPHODYNAMICS OF COASTAL EMBRYO DUNES AT PADRE ISLAND NATIONAL SEASHORE, TEXAS

A Dissertation

Submitted to the Graduate Faculty of the
Louisiana State University and
Agricultural Mechanical College
in partial fulfillment of the
requirements for the degree of
Doctor of Philosophy

in

The Department of Geography and Anthropology

by
Katherine Anne Renken
B.S., University of North Carolina at Chapel Hill, 2006
M.A., East Carolina University, 2008
August 2015

Acknowledgments

First and foremost, I would like to express gratitude to my advisor, Dr. Steven Namikas. This endeavor would never have been possible without your willingness to provide me with guidance and insight. I am also thankful to Dr. Robert Rohli and Dr. Lei Wang for serving on my committee, and Dr. Julie Anderson Lively, for serving as my Dean's Representative.

I would also like to thank those people who worked with me along the way. Dr. Brandon Edwards, Dr. Phillip Schmutz, and Dr. Katherine Parys were mentors in many capacities, and for their support I am eternally grateful. Dennis Renken, Patrick Remson, and Clay S. Tucker provided much appreciated assistance during field work. Wade Stablein and the staff at Padre Island National Seashore also provided assistance and housing during field seasons. In addition, Dr. David Blouin and Roxie Chen provided valuable statistical advice. The staff in the Cartography section of the Louisiana Geological Survey looked after me for four of the seven years.

It takes a village. Many people have provided emotional support during the past seven years. My parents, above all else, are the two people who have shown the most love, guidance, and encouragement. They led by example and taught me to work hard, persevere against the odds, and never ever quit. My running family in Louisiana Ultra Runners, particularly Jerry, Rhea, and David, and in Forge Racing have given me an outlet for all the pent up energy from sitting and writing. There are many people I do not have time to thank here, but please know that I am very grateful for your support.

Finally, I would like to thank my partner, Patrick Remson. You have shown incredible patience and understanding throughout this journey. By making me keep things in perspective, you helped me realize this dream. Now, let's get to yours!

Table of Contents

Abstract

This dissertation is an investigation into the interplay between vegetation and aeolian processes in the coastal embryo dune environment at Padre Island National Seashore, Texas. Vegetation is a geomorphic agent, altering aeolian process dynamics. This research adopted a three-pronged approach to improving our understanding of ecogeomorphodynamics in the coastal environment.

The first study analyzed large-scale spatiotemporal trends in the vegetation community of the embryo dune environment in order to contextualize smaller scale aeolian processes. Results of this study demonstrated that there was a clear transition in community assemblage from the seaward edge of the embryo dune zone, where species functioned as pioneer builders promoting deposition, to foredune toe, where species stabilized and protected the substrate from erosion.

The second study documented morphology of different vegetation types (tall grass, short grass, and shrub) as well as their response to wind velocity. While tall grass occupied the greatest area, it also had the highest porosity. Short grasses occupied less space than the tall grasses, with roughly half the optical porosity. Shrubs occupied the lowest volume but were the densest roughness element with the highest optical porosity.

The final study documented spatial patterns of fluid flow and sediment erosion and deposition around vegetation of different morphology types (tall grass, short grass, and shrub). Tall grasses and shrubs were more effective at reducing velocity in their lee than short grasses, with tall grasses creating a larger deceleration zone than shrubs. However, the greatest deposition occurred around patches of short grass, which was the shortest morphology type.

Findings of this dissertation suggest that both optical porosity and element size influence patterns of aeolian flow and sediment deposition. There is a tradeoff between overall size of a

roughness element in the flow field and the porosity of that element. Objects with lower optical porosity but smaller size are less effective at trapping sediment than elements with greater size and higher optical porosity. Results indicate that large, continuous patches of short, dense vegetation are in fact more effective at trapping and retaining sediment than tall grasses which obtrude into the boundary layer and cause greater flow deceleration.

Chapter 1. Introduction

1.1 Project Context and Research Needs

Coastal dunes perform many vital functions. They represent a key reserve of sediment within the larger littoral system (Sherman and Bauer, 1993; Bauer and Sherman, 1999), and provide a first line of defense for coastal infrastructure against storm waves, storm surge, and shoreline retreat due to sea level rise and negative sediment budgets (Nordstrom and Psuty, 1980; Martínez et al., 2008; Nordstrom, 2008; Debaine and Robin, 2012). In addition to aesthetically pleasing, representing a key component of the allure and attraction of beaches, and contributing to the vast tourism industry associated with beaches (Nordstrom and Lotstein, 1989; Bauer and Sherman, 1999), coastal dunes function as a critical habitat for a large variety of organisms, including a number of threatened or endangered species (e.g., *Forelius pruinosus* and *Dorymyrmex flavus* (ants), *Ocypode quadrata* (ghost crabs), *Charadrius melodus* (piping plover), *Pelecanus occidentalis* (brown pelican), etc.) (Bauer and Sherman, 1999; Martínez et al., 2008; Maun, 2009). Despite the significance and importance of coastal dunes, our ability to model their development and dynamics remains far too crude to effectively contribute to the successful management of this highly dynamic environment. Given a general model of the basic physical dynamics involved in the interaction between vegetation and aeolian processes, local managers could apply site-specific characteristics to improve the efficacy of dune restoration projects. This dissertation improves quantitative understanding of the physical process dynamics involved in the interactions between key vegetation species and wind flow and sediment transport in the embryonic dune zone.

This dissertation presents investigations into the dynamics between vegetation and aeolian process dynamics in the coastal embryo dune zone. The embryo dune zone is the zone of minor, hummocky dunes formed as a result of deposition around vegetation seaward of the foredune ridge.

Vegetation obstructs and alters fluid flow by increasing drag, resulting in increased turbulence and deposition in the area surrounding the vegetation and within vegetation (Buckley, 1987; Crawley and Nickling, 2003; Gillies et al., 2006; Gillies et al., 2007; Grant and Nickling, 1998; King et al., 2005; Lancaster and Baas, 1998; Leenders et al., 2011; Leenders et al., 2007; Lightbody and Nepf, 2006; Luhar et al., 2008; Musick et al., 1996; Nepf, 1999; Neumeier and Amos, 2006; Neumeier and Ciavola, 2004; Okin, 2008; Pasquill, 1950; Suter-Burri et al., 2013; Wolfe and Nickling, 1993; Wolfe and Nickling, 1996; Wyatt and Nickling, 1997; Zong and Nepf, 2010). It is possible to model the effect of roughness elements on the distribution of shear stress, which is the driving force of sediment transport, around roughness elements such as vegetation (Marshall, 1971; Raupach, 1992; Raupach et al., 1993; Schlichting, 1936). Many studies have evaluated the applicability of the Raupach et al. (1993) model where rigid roughness elements, either synthetic rods or shrub species, have been used to represent simplified vegetation elements (Brown et al., 2008; Gillies et al., 2000; Gillies et al., 2007; King et al., 2005; Musick et al., 1996; Sutton and McKenna-Neuman, 2008; Wolfe and Nickling, 1996; Wyatt and Nickling, 1997).

However, there are fundamental limitations in applying the Raupach et al. (1993) model to environments which have live, flexible, porous grasses. Primarily, the morphology of live vegetation is dynamic because blades, leaves, and stems bend and flex in response to increasing wind flow, which causes a change in drag coefficients of these roughness elements (Burri et al., 2011; Gillies et al., 2002; King et al., 2005; Okin, 2008; Walter et al., 2012a; Walter et al., 2012b; Webb et al., 2014). Additionally, the response of vegetation to increased wind flow differs by species because vegetation morphology depends on a variety of variables such as blade/leaf size, shape, and rigidity, as well as stem and blade density (Arens et al., 2001; de Langre, 2008; Moller, 2006; Neumeier, 2005; Nilsson et al., 1958; Pavlik, 1984; Steudle et al., 1977). Moreover, the

Raupach et al. (1993) model assumes that all roughness elements have the same geometry. Yet coastal embryo and foredune systems contain a wide variety of vegetation species with different morphologies that range from tall grasses to short grasses to shrubs and vines.

Due to the inherent complexity of the interaction between vegetation and aeolian processes in the natural dune environment, deterministic modeling of the initiation and development of coastal dunes is still not possible because of the lack of detailed, quantitative understanding of how coastal dune vegetation alters and modifies the aeolian sediment transport system in real embryo dune environments. In order to develop theory describing the interactions between plants and wind flow it is necessary to characterize the response of plant morphology to fluctuations in fluid flow as well as the response of the wind field and resulting sediment transport to the presence of plants with varying morphologies.

1.2 Research Objectives

The overall goal of this dissertation is to enhance understanding of how vegetation influences fluid flow and sediment deposition and erosion in coastal embryo dune environments. The specific objectives pursued in order to achieve this goal were to:

1. document and quantify spatiotemporal variation in vegetation community composition in the embryo dune zone at Padre Island National Seashore, including ecological characteristics such as species abundance and diversity;
2. identify the effect of wind velocity on the shape of three common morphology types of native dune species (tall grass, short grass, and shrub), in terms of fluid-dynamically meaningful morphological parameters, including plant area, pore area, and optical porosity;

3. document and analyze differences in spatial patterns of fluid flow across a range of wind velocities around common, native vegetation species that exhibit very different morphologies; and
4. document and analyze patterns of erosion and deposition of sediment around species with different morphologies.

The first objective of this investigation was necessary in order to contextualize further research into process dynamics of different vegetation morphology types. The second, third, and fourth objectives were undertaken in order to build a framework for development of a shear stress partitioning model which incorporates the inherent variability in roughness element morphology that vegetation in coastal dunes presents. A model that accounts for the dynamic morphology of live vegetation as well as morphology-dependent flow dynamics would substantially improve our ability to model the fluid dynamics associated with the presence of these types of vegetation and enhance our ability to model changes in morphology and dune growth resulting from the presence of vegetation.

1.3 Chapter Synopses

Chapters 2-4 focus on field experiments which address these research needs and objectives in the following ways. Chapter 2 documents temporal and spatial variation in vegetation ecology in the embryo dune and foredune environments at Padre Island National Seashore. The goal of this chapter was to determine what, if any, were the trends in species composition and abundance through time and space and relate those changes to geomorphology. An understanding of spatial-temporal trends in larger scale ecogeomorphology was deemed necessary to contextualize the process dynamics involved in vegetation-aeolian fluid flow interactions.

Chapters 3 and 4 focus on process dynamics between vegetation and wind. Remotely sensed imagery from three perspectives was used to derive measures of vegetation morphology, such as plant area, pore area, and optical porosity, which were then analyzed as a function of wind velocity. By focusing on changes in vegetation morphology from three perspectives, Chapter 3 presents a new methodology for quantifying the change in shape of different vegetation morphology brought on as a result of changes in wind velocity. Chapter 4 examines the differences in spatial patterns of fluid flow and surface elevation changes around isolated clumps of vegetation in the embryo dune environment. The goal of this chapter was to distinguish flow and sediment transport patterns based on vegetation morphology type. Chapter 5 summarizes the findings and presents avenues for future research.

The coastal embryo dune systems is highly complex, with a multitude of dynamic vegetation morphologies altering fluid flow to varying degrees and creating hummocky terrain. By investigating the response of vegetation to aeolian flow as well as the how aeolian processes are altered by the presence of discrete patches of vegetation, this dissertation provides a holistic approach to examining the interplay between vegetation and geomorphological processes in this complex ecosystem. This dissertation establishes a foundation for developing a shear stress partitioning model which accounts for the dynamic morphology of live vegetation.

1.4 References

Arens, S.M., Baas, A.C.W., Van Boxel, J.H., Kalkman, C., 2001. Influence of reed stem density on foredune development. Earth Surface Processes and Landforms, 26(11), 1161-1176.

Bauer, B.O., Sherman, D.J., 1999. Coastal dunes dynamics: Problems and prospects. In: A.S. Goudie, I. Livingstone, and S. Stokes (Ed.), Aeolian Environments, Sediments and Landforms. John Wiley & Sons, Ltd, pp. 71-103.

Brown, S., Nickling, W.G., Gillies, J.A., 2008. A wind tunnel examination of shear stress partitioning for an assortment of surface roughness distributions. Journal of Geophysical Research-Earth Surface, 113(F2).

Buckley, R., 1987. The effect of sparse vegetation on the transport of dune sand by wind. Nature, 325(6103), 426-428.

Burri, K., Gromke, C., Lehning, M., Graf, F., 2011. Aeolian sediment transport over vegetation canopies: A wind tunnel study with live plants. Aeolian Research, 3(2), 205-213.

Crawley, D.M., Nickling, W.G., 2003. Drag partition for regularly-arrayed rough surfaces. Boundary-Layer Meteorology, 107(2), 445-468.

de Langre, E., 2008. Effects of wind on plants. Annual Review of Fluid Mechanics, 40(1), 141-168.

Debaine, F., Robin, M., 2012. A new GIS modelling of coastal dune protection services against physical coastal hazards. Ocean & Coastal Management, 63(0), 43-54.

Gillies, J.A., Lancaster, N., Nickling, W.G., Crawley, D.M., 2000. Field determination of drag forces and shear stress partitioning effects for a desert shrub (Sarcobatus vermiculatus, greasewood). J. Geophys. Res.-Atmos., 105(D20), 24871-24880.

Gillies, J.A., Nickling, W.G., King, J., 2002. Drag coefficient and plant form response to wind speed in three plant species: Burning Bush (Euonymus alatus), Colorado Blue Spruce (Picea pungens glauca.), and Fountain Grass (Pennisetum setaceum). J. Geophys. Res.-Atmos., 107(D24).

Gillies, J.A., Nickling, W.G., King, J., 2006. Aeolian sediment transport through large patches of roughness in the atmospheric inertial sublayer. Journal of Geophysical Research-Earth Surface, 111(F2).

Gillies, J.A., Nickling, W.G., King, J., 2007. Shear stress partitioning in large patches of roughness in the atmospheric inertial sublayer. Boundary-Layer Meteorology, 122(2), 367-396.

Grant, P.F., Nickling, W.G., 1998. Direct field measurement of wind drag on vegetation for application to windbreak design and modelling. Land Degradation & Development, 9(1), 57-66.

King, J., Nickling, W.G., Gillies, J.A., 2005. Representation of vegetation and other nonerodible elements in aeolian shear stress partitioning models for predicting transport threshold. Journal of Geophysical Research-Earth Surface, 110(F4).

Lancaster, N., Baas, A., 1998. Influence of vegetation cover on sand transport by wind: Field studies at Owens Lake, California. Earth Surface Processes and Landforms, 23(1), 69-82.

Leenders, J.K., Sterk, G., Van Boxel, J.H., 2011. Modelling wind-blown sediment transport around single vegetation elements. Earth Surface Processes and Landforms, 36(9), 1218-1229.

Leenders, J.K., van Boxel, J.H., Sterk, G., 2007. The effect of single vegetation elements on wind speed and sediment transport in the Sahelian zone of Burkina Faso. Earth Surface Processes and Landforms, 32(10), 1454-1474.

Lightbody, A.F., Nepf, H.M., 2006. Prediction of velocity profiles and longitudinal dispersion in emergent salt marsh vegetation. Limnology and Oceanography, 51(1), 218-228.

Luhar, M., Rominger, J., Nepf, H., 2008. Interaction between flow, transport and vegetation spatial structure. Environ. Fluid Mech., 8(5-6), 423-439.

Marshall, J.K., 1971. Drag measurements in roughness arrays of varying density and distribution. Agricultural Meteorology, 8(4-5), 269-&.

Martínez, M.L., Psuty, N.P., Lubke, R.A., 2008. A perspective on coastal dunes. In: M.L. Martínez, N. Psuty (Eds.), Coastal Dunes. Ecological Studies. Springer Berlin Heidelberg, pp. 3-10.

Maun, M.A., 2009. The Biology of Coastal Sand Dunes. Oxford University Press, Oxford, UK.

Moller, I., 2006. Quantifying saltmarsh vegetation and its effect on wave height dissipation: Results from a UK East coast saltmarsh. Estuar. Coast. Shelf Sci., 69(3-4), 337-351.

Musick, H.B., Trujillo, S.M., Truman, C.R., 1996. Wind-tunnel modelling of the influence of vegetation structure on saltation threshold. Earth Surface Processes and Landforms, 21(7), 589-605.

Nepf, H.M., 1999. Drag, turbulence, and diffusion in flow through emergent vegetation. Water Resources Research, 35(2), 479-489.

Neumeier, U., 2005. Quantification of vertical density variations of salt-marsh vegetation. Estuar. Coast. Shelf Sci., 63(4), 489-496.

Neumeier, U., Amos, C.L., 2006. The influence of vegetation on turbulence and flow velocities in European salt-marshes. Sedimentology, 53(2), 259-277.

Neumeier, U., Ciavola, P., 2004. Flow resistance and associated sedimentary processes in a Spartina maritima salt-marsh. Journal of Coastal Research, 20(2), 435-447.

Nilsson, S.B., Hertz, C.H., Falk, S., 1958. On the relation between turgor pressure and tissue rigidity. II. Physiologia Plantarum, 11(4), 818-837.

Nordstrom, K.F., 2008. Beach and Dune Restoration. Cambridge University Press.

Nordstrom, K.F., Lotstein, E.L., 1989. Perspectives on resource use of dynamic coastal dunes. Geogr. Rev., 79(1), 1-12.

Nordstrom, K.F., Psuty, N.P., 1980. Dune district management: A framework for shorefront protection and land use control. Coastal Zone Management Journal, 7(1), 1-23.

Okin, G.S., 2008. A new model of wind erosion in the presence of vegetation. Journal of Geophysical Research-Earth Surface, 113(F2).

Pasquill, F., 1950. The aerodynamic drag of grassland. Proceedings of the Royal Society of London Series a-Mathematical and Physical Sciences, 202(1068), 143-153.

Pavlik, B.M., 1984. Seasonal changes of osmotic pressure, symplasmic water content and tissue elasticity in the blades of dune grasses growing in situ along the coast of Oregon. Plant, Cell & Environment, 7(7), 531-539.

Raupach, M.R., 1992. Drag and drag partition on rough surfaces. Boundary-Layer Meteorology, 60(4), 375-395.

Raupach, M.R., Gillette, D.A., Leys, J.F., 1993. The effect of roughness elements on wind erosion threshold. J. Geophys. Res.-Atmos., 98(D2), 3023-3029.

Schlichting, H., 1936. Experimental investigation of the problem of surface roughness. Ingeniur Archiv., 7, 1-34.

Sherman, D.J., Bauer, B.O., 1993. Dynamics of beach-dune interactions. Progress in Physical Geography, 17, 413-447.

Steudle, E., Zimmermann, U., Lüttge, U., 1977. Effect of turgor pressure and cell cize on the wall elasticity of plant cells. Plant Physiology, 59(2), 285-289.

Suter-Burri, K., Gromke, C., Leonard, K.C., Graf, F., 2013. Spatial patterns of aeolian sediment deposition in vegetation canopies: Observations from wind tunnel experiments using colored sand. Aeolian Research, 8(0), 65-73.

Sutton, S.L.F., McKenna-Neuman, C., 2008. Variation in bed level shear stress on surfaces sheltered by nonerodible roughness elements. Journal of Geophysical Research-Earth Surface, 113(F3).

Walter, B., Gromke, C., Lehning, M., 2012a. Shear-Stress Partitioning in Live Plant Canopies and Modifications to Raupach's Model. Boundary-Layer Meteorology, 144(2), 217-241.

Walter, B., Gromke, C., Leonard, K.C., Manes, C., Lehning, M., 2012b. Spatio-Temporal Surface Shear-Stress Variability in Live Plant Canopies and Cube Arrays. Boundary-Layer Meteorology, 143(2), 337-356.

Webb, N.P., Okin, G.S., Brown, S., 2014. The effect of roughness elements on wind erosion: The importance of surface shear stress distribution.

Wolfe, S.A., Nickling, W.G., 1993. The protective role of sparge vegetation in wind erosion. Progress in Physical Geography, 17(1), 50-68.

Wolfe, S.A., Nickling, W.G., 1996. Shear stress partitioning in sparsely vegetated desert canopies. Earth Surface Processes and Landforms, 21(7), 607-619.

Wyatt, V.E., Nickling, W.G., 1997. Drag and shear stress partitioning in sparse desert creosote communities. Can. J. Earth Sci., 34(11), 1486-1498.

Zong, L., Nepf, H., 2010. Flow and deposition in and around a finite patch of vegetation. Geomorphology, 116(3–4), 363-372.

Chapter 2. Embryo Dune and Foredune Vegetation Ecogeomorphodynamics at Padre Island National Seashore

2.1 Introduction

Vegetation is integral to the formation and evolution of foredunes in coastal environments (Arens, 1996; Arens et al., 2001; Baas and Nield, 2007; Buckley, 1987; Burri et al., 2011; Delgado-Fernandez, 2011; Durán and Moore, 2013; King et al., 2005; Kuriyama et al., 2005; Luna et al., 2011; Miller, 2015; Psuty, 2004; Pye, 1983; Pye, 1992; Zarnetske et al., 2012). In order to contextualize small-scale, fluid dynamic processes of aeolian sediment transport influenced by the numerous species found in the embryo dune zone (EDZ), it is necessary to document and analyze spatiotemporal trends in vegetation species abundance, richness, and diversity along with geomorphology. Once larger scale vegetation community dynamics are documented it will be possible to extend small-scale process dynamics to larger-scale, longer-term models of coastal dune formation and evolution.

The purposes of this study were to 1) investigate the dynamics between plant species and geomorphology in the EDZ, 2) analyze temporal changes in community composition in different cross-shore habitats, 3) investigate ecogeomorphic functions of the various species found in the EDZ, and 4) produce an inventory of species present in the embryo dune and foredune zones. Field surveys of ecology and topography were conducted in the summer of 2012, 2013, and 2014 in order to accomplish these objectives.

2.2 Background

While the effects of the environmental stresses on coastal dune vegetation are well documented, there is currently no detailed information on spatiotemporal variation in vegetation abundance and diversity in the coastal embryo and foredune environments available for Padre

Island National Seashore (PINS). Padre Island, Texas, is the largest barrier island in the United States, extending 182 km from Corpus Christi Pass in the north to Brazos Santiago Pass in the south, and separating Laguna Madre from the Gulf of Mexico. Judd et al. (1977) documented species distribution in relation to topography on South Padre Island in five zones on three cross-island transects which were approximately 64 km south of the study site used in this research, though the season and year in which surveys were conducted was not identified. This study is not fully applicable to northern PINS because anthropogenic disturbance, which is common in South Padre Island with areas of dense development and altered natural processes, is largely absent in the northernmost portion of PINS. Carls et al. (1991) documented the presence of species in five cross-island zones in May and July 1987. Both of these studies documented vegetation in cross-island transects from the beach to the backside of the barrier island and grouped the entire EDZ into one sub-environment called the "backshore" (Carls et al., 1991; Judd et al., 1977). This coarse grouping obscures variation in biotic and abiotic factors that control vegetation distribution within this zone, which was ~40 m wide during the study period. Furthermore, neither of these studies analyzed temporal change in community assemblage and species abundance. Knowledge and understanding of spatiotemporal distribution of species in the embryo dune and foredune zones are essential to modeling geomorphic changes in this zone, as vegetation species are agents of geomorphic change.

Vegetation in coastal dune environments is specially adapted to living in this high stress environment, where burial, erosion, sand abrasion, salt spray, low nutrient availability, low soil moisture, and high exposure to sun are present (Dech and Maun, 2005; Gilbert et al., 2008; Maun, 1998; Maun, 2009; Miller, 2015; Moreno-Casasola, 1986; Moreno-Casasola and Vasquez, 1999; Oosting and Billings, 1942; Ruocco et al., 2014; van der Maarel, 2005). The intensity of

environmental stress caused by these variables varies along a shore-perpendicular gradient, wherein stresses are higher closer to the shoreline and lower farther from the shoreline (Arens, 1996; Bauer and Davidson-Arnott, 2003; Gilbert et al., 2008; Grootjans et al., 1998; Houser and Ellis, 2013; Lubke, 2004; Martinez et al., 1997; Martinez et al., 2001; Maun, 2009; Moreno-Casasola, 1986; Moreno-Casasola and Vasquez, 1999; Oosting, 1945; Oosting and Billings, 1942; Zuo et al., 2008). Based on the distribution of stresses smaller micro-habitats exist within the EDZ and foredune zones. Adaptation to and ability to cope with these various environmental stresses determine the spatial distribution of species as well as their abundance (Gilbert et al., 2008; Maun, 1998; Maun, 2009). Thus, species abundance and diversity were measured through time and related to changes in surface elevation since sand transport and consequent deposition and erosion is the predominant variable that influences dune vegetation species (Dech and Maun, 2005; Gilbert et al., 2008; Hesse and Simpson, 2006; Martinez et al., 1997; Martinez et al., 2001; Maun, 1998; Maun, 2009; Miller, 2015; Moreno-Casasola, 1986b).

Vegetation and geomorphology are interdependent. Not only do geomorphic processes influence the spatial distribution and abundance of species, but also different species perform different functions as geomorphic agents. Zonation of communities is thought to be representative of successional processes. Pioneer species are those which first colonize a previously uninhabited surface, altering the local environmental conditions through time and enabling colonization of other species. New species colonize a location in successive waves as environmental conditions change further. These are called secondary and tertiary species and so forth. Typically, the pioneer species will be the builders of the landscape in coastal dune environment, as they are located at the edge of vegetation closest to the source of wind-blown sand and trap deposition with upright growth habits (Hernández-Cordero et al., 2015). Secondary and tertiary waves of species are

typically stabilizers and can be classified by whether they are burial tolerant or intolerant (Hernández-Cordero et al., 2015). Stabilizers protect the surface from erosion and stabilize the substrate. Thus, by looking at concurrent change in geomorphology, it can be determined what function individual or groups of species perform as geomorphic agents based on their location in the embryo dune and foredune environments and the concurrent change in geomorphology. For example, Tobias (2015) conducted very thorough surveys and determined the functions of different species found along the coast of California. However, none of the species mentioned were found at PINS in this study or in the catalogs of Judd et al. (1977) or Carls et al. (1991). This study will determine the functions of the species that characterize the Texas coast by examining an essentially unaltered coastal dune ecosystem.

2.3 Methodology

2.3.1 Study Site

Vegetation species and abundance and topography were documented at PINS, which is located in the Gulf of Mexico, approximately 160 km north of the United States – Mexico border (Figure 2.1 inset). Beach sediment is predominantly very-well sorted, fine to very-fine quartz sand with a mean diameter of about 0.15 mm (Schmutz, 2007). In the northern portion of the park where the study sites were located, there is a 7.25 km section of beach on which public driving has been prohibited since the park was established in 1962. The beach at PINS is dissipative, with a continuous primary foredune ridge that has very few and minor blowouts. Seaward of the foredune ridge is a partially vegetated, hummocky EDZ that ranges from about 30 to 40 m in width (Figure 2.2). The general climate of PINS is regarded as subtropical and semi-arid. The average temperature is 14°C in winter and is 28°C in summer, while the mean annual rainfall is 81 cm

(SRCC, 2015). During summer, winds are dominated by the sea breeze so that the dominant wind direction is from the southeast (Weise and White, 1980). During winter, passage of cold polar frontal systems through the area generates strong northerly winds (Weise and White, 1980).

Figure 2.1. Map of location of study site (inset) and transects (red lines with white numbers).

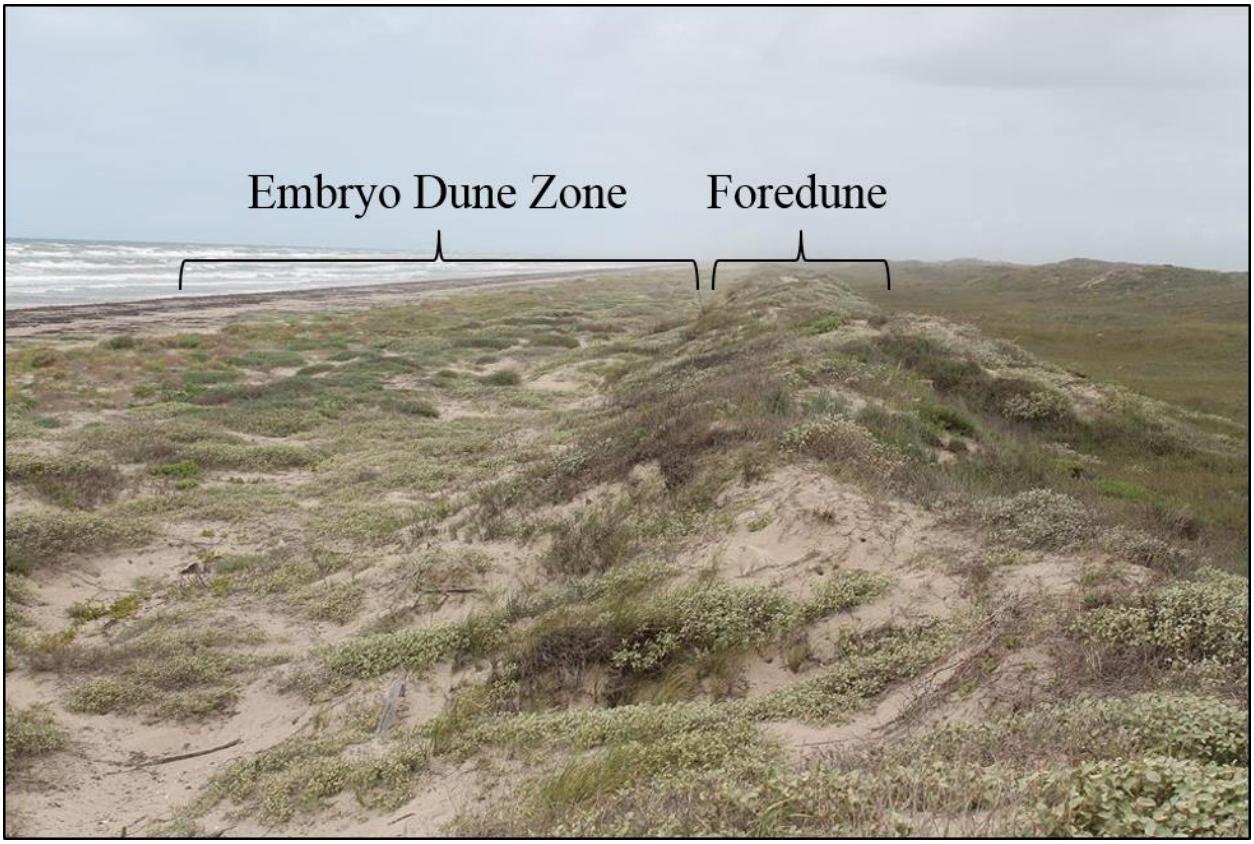

Figure 2.2. Image of the study site from the crest of the foredune, looking to the southwest with the Gulf of Mexico to the left and Laguna Madre out of the frame to the right.

PINS has several important advantages as a study site including dune morphology and vegetation that are fairly typical and representative of northern and western Gulf of Mexico barrier islands. This section of the shoreline is relatively unaffected by human development. Only a few park vehicles agitate the surface to contribute to increased sediment transport into the embryo dune. It is abundantly clear that heavy vehicular traffic contributes to a large amount of aeolian sediment transport into the embryo dune and foredune zones and results in a decrease in vegetation abundance, density, and diversity (Anders and Leatherman, 1987; Hosier and Eaton, 1980; McAtee and Drawe, 1980; Rickard et al., 1994; Schlacher and Morrison, 2008; Schlacher and Thompson, 2008; Thompson and Schlacher, 2008). Thus this portion of the shoreline exhibits a vegetation ecology and geomorphological dynamics that are as natural as can be found in the state.

2.3.2 Data Collection

Three sets of field data were collected at PINS – on 6-8 August 2012, 27 July 2013, and 9-10 June 2014. The survey dates were determined to be representative of the peak growing season. No significant tropical storms affected the study area prior to or during surveys. During these surveys, vegetation presence and abundance as well as topography were measured along five transects perpendicular to the shoreline, extending from the foredune crest (FDC) to the seaward edge of vegetation, also referred to as the leading edge of the EDZ.

In order to capture trends alongshore variation in vegetation, five cross-shore transects were established in the northernmost 5 km of the vehicle-prohibited zone at PINS (Figure 2.1) for vegetation and geomorphology monitoring. Transects were located approximately 4.25 km (transect 1), 3.25 km (transect 2), 2.25 km (transect 3), 1.25 km (transect 4), and 0.25 km (transect 5) from the northern boundary of the restricted area. A benchmark was emplaced at the crest of the foredune for each transect in 2012 as a control point for subsequent surveys. The location of the benchmarks were recorded in UTM NAD 83 using a handheld eTrex GPS (Table 2.1). Transect orientations were also recorded to ensure that the same locations were surveyed during subsequent surveys.

Table 2.1. Coordinates (NAD 83 UTM Zone 14R) for the benchmark at the start of each transect and the orientation of each transect.

transect	starting x	starting y	site line
1	0669007	3036570	291°
2	0669370	3037519	289°
3	0669735	3038459	285°
4	0670105	3039380	284°
5	0670474	3040300	289°

Topographic data for each transect were collected using a total station. Vegetation surveys were conducted using the visual estimate method within a 1 m^2 quadrat, or plot (Figure 2.3). The visual estimate method is a standard methodology for monitoring plant assemblages (Barbour et al., 1987; Bråkenhielm and Qinghong, 1995; Vanha-Majamaa et al., 2000; Kercher et al., 2003; Carlsson et al., 2005; Godínez-Alvarez et al., 2009), which is executed by establishing plots using a quadrat of known size on the surface, visually identifying each species, and estimating the percentage of the area of the plot that each species occupies, resulting in a percent cover estimate.

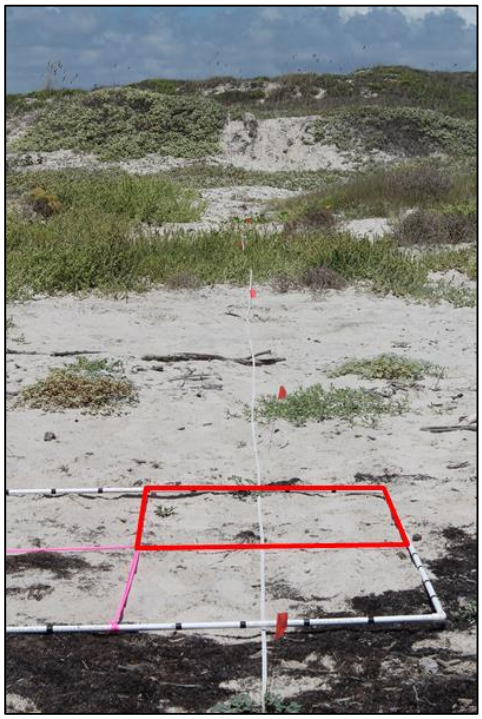

Figure 2.3. Example of transect for measuring topography and species distribution. Species cover was estimated within the 1 m by 1 m space outlined by the red box.

Although visual estimates fluctuate somewhat between surveyors, this method has been found to be the least time-consuming and most accurate approach in sparse grassland environments (Bråkenhielm and Qinghong, 1995; Vanha-Majamaa et al., 2000; Kercher et al., 2003; Carlsson et al., 2005; Godínez-Alvarez et al., 2009). In this study, all surveys were conducted by the same

person, who had training in visual estimate methods. If a species was not easily identified in the field, it was photographed *in situ*, extracted and pressed for identification by a botanist at Louisiana State University Herbarium.

2.3.3 Ecological Data Analysis

The ecology database for analysis had five transects with 35-45 plots in each, in which species percent cover was estimated, for a total of 566 plots. In order to analyze community structure in the embryo dune and foredune environments at PINS, percent cover of each species, richness, and Simpson's Diversity Index were related to distance from the FDC and year of data collection. Species richness is simply the total number of species present in a given plot and does not take into account the abundances of the species present. Species richness is not a complete representation of community structure as it does not take into account the evenness, or homogeneity of abundance, of species present. For example consider two plots, both of which have the same richness value with three species present. One plot has 60% cover of species A, 30% cover of species B, and 10% cover of species C. It is evident that species A dominates this plot. The second plot has 30% cover of species A, 35% cover of species B, and 35% cover of species C. The species in the second plot share roughly equal area within the plot and thus no one species dominates.

Many diversity indices incorporate evenness to capture differences in community structure (Krebs, 1972), and Simpson's Diversity Index was chosen to measure species diversity in this study. Simpson's Diversity Index was calculated for each plot using the following equation:

$$D = \frac{\Sigma_{i=1}^{S} n_i(n_i-1)}{N(N-1)}$$

where the values of *D* range from 0 to 1, *S* is the number of species in each plot, *N* is the total percentage cover in each plot and *n* is the percentage cover of a species within a plot. As the value of D increases, diversity decreases. Simpson's Diversity Index (Simpson, 1949) is more appropriate for use in coastal dune vegetation communities over the widely used Shannon-Weiner Index because the Shannon-Weiner Index emphasizes species richness while Simpson's Diversity Index does not (Magurran, 1988; van der Maarel, 2005). Species richness is rather low in dune environments (often no more than 15) and fluctuates greatly between plots. Richness in plots in this study range from 1 to 7. Accuracy in diversity calculated by the Shannon-Weiner index is affected by richness, (Magurran, 1988; van der Maarel, 2005). On the other hand, Simpson's Diversity Index emphasizes dominance (Magurran, 1988; van der Maarel, 2005), which varies as different species dominate the various plots along transects. For diversity indices to be useful, the total cover must add up to 100% and therefore bare sand coverage is used as a "species" in this analysis, as suggested by Magurran (1988) because vegetation often covers less than 100% of the surface in dunes and semi-arid grasslands.

2.4 Results

2.4.1 Geomorphology

Data from the GPS total station were interpolated to generate topographic profiles representing the different data years (Figure 2.4). The elevations of the starting point of transects in 2013 and 2014 were adjusted to match the benchmark recorded in 2012, because the surface elevation at this point changed less than 2 cm between 2012 and 2014. Profiles were truncated at the seaward edge of the vegetated zone because the focus on ecogeomorphodynamics requires the presence of vegetation. The average from each year of the five transects was used to determine

height change through time. The five transects were treated as replicates representing a moment in time because the focus was on the community, not the individual transects.

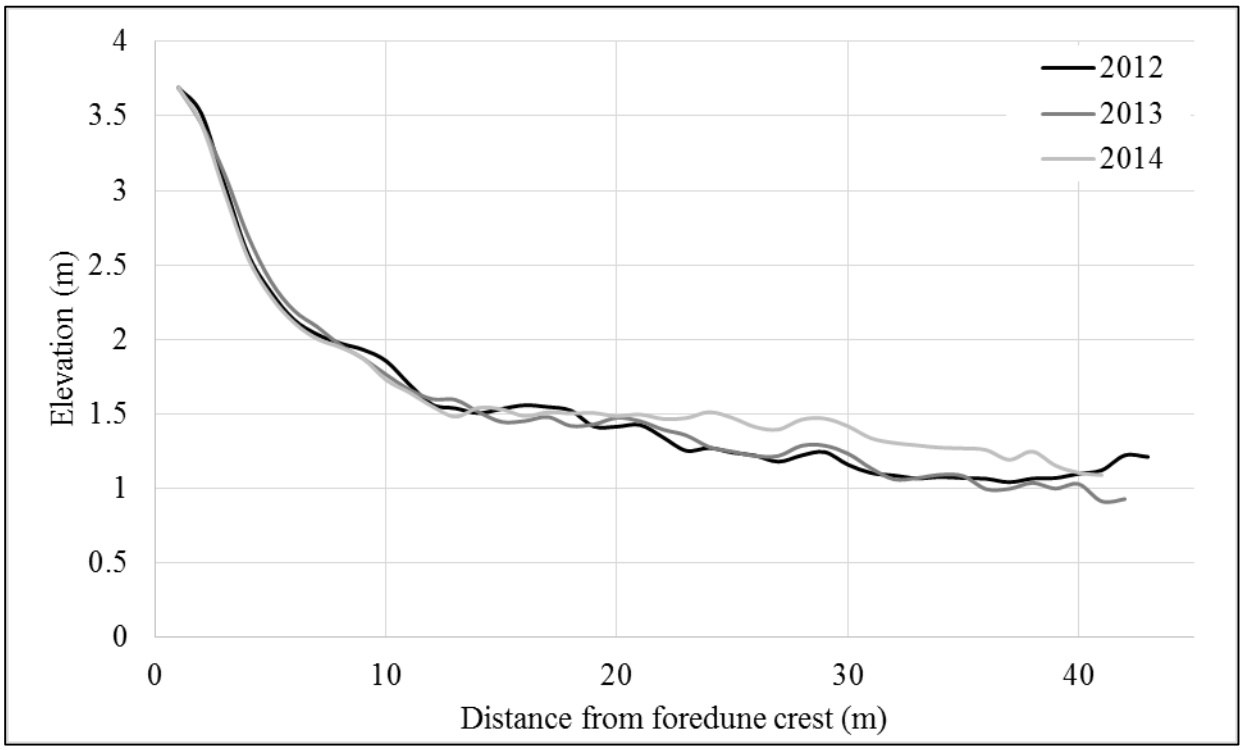

Figure 2.4. Average topographic profiles for 2012, 2013, and 2014.

A general linear mixed model ("Proc Glimmix" in SAS) was used to test the effect of the independent variables: distance from the FDC, year, and distance*year on the dependent variable elevation. The interactive term "distance*year" was used to test the simultaneous influence of these two variables on elevation. Distance and Distance*year were random variables and year was a fixed variable. Use of a linear model is not appropriate when both fixed and random effects are present in the data. Furthermore, a general linear mixed model is the most appropriate model for unbalanced and non-normal data as are found in this dataset. The use of a general linear mixed model allows grouping of various effects and responses by year and distance from the FDC.

There were significant differences in plot elevation along all transects as functions of a) distance from FDC ($p<0.0001$), b) year ($p<0.0001$), and c) the interaction between year and distance ($p=0.0376$). Elevation decreased along all transects away from the FDC, as to be expected, and elevation increased through time, signifying deposition along transects between 2012 and 2014.

A second model was tested in SAS to determine the effects of the independent variables distance, time period, and the simultaneous interaction between distance and time period on the dependent variables elevation change. The time periods tested were 2012-2013 and 2013-2014. There were significant differences in elevation change along all transects as a function of a) distance ($p<0.0001$) and b) time period ($p<0.0001$), but not as a function of the interaction of distance and time period ($p=0.5972$). Elevation changes from 2012-2013 (average=0.0002 m) were significantly lower than from 2013-2014 (average=0.079 m) or 2012-2014 (average=0.096 m) (Table 2.2). The average elevation change along transects was graphed for each time period in Figure 2.5.

Table 2.2. Elevation change statistics.

	2012-2013	2013-2014	2012-2014
Average change along all five transects (m)	0.0002	0.0794	0.0957
Maximum erosion along all five transect (m)	0.12	0.15	0.13
Maximum deposition along all five transects (m)	0.12	0.31	0.31
Slope of line relating average elevation in a year to distance	-0.19	0.85	0.88

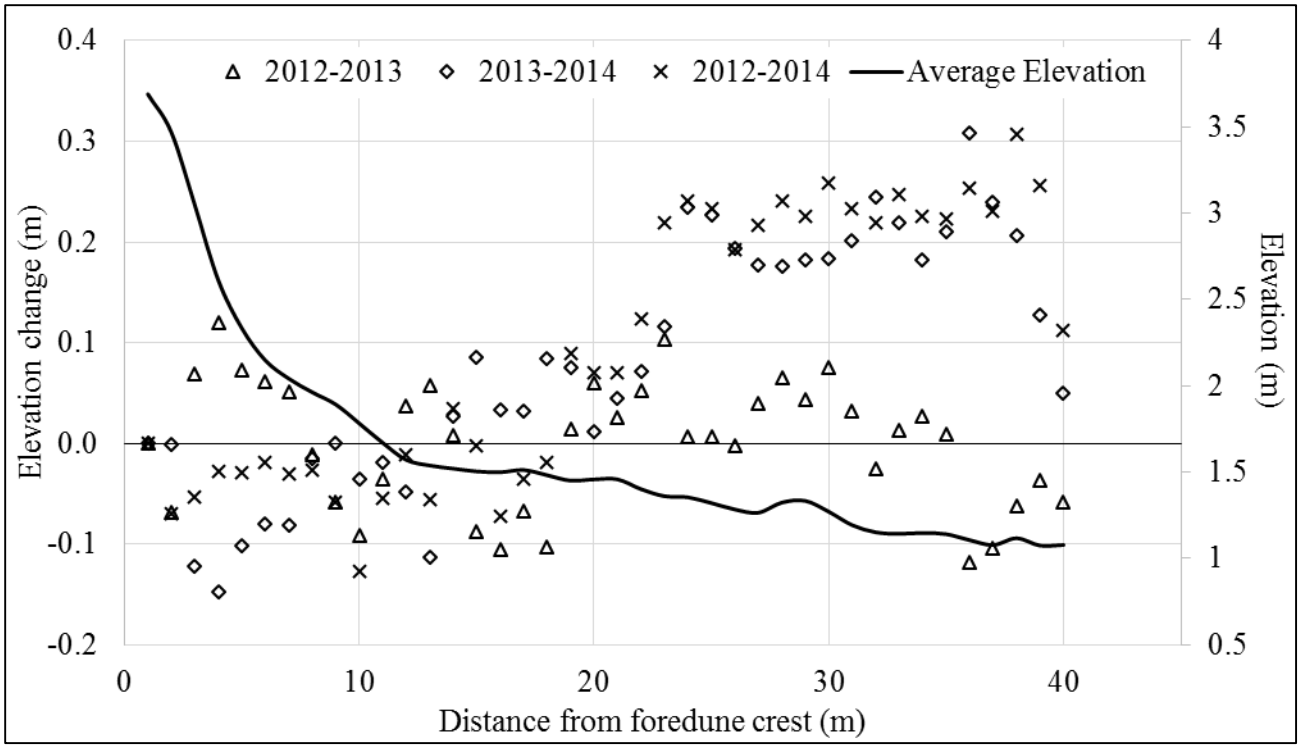

Figure 2.5. Elevation change for all transects averaged for the study periods. Average elevation of all transects and data years depicted as profile line.

The foredune slope (FDS) (0-12 m from the FDC) experienced small amounts of deposition (0.05-0.12 m) between 2012 and 2013 and small amounts of erosion (0.08-0.15 m) between 2013 and 2014 (Figure 2.5). The result was net erosion of less than 0.05 m in this area between 2012 and 2014. Changes in elevation at the rear portion of the EDZ (EDZ) (12-18 m from the FDC) ranged from -0.11 m to 0.09 m between 2012 and 2013 and between 2013 and 2014. The net change in this area was erosion less than 0.08 m between 2012 and 2014. The rear of the EDZ (12-23 m from the FDC) experienced minor amounts of deposition (0.01-0.13 m). Between 2012 and 2013 minor deposition (up to 0.08 m) occurred in the middle of the EDZ (24-35 m from the FDC) and erosion (up to -0.12 m) occurred at the leading edge of the EDZ (36-40 m from the FDC). Between 2013 and 2014 deposition (0.18-0.31 m) dominated the middle to leading edge of the EDZ. In summary, deposition occurred along the FDS and minor amounts of erosion occurred

throughout the EDZ between 2012 and 2013 whereas erosion occurred along the FDS and rear of the EDZ and deposition occurred in the middle and leading edge of the EDZ between 2013 and 2014. Net elevation changes from 2012 to 2014 match more closely those changes from 2013 to 2014 than from 2012 to 2013. During the entire study period, net erosion occurred along the FDS and rear of the EDZ and deposition dominated from the middle to the leading edge of the EDZ.

2.5.2 Trends in Community Ecology

For the purpose of analyzing trends in community ecology, the presence or absence of all species in all plots was displayed as a function of distance using box and whisker plots, which show the total range of distribution as lines and 50% of occurrences as boxes (Figure 2.6). The following species occurred on every profile: *Amaranthus greggii* S. Watson, *Atriplex acanthocarpa* (Torr.) S. Watson, *Croton punctatus* Jacq., *Ipomoea imperati* (Vahl) Griseb., *Ipomoea pes-caprae* (L.) R. Br., *Oenethera drummondii* Hook., *Panicum amarum* Elliott, *Salicornia spp.*, *Sesuvium portulacastrum* (L.) L., *Sporobolus virginicus* (L.) Kunth, and *Tidestromia lanuginosa* (Nutt.) Standl. There was a tendency for certain species to occupy similar areas of the embryo dune and foredune environment. Generally, *Croton* dominated the vegetation community closest to the foredune, with minor occurrences of *Panicum*, *Atriplex*, *I. imperati*, and *Oenethera*. Some species, such as *I. pes-caprae* and *Sporobolus* were found primarily at the rear to middle of the EDZ. *Amaranthus*, *Salicornia spp*., *Sesuvium* and *Tidestromia* were not present in this area but were found predominantly from the middle to the leading edge of the EDZ.

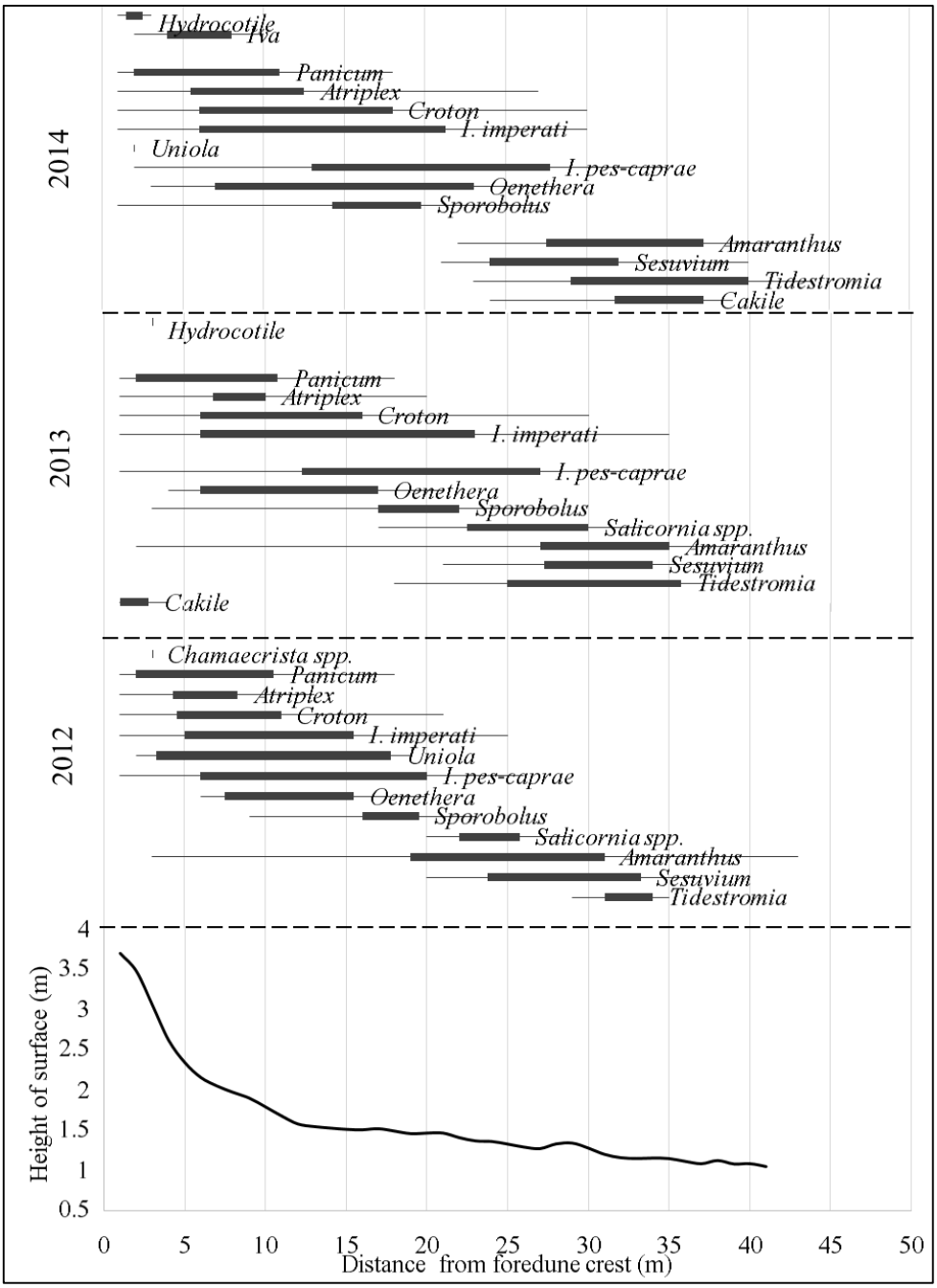

Figure 2.6. Box and whisker plots of species presence at distances from foredune crest in 2012, 2013, and 2014. Average elevation of all transects plotted in bottom graph for reference.

Five species were deemed rare because they occurred in fewer than 15 of the 566 plots. These species were *Cakile geniculata* (B.L. Rob.) Millsp. with 14 occurrences, *Chamaecrista spp.* with 1 occurrence, *Hydrocotile bonariensis* Comm. ex Lam. with 4 occurrences, *Iva imbricata*

Walter with 2 occurrences, and *Uniola paniculata* L. with 7 occurrences. Contrary to expectations based on published catalogs of common coastal dune vegetation in the area (Carls et al., 1991; Judd et al., 1977; Weise and White, 1980), *Uniola* was not a dominant species. The low occurrence of *Uniola* in the dataset is simply coincidental and attributable to placement of transects. *Uniola* was observed throughout the EDZ in discrete tussocks during all three field seasons.

Graphical representations of percent cover of each non-rare species in each plot along each transect in each year are presented in Appendix A. These graphs were difficult to read, provide limited insight into spatial and temporal trends, and produce descriptive results at best, but they illustrate the complexity of the dataset. The next issue to be investigated was whether percent cover of each species, richness, or diversity is related to distance from the FDC or the year in which data were collected.

A general linear mixed model (Proc Glimmix in SAS) was used to analyze the effect of the independent variables distance from FDC, year, and distance*year on the dependent variables percent cover of all species, richness, and diversity. Distance and distance*year were random effects and year was a fixed effect. The interactive term "distance*year" was used to test the simultaneous influence of these two variables on percent cover, richness, or diversity. Results are presented in Table 2.4. No significant relationships were found between percent cover of *I. imperati*, *I. pes-caprae*, *Panicum*, *Sesuvium*, or *Sporobolus* and distance or year. Distance from the FDC had a significant effect on percent bare cover ($p=0.0023$), dead cover ($p=0.0459$), and *Oenethera* ($p<0.0001$). Percent cover of the plots occupied by bare sand and by *Oenethera* increased from the FDC to the leading edge of the EDZ while percent cover by dead material in all plots decreased along this same gradient.

Table 2.4. P-values for relationships between independent (distance, year, distance*year) and dependent (richness, Simpson's Diversity, and percent cover of species) variables.

	distance	year	distance*year
Amaranthus	0.7813	0.0017	0.8464
Atriplex	0.8632	0.0092	0.5916
bare cover	0.0023	0.0107	0.0572
Croton	0.4117	0.0036	0.004
dead cover	0.0459	0.0722	0.5174
I. imperati	0.6245	0.1056	0.4116
I. pes-caprae	0.8773	0.4873	0.9996
Oenethera	<.0001	0.0073	0.0012
Panicum	0.6313	0.8224	0.8948
richness	<.0001	<.0001	0.341
Salicornia spp.	0.2512	0.1256	0.0026
Sesuvium	0.6915	0.0575	0.674
Simpson's	<.0001	0.423	0.9534
Sporobolus	0.9736	0.1481	0.5616
Tidestromia	0.1053	0.0013	0.2322

Sediment transport and salt spray increased along a gradient from the FDC to the leading edge of the EDZ, causing higher environmental stress in more seaward areas of the EDZ. Greater stresses at the leading edge of the EDZ were associated with lower vegetation cover and greater bare sand cover in this area. At the rear of the EDZ and along the FDS, environmental conditions were more stable and less stressful and therefore the community there had undergone some successional transition, leading to build-up of detritus from previous waves of succession.

The simultaneous effect of year and distance had a significant effect on the percent cover of *Croton* (p=0.004), *Oenethera* (p=0.0012), and *Salicornia spp*. (p=0.0026). Both *Croton* and *Oenethera* migrated seaward through time. *Salicornia spp*. is an annual species which was found in minor amounts in 2012, greater amounts and more seaward in 2013, and not at all in 2014 in the survey plots.

There were significant changes through time in percent cover of *Amaranthus* ($p=0.0014$), *Atriplex* ($p=0.0092$), *Croton* ($p=0.0036$), *Oenethera* ($p=0.0073$), *Tidestromia* ($p<0.0001$), and bare ground ($p=0.0013$). Overall the percent cover of plots occupied by *Atriplex*, *Oenethera*, and bare cover increased from 2012 to 2014, while the percent cover of plots occupied by *Amaranthus*, *Croton*, and *Tidestromia* decreased through time. Bare cover increased through time as the result of deposition. It is not clear if this was part of a longer-term trend in community composition caused by large-scale factors such as barrier island progradation. Vegetation surveys need to be conducted in the growing season for several more years expand and strengthen the dataset. For all other species there was not a significant change in the percent cover through time.

Treated as separate effects, year ($p<0.001$) and distance ($p<0.001$) from FDC both had a significant effect on species richness, even though the simultaneous effect of distance and year did not significantly affect richness. Richness increased through time so that the average richness across all plots on all transects in 2012 was 1.75, in 2013 was 2.07, and in 2014 was 2.31. Richness increasing through time indicated that the foredune and embryo dune environment as a whole was experiencing transition in succession, wherein a larger number of species are present because species of the previous stage co-exist with species of the next stage of succession. Successional transition is occurring because this coastline has been prograding since the 1970s (Weise and White, 1980) and so community assemblage has changed through time as the barrier island has widened. Species richness decreased with increasing distance from the FDC (Figure 2.7). There was a spike in richness in the middle of the EDZ (23-34 m from the FDC) in 2014. Richness was lower at the leading edge of the EDZ, where environmental stresses were greatest along transects, and increased toward the FDC, where environmental stresses such as sediment transport and salt spray were less.

While time did not have a significant effect on diversity distance from FDC did have a significant effect on diversity ($p<0.001$). Along each transect, diversity was higher at the FDC, lower at the FDT, and then decreased across the EDZ so that it was lowest at the leading edge of the EDZ (Figure 2.8). This was due to the increase in environmental stresses from the FDC to the leading edge of the EDZ.

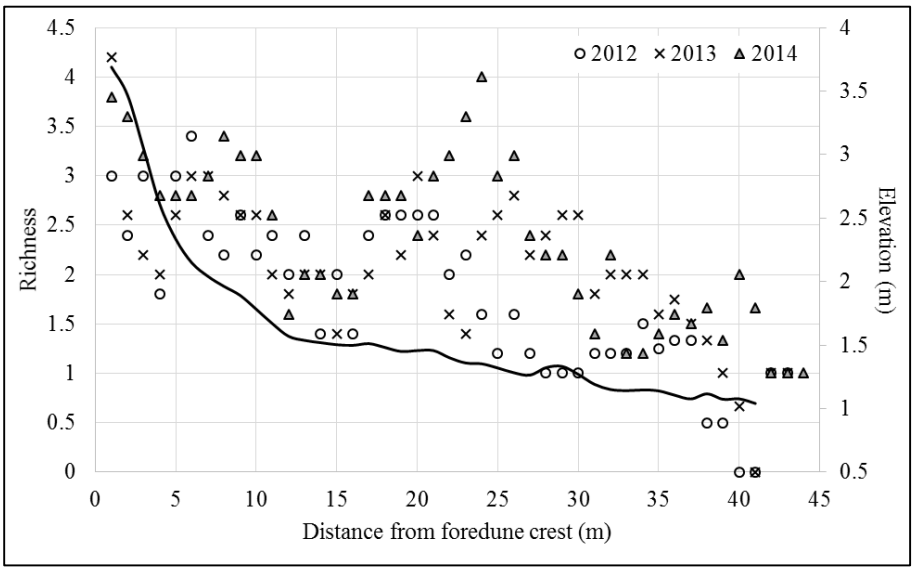

Figure 2.7. Richness averaged for all transects in a study year. Elevation profile included for reference.

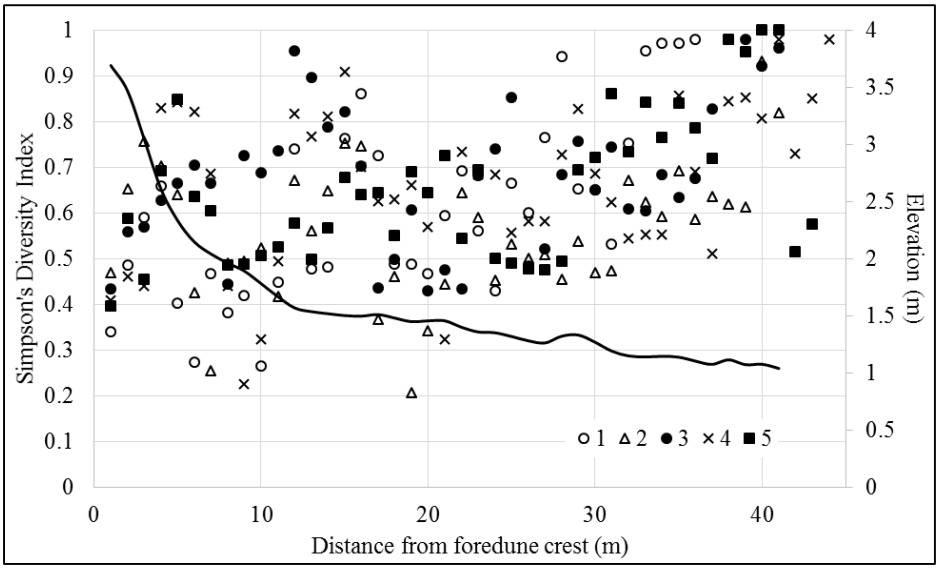

Figure 2.8. Simpson's Diversity Index, averaged through time along each transect. Elevation profile included for reference.

2.5.3 Effects of Elevation Change on Community Ecology

The final issue was to examine the relationship between sediment transport and changes in percent cover of species found in the EDZ as well as richness and diversity. In order to examine the effect of elevation change, as a representative of rates of deposition and erosion, on ecology, rates of change of percent cover were calculated for all species and correlated to elevation change in each plot. Time periods examined were 2012-2013 and 2013-2014. The results are presented in Table 2.5.

Table 2.5. Pearson correlation coefficients and p-values for correlations of elevation change to change in percent cover of all species, richness, and diversity.

	R	p-value
Amaranthus	0.01425	0.8607
Atriplex	-0.02230	0.8612
bare cover	0.01109	0.8332
Croton	0.15266	0.0370
dead cover	-0.05507	0.3746
I. imperati	-0.24688	0.0050
I. pes-caprae	-0.07515	0.3828
Oenethera	0.08419	0.4607
Panicum	-0.02567	0.8671
richness	-0.08827	0.1575
Salicornia spp.	-0.29788	0.0151
Sesuvium	-0.10612	0.3009
Simpson's	0.01745	0.7380
Sporobolus	0.04528	0.7181
Tidestromia	-0.21276	0.0969

Change in percent cover of *Croton*, *I. imperati*, and *Salicornia spp.* were significantly related to elevation change (p=0.0370, 0.0050, and 0.0151, respectively). *Croton* cover increased where deposition occurred whereas *I. imperati* and *Salicornia spp.* decreased where deposition occurred. Change in the percent cover of the other species, richness, and diversity did not correlate

to elevation change. It is likely that species response to deposition and erosion occurs at longer time intervals than those examined herein.

2.5.4 Comparison to Previous Species Catalogs for Padre Island

Prior to when PINS was established as a National Seashore in 1962, the land was primarily used for cattle ranching (Weise and White, 1980), a practice which reduced vegetation cover in the park. As time passed, the ecosystem has recovered from grazing disturbance. To the author's knowledge there has been no vegetation catalogue for embryo dune and foredune species published for PINS since the late 1980s. There are substantial differences between species recorded by Judd et al. (1977), Carls et al. (1991), and this study in both the EDZ and the foredune zone (Table 2.5). These differences suggest that the community is actively undergoing succession, attributable to larger-scale disturbances, such as island-wide cattle grazing, or smaller scale disturbances, such as scarping or overwash during periodic storms or fires. Without long-term census data and records of these disturbances, it is not possible to determine where in the succession process the communities are the recorded times.

Species that occurred in the EDZ during all three studies were *Sesuvium, Panicum*, *I. imperati*, *I. pes-caprae*, and *Croton*. Six other species were present in the EDZ in this study which were not present in previous studies – *Atriplex*, *Sporobolus*, *Amaranthus*, *Tidestromia*, *Cakile*, and *Salicornia spp.* Species which occurred in the foredune zone in all three studies include *Uniola*, *Croton*, *Panicum*, and *Oenethera*. Six species were present in the foredune in this study which were not present in previous studies – *Cakile*, *Atriplex*, *I. pes-caprae*, *Sporobolus*, *Amaranthus*, and *Iva*. This study focused on ecology in the EDZ and thus did not extend landward of the FDC so that the list of foredune species is not as comprehensive as previous studies that surveyed the

whole foredune complex. It is unclear how exactly the boundaries of the zones termed backshore and foredune were defined in the earlier studies, so there may be some overlap in the two environments. In this study, the boundary between the EDZ and the foredune is the dune toe, or the break in slope at the windward bottom of the foredune.

Table 2.5. Species catalogues of various studies.

	Judd et al. (1977)	Carls et al. (1991)	Renken (2015)
Embryo dune zone (or backshore in Judd et al. (1977) and Carls et al. (1991))	*Croton punctatus* *Fimbristylis castanea* *Ipomoea pes-caprae* *Ipomoea stolonifera* *Panicum amarulum* *Schizachyrium scoparium* *Sesuvium portulacastrum* *Uniola paniculata*	*Croton punctatus* *Ipomoea imperati* *Ipomoea pes-caprae var. emarginata* *Oenothera drummondii* *Panicum amarum* *Senecio riddellii* *Sesuvium portulacestrum* *Uniola paniculata*	*Amaranthus greggii* *Atriplex acanthocarpa* *Cakile geniculate* *Croton punctatus* *Ipomoea imperati* *Ipomoea pes-caprae* *Oenethera drumondii* *Panicum amarum* *Salicornia spp.* *Sesuvium portulacastrum* *Sporobolus virginicus* *Tidestromia lanuginosa*
Foredune	*Cassia fasciculata* *Croton punctatus* *Fimbristylis castanea* *Heterotheca subaxillaris* *Heterotheca subaxillaris* *Ipomoea stolonifera* *Oenothera drummondii* *Panicum amarulum* *Paspalum monostachyum* *Rhynchosia minima* *Schizachyrium scoparium* *Uniola paniculata*	*Andropogon glomeratus* *Chamaecrista fasciculate* *Croton punctatus* *Eleocharis sp.* *Eragrostis secundiflora* *Euphorbia serpens* *Heterotheca subaxillari* *Hydrocotyle bonariensis* *Ipomoea imperati* *Leptoloma cognatum* *Machaeranthera phyllocephala* *Oenothera drummondii* *Panicum amarum* *Paspalum monostachyum* *Paspalum setaceum* *Phyla nodiflo* *Physalis viscosa* *Schizachyrium scoparium var. littoralis* *Scirpus pungens var. longispicatus* *Sporobolus pyramidatus* *Uniola paniculata*	*Amaranthus greggii* *Atriplex acanthocarpa* *Cakile geniculate* *Chamaecrista spp.* *Croton punctatus* *Hydrocotile bonariensis* *Ipomoea imperati* *Ipomoea pes-caprae* *Iva imbricata* *Oenethera drumondii* *Panicum amarum* *Sporobolus virginicus* *Uniola paniculata*

2.6 Summary and Conclusions

Spatial and temporal trends in community composition were examined and compared to geomorphology. There were significant inter-annual variations between species percent cover for 5 of the 12 major species – *Atriplex* and *Oenethera* increased through time while *Amaranthus*, *Croton*, and *Tidestromia* decreased through time. The change in community composition during this three-year study signifies the active process of community succession, whereby a newer community of species replaces an older community of species as environmental conditions are changed by the older community.

Species tended to co-occupy similar zones in the EDZ and the foredune. The community at the leading edge of the EDZ consisted of *Tidestromia*, *Amaranthus*, and *Sesuvium*. These species are exposed to high environmental stresses and thus their composition and cover fluctuate greatly through time. These species were leading edge pioneers (Tobias, 2015), which tend to trap moving sand particles resulting in deposition. Indeed, deposition was greatest at the leading edge of the EDZ. Diversity was found to be lowest here, with a small number of species occupying small areas within plots here.

The middle of the EDZ was a transition zone in the EDZ community, with some species extending seaward from the FDS and FDT into this area (i.e. *I. pes-caprae*, and *I. imperati*) and other species extending landward from the leading edge of the EDZ in this area (i.e., *Salicornia spp.* and *Amaranthus*). The rear of the EDZ and the FDS were relatively stable and experienced little change in morphology. Biodiversity was greatest here and richness was moderate. The rear portion of the EDZ, the FDT, and the FDS housed a particular suite of species, including *Croton*, *Atriplex*, *Oenethera*, and *Panicum*. These species are mid-strand stabilizers (Tobias, 2015), which

establish themselves after other plants have colonized the surface and continue to protect and stabilize the substrate.

Even though all species present in the coastal dune environment located seaward of the crest of the foredune can be considered pioneer species because they are first to colonize the highly unstable substrate of the coastal barrier island, the distribution of the various species along the five transects indicate the proclivity of some species to be *more* pioneer than others, colonizing the leading edge of the EDZ (i.e., *Sesuvium*) while others prefer the more stable portion of the EDZ nearest the foredune (i.e., *Croton*).

In previous research, the foredune zone and the EDZ have been clumped together as one community or the embryo dune environment has been considered uniform (Freestone and Nordstrom, 2001; Judd et al., 1977; Miller, 2015). However, this study shows that there are clear and distinct differences in the ecological community across the EDZ to the crest of the foredune, as evidenced by analysis of not only species presence but also species richness and species diversity. Differences in morphological evolution played a large role in the development of ecological zones within the embryo dune sub-environment. There was a clear transition in the composition of the ecological community from the foredune to the seaward edge of vegetation. *Croton*, *Panicum*, *Atriplex*, *Oenethera*, and *I. imperati* as well as two rare species *Chamaecrista spp*. and *Hydrocotile* occupied the FDS and rear of EDZ, which was the most stable, with little geomorphic change through time. *Sporobolus*, *Oenethera*, *I. imperati*, *Salicornia spp*., *I. pes-caprae*, and *Amaranthus* occupied the middle of the EDZ, which had a relatively stable substrate and experienced minor deposition through time. *Tidestromia*, *Sesuvium*, and *Amaranthus* occupied the leading edge of the EDZ together. These are the pioneer species that promote deposition of sand being transported from the beach by wind.

The interactions between ecology and geomorphology are such that it appears possible to predict community composition based on the location within the EDZ as well as trends in geomorphic change. In future studies, employment of a variety of instruments to measure environmental variables such as soil moisture, pH, organic content, and soil nutrients would allow for a more thorough analysis of the numerous variables that influence species zonation in embryo dunes and foredunes.

2.7 References

Anders, F.J., Leatherman, S.P., 1987. Effects of off-road vehicles on coastal foredunes at Fire Island, New York, USA. Environmental Management, 11(1), 45-52.

Arens, S.M., 1996. Patterns of sand transport on vegetated foredunes. Geomorphology, 17(4), 339-350.

Arens, S.M., Baas, A.C.W., Van Boxel, J.H., Kalkman, C., 2001. Influence of reed stem density on foredune development. Earth Surface Processes and Landforms, 26(11), 1161-1176.

Baas, A.C.W., Nield, J.M., 2007. Modelling vegetated dune landscapes. Geophysical Research Letters, 34(6).

Barbour, M.G., Burk, J.H., Pitts, W.D., 1987. Method of sampling the plant community, Terrestrial Plant Ecology. Benjamin/Cummings Publishing Co., Menlo Park, CA.

Bauer, B.O., Davidson-Arnott, R.G.D., 2003. A general framework for modeling sediment supply to coastal dunes including wind angle, beach geometry, and fetch effects. Geomorphology, 49(1-2), 89-108.

Bråkenhielm, S., Qinghong, L., 1995. Comparison of field methods in vegetation monitoring. Water, Air, & Soil Pollution, 79(1-4), 75-87.

Buckley, R., 1987. The effect of sparse vegetation on the transport of dune sand by wind. Nature, 325(6103), 426-428.

Burri, K., Gromke, C., Lehning, M., Graf, F., 2011. Aeolian sediment transport over vegetation canopies: A wind tunnel study with live plants. Aeolian Research, 3(2), 205-213.

Carls, E.G., Lonard, R.I., Fenn, D.B., 1991. Notes on the vegetation and flora of North Padre Island, Texas. The Southwestern Naturalist, 36(1), 121-125.

Carlsson, A.L.M., Bergfur, J., Milberg, P., 2005. Comparison of data from two vegetation monitoring methods in semi-natural grasslands. Environmental Monitoring and Assessment, 100(1-3), 235-248.

Dech, J.P., Maun, M.A., 2005. Zonation of vegetation along a burial gradient on the leeward slopes of Lake Huron sand dunes. Canadian Journal of Botany, 83, 227-236.

Delgado-Fernandez, I., 2011. Meso-scale modelling of aeolian sediment input to coastal dunes. Geomorphology, 130(3-4), 230-243.

Durán, O., Moore, L.J., 2013. Vegetation controls on the maximum size of coastal dunes. Proceedings of the National Academy of Sciences, 110(43), 17217-17222.

Freestone, A.L., Nordstrom, K.F., 2001. Early development of vegetation in restored dune plant microhabitats on a nourished beach at Ocean City, New Jersey. J Coast Conserv, 7(2), 105-116.

Gilbert, M., Pammenter, N., Ripley, B., 2008. The growth response of coastal dune species are determined by nutrient limitation and sand burial. Oecologia, 156, 169-178.

Godínez-Alvarez, H., Herrick, J.E., Mattocks, M., Toledo, D., Van Zee, J., 2009. Comparison of three vegetation monitoring methods: Their relative utility for ecological assessment and monitoring. Ecological Indicators, 9(5), 1001-1008.

Grootjans, A.P., Ernst, W.H.O., Stuyfzand, P.J., 1998. European dune slacks: strong interactions of biology, pedogenesis and hydrology. Trends in Ecology and Evolution, 13, 96-100.

Hernández-Cordero, A.I., Hernández-Calvento, L., Espino, E.P.-C., 2015. Relationship between vegetation dynamics and dune mobility in an arid transgressive coastal system, Maspalomas, Canary Islands. Geomorphology, 238(0), 160-176.

Hesse, P.P., Simpson, R.L., 2006. Variable vegetation cover and episodic sand movement on longitudinal desert sand dunes. Geomorphology 81, 276-291.

Hosier, P.E., Eaton, T.E., 1980. The impact of vehicles on dune and grassland vegetation on a south-eastern North Carolina barrier beach. Journal of Applied Ecology, 17(1), 173-182.

Houser, C., Ellis, J., 2013. Beach and dune interaction. In: J.F. Shroder (Ed.), Treatise on Geomorphology. Academic Press, San Diego, pp. 267-288.

Judd, F.W., Lonard, R.I., Sides, S.L., 1977. The vegetation of South Padre Island, Texas in relation to topography. The Southwestern Naturalist, 22(1), 31-48.

Kercher, S.M., Frieswyk, C.B., Zedler, J.B., 2003. Effects of sampling teams and estimation methods on the assessment of plant cover. Journal of Vegetation Science, 14(6), 899-906.

King, J., Nickling, W.G., Gillies, J.A., 2005. Representation of vegetation and other nonerodible elements in aeolian shear stress partitioning models for predicting transport threshold. Journal of Geophysical Research-Earth Surface, 110(F4).

Krebs, C.J., 1972. Ecology. The Experimental Analysis of Distribution and Abundance. . Harper and Row, New York.

Kuriyama, Y., Mochizuki, N., Nakashima, T., 2005. Influence of vegetation on aeolian sand transport rate from a backshore to a foredune at Hasaki, Japan. Sedimentology, 52(5), 1123-1132.

Lubke, R.A., 2004. Vegetation dynamics and succession on sand dunes of the eastern coasts of Africa. In: M.L. Martínez, N. Psuty (Eds.), Coastal Dunes. Ecological Studies. Springer Berlin Heidelberg, pp. 67-84.

Luna, M.C.d.M., Parteli, E.J.R., Duran, O., Herrmann, H.J., 2011. Model for the genesis of coastal dune fields with vegetation. Geomorphology, 129(3-4), 215-224.

Magurran, A.E., 1988. Ecological Diversity and its Measurement. Princeton University Press, Princeton, NJ.

Martinez, M.L., P., M.-C., Vazquez, G., 1997. Effects of disturbance by sand movement and inundation by water on tropical dunes vegetation dynamics. Canadian Journal of Botany, 75, 2005-2014.

Martinez, M.L., Vasquez, G., Sanchez, C.S., Colon, S., 2001. Spatial and temporal variability during primary succession on tropical coastal sand dunes. Journal of Vegetation Science, 12, 361-372.

Maun, M.A., 1998. Adaptations of plants to burial in coastal sand dunes. Canadian Journal of Botany, 76, 713-738.

Maun, M.A., 2009. The Biology of Coastal Sand Dunes. Oxford University Press, Oxford, UK.

McAtee, J.W., Drawe, D.L., 1980. Human impact on beach and foredune vegetation of North Padre Island, Texas. Environmental Management, 4(6), 527-538.

Miller, T.E., 2015. Effects of disturbance on vegetation by sand accretion and erosion across coastal dune habitats on a barrier island. AoB Plants.

Moreno-Casasola, P., 1986. Sand movement as a factor in the distribution of plant communities in a coastal dune system. Vegetatio, 65, 67-76.

Moreno-Casasola, P., Vasquez, G., 1999. Succession in tropical dune slacks after disturbance by water-table dynamics. Journal of Vegetation Science, 10, 515-524.

Oosting, H.J., 1945. Tolerance to salt spray of plants of coastal dunes. Ecology, 26(1), 85-89.

Oosting, H.J., Billings, W.D., 1942. Factors affecting vegetational zonation on coastal dunes. Ecology, 23(2), 131-142.

Psuty, N.P., 2004. The coastal foredune: a morphological basis for regional coastal dune development. In: M.L. Martínez, N. Psuty (Eds.), Coastal Dunes. Ecological Studies. Springer Berlin Heidelberg, pp. 11-27.

Pye, K., 1983. Coastal Dunes. Progress in Physical Geography, 7, 531-557.

Pye, K., 1992. Coastal dunes: form and process, edited by K. Nordstorm, N. Psuty and R. W. G. Carter, John Wiley & Sons, Chichester. No. of pages: xvii + 392. U.K. Price: $60. Hardback ISBN 0-471-91842-3. Earth Surface Processes and Landforms, 17(2), 201-201.

Rickard, C.A., McLachlan, A., Kerley, G.I.H., 1994. The effects of vehicular and pedestrian traffic on dune vegetation in South Africa. Ocean & Coastal Management, 23(3), 225-247.

Ruocco, M., Bertoni, D., Sarti, G., Ciccarelli, D., 2014. Mediterranean coastal dune systems: Which abiotic factors have the most influence on plant communities? Estuar. Coast. Shelf Sci., 149, 213-222.

Schlacher, T.A., Morrison, J.M., 2008. Beach disturbance caused by off-road vehicles (ORVs) on sandy shores: Relationship with traffic volumes and a new method to quantify impacts using image-based data acquisition and analysis. Marine Pollution Bulletin, 56(9), 1646-1649.

Schlacher, T.A., Thompson, L.M.C., 2008. Physical impacts caused by off-road vehicles to sandy beaches: spatial quantification of car tracks on an Australian barrier island. Journal of Coastal Research, 234-242.

Schmutz, P., 2007. Investigation of utility of delta-t thetaprobe for obtaining surficial moisture measurements on beaches. M.S., Louisiana State University, Baton Rouge, 114 pp.

Simpson, E.H., 1949. Measurement of diversity. Nature, 163, 688.

SRCC, 2015. Southern Regional Climate Center: 1981 - 2010 NCDC Monthly Normals.

Steudle, E., Zimmermann, U., Lüttge, U., 1977. Effect of turgor pressure and cell size on the wall elasticity of plant cells. Plant Physiology, 59(2), 285-289.

Thompson, L.C., Schlacher, T., 2008. Physical damage to coastal dunes and ecological impacts caused by vehicle tracks associated with beach camping on sandy shores: a case study from Fraser Island, Australia. J Coast Conserv, 12(2), 67-82.

Tobias, M.M., 2014. California foredune plant biogeomorphology. Physical Geography, 36(1), 19-33.

van der Maarel, E., 2005. Vegetation Ecology. Blackwell Publishing, Oxford.

Vanha-Majamaa, I., Salemaa, M., Tuominen, S., Mikkola, K., 2000. Digitized photographs in vegetation analysis - a comparison of cover estimates. Applied Vegetation Science, 3(1), 89-94.

Weise, B.R., White, W.A., 1980. Padre Island National Seashore: a guide to the geology, natural environments, and history of a Texas barrier island. Bureau of Economic Geology, Austin, Texas.

Zarnetske, P.L., Hacker, S.D., Seabloom, E.W., Ruggiero, P., Killian, J.R., Maddux, T.B., Cox, D., 2012. Biophysical feedback mediates effects of invasive grasses on coastal dune shape. Ecology, 93(6), 1439-1450.

Zuo, X., Zhao, H., Zhao, X., Guo, Y., Li, Y., Luo, Y., 2008. Plant distribution at the mobile dune scale and its relevance to soil properties and topographic features. Environmental Geology, 54, 1111-1120.

Chapter 3. The Response of Coastal Dune Vegetation Morphology to Fluctuating Wind Energy

3.1 Introduction

It is widely recognized that vegetation behaves as a roughness element that impedes fluid flow at the surface and alters sediment transport patterns (Arens et al., 2001; Baas and Nield, 2007; Brown et al., 2008; Buckley, 1987; Burri et al., 2011; Dallavis et al., 2011; Dijkstra and Uittenbogaard, 2010; Dong et al., 2008; Gillies et al., 2000; Gillies et al., 2002; Grant and Nickling, 1998; Kim and Stoesser, 2011; Kuriyama et al., 2005; Lancaster and Baas, 1998; Leenders et al., 2011; Leenders et al., 2007; Leonard and Croft, 2006; Leonard and Luther, 1995; Lightbody and Nepf, 2006; Luhar et al., 2008; Moller, 2006; Musick and Gillette, 1990; Nepf, 1999; Neumeier, 2007; Neumeier and Amos, 2006; Neumeier and Ciavola, 2004; Okin, 2008; Suter-Burri et al., 2013; Udo and Takewaka, 2007; Wolfe and Nickling, 1993; Woodhouse, 1978; Wyatt and Nickling, 1997; Zong and Nepf, 2010). However, as a result of the complexity of interactions between aeolian processes and biological elements, there remains a lack of quantitative understanding of the influence of vegetation on mechanics of wind flow in coastal embryo dunes and foredunes. The adjustment of wind flow patterns is interactive with vegetation morphology, which continuously varies as vegetation bends and flexes in response to wind forces. Furthermore, this dynamic response of vegetation morphology to wind velocity differs between species due to different blade/leaf size, shape, and rigidity, or ability to flex based on cell structure and water pressure within the blades/leaves/stems (de Langre, 2008; Nilsson et al., 1958; Pavlik, 1984; Steudle et al., 1977) as well as varying stem and blade density (Arens et al., 2001; Moller, 2006; Neumeier, 2005). The coastal embryo dune environment is host to a wide variety of species, from short grasses such as *Sporobolus virginicus,* to tall grasses such as *Uniola paniculata,* to vines

such as *Ipomoea sp.*, to prostrate shrubs such as *Sesuvium portulacastrum*, and to taller shrubs such as *Croton punctatus*.

The goal of this research was to quantify the effect of wind on the morphology of multiple vegetation morphology types commonly found in the embryo dune zone in terms of fluid-dynamically meaningful variables, such as plant area, pore area, and optical porosity. This research will improve understanding of the interactions between vegetative elements and aeolian processes, building a foundation for incorporating different plant types into models of the distribution of surface shear stress, which is the force driving sediment transport.

3.2 Background

As with all roughness elements, vegetation creates drag on fluid flow, altering the bed shear stress distribution and velocity (Gillies et al., 2002; Jia et al., 1998; Marshall, 1971; Wyatt and Nickling, 1997). The predominant models of the spatial distribution of shear stress around vegetation elements were developed using rigid elements such as solid rods and cylinders to represent vegetation (Brown et al., 2008; Gillette and Stockton, 1989; King et al., 2005; Marshall, 1971; Okin, 2008; Raupach, 1992; Raupach et al., 1993; Sutton and McKenna-Neuman, 2008). The model has been to apply to flow around rigid, desert shrub species (Dong et al., 2008; Gillies et al., 2000; Gillies et al., 2002; Leenders et al., 2011; Leenders et al., 2007; Musick and Gillette, 1990). However, a few studies have demonstrated that flexible grasses, which often dominate coastal dune environments (Martinez et al., 2001; Maun, 2009), produce significantly different flow dynamics than rigid shrub species (Burri et al., 2011; Gillies et al., 2002; Walter et al., 2012a; Walter et al., 2012b), because the morphologies of grasses and other natural vegetation are highly

dynamic in response to wind flow. Thus it is necessary to investigate the effect of wind on vegetation morphologies which are common within the embryo dune environment.

Frontal area and optical porosity are two morphological variables that have been used in previous investigations of the influence of vegetation on fluid dynamics (Gillies et al., 2002; Grant and Nickling, 1998; Guan et al., 2009; Jia et al., 1998; Kenney, 1987; Loeffler et al., 1992; Marshall, 1971; Wyatt and Nickling, 1997). In these studies, frontal area was defined as the width times the height of the object and was used to calculate roughness density, a variable used to model shear stress around roughness elements, the drag coefficient of roughness elements in the flow field, and the effect of vegetation on velocity profiles and turbulence (Brown et al., 2008; Crawley and Nickling, 2003; Gillies et al., 2000; Gillies et al., 2002; Gillies et al., 2007; Jia et al., 1998; King et al., 2005; Marshall, 1971; Okin, 2008; Raupach, 1992; Raupach et al., 1993; Walter et al., 2012a; Walter et al., 2012b; Wolfe and Nickling, 1996; Wyatt and Nickling, 1997). This approach is practical for solid objects, but is less appropriate for porous objects such as vegetation. It is also not appropriate for objects that do not have a standard and uniform geometry, such as vegetation. To determine frontal area, an image of a plant can be projected onto a two-dimensional surface. Because porous objects such as vegetation have aerodynamics porosity it was necessary to distinguish between area occupied by plant and area occupied by pores within the perimeter of the plant. In the present study, frontal area was subdivided into plant area (PLA) and pore area (POA).

Optical porosity (OP) has also been used to characterize the morphology of vegetation in relation to aeolian fluid flow (Gillies et al., 2002; Grant and Nickling, 1998; Kenney, 1987; Leenders et al., 2011; Loeffler et al., 1992; Musick et al., 1996). OP is defined as the proportion of pore area to total area (which is the sum of plant area and pore area). OP ranges from 0, when an object is completely solid, to 1, when an object is non-existent. Elements with lower OP have

greater flow decrease in their lee (Leenders et al., 2011; Loeffler et al., 1992) and are more effective at increasing the transportation threshold surrounding them than elements with higher OP (Musick et al., 1996). The OPs of grasses and shrubs behave differently in response to changes in wind velocity, so that OP of grasses decreases at higher velocity as plants bend and compress to become more streamlined and OP of shrubs increases at higher velocities as the flat surfaces of leaves align parallel to wind flow (Gillies et al., 2002). OP provides a useful improvement over pore area since it is not dependent on the plant size.

In previous research vegetation morphology has been measured from one direction only, the upwind or "front" direction. Analyzing vegetation morphology from only the front, or upwind perspective, to predict the effect of plants on flow disregards the three-dimensional nature of vegetation as well as wind direction variability. In Figure 3.1 the plant area from the front perspective of the two different plant distributions (A and B) is the same.

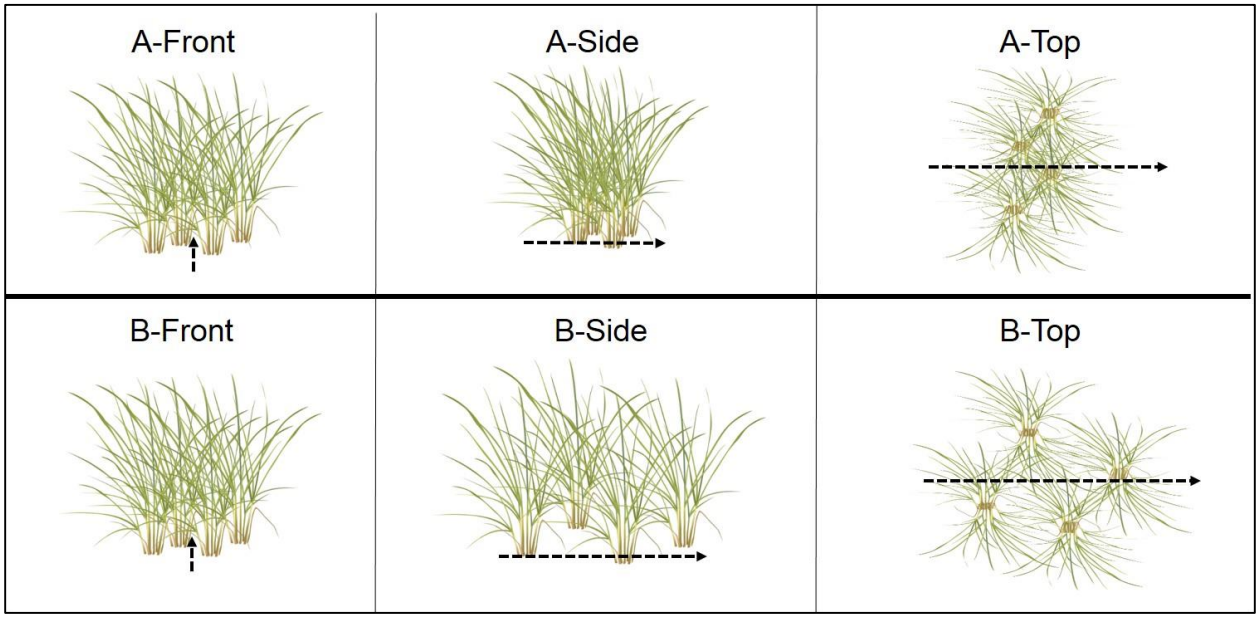

Figure 3.1. Front, side, and top views of two hypothetical vegetation spatial arrangements. Dashed black line with arrow indicates wind direction. The front view, used to determine optical porosity in previous studies, is equal. Side and top views reveal very different spatial arrangements that affect fluid flow for the two cases.

However, incorporation of side and top views in analysis would produce very different measures of morphology and aerodynamic roughness. Hence this study examined vegetation morphology in terms of PLA, POA, total area, and OP from three perspectives – upwind, perpendicular to the wind, and overhead. Total area from the front perspective only equates to the frontal area metric used in previous studies.

Research on flexible grasses in aquatic environments clearly shows significant interspecies differences in how grasses impact fluid dynamics and sediment transport rates (Leonard and Croft, 2006; Leonard and Luther, 1995; Luhar et al., 2008; Moller, 2006; Nepf, 1999; Neumeier, 2005; Neumeier, 2007; Neumeier and Ciavola, 2004). However, differences in the fluid-dynamic influence of different species in aeolian environments has heretofore been limited to non-coastal species such as shrubs and ornamental grasses (Burri et al., 2011; Gillies et al., 2002; Loeffler et al., 1992; Walter et al., 2012a). It is therefore necessary to investigate the physical dynamics of different species in the embryo dune environment in order to develop a framework to improve the ability to model aeolian fluid flow around vegetation and resulting dune formation and evolution in the embryo dune environment and thus to improve the effectiveness of dune restoration projects. Dune restoration projects typically employ a single species, often whatever is native or indigenous to the area and perceived to be the most effective at trapping sediment (Freestone and Nordstrom, 2001; Nordstrom, 2008; Woodhouse, 1978). Inclusion of only one species has been the default for decades, without any explicit scientific reasoning for not including more than one species. However, natural dune environments are commonly occupied by 5 to 25 different species indigenous to the embryo and foredune zones (Agır et al., 2014; Barbour et al., 1985; Carls et al., 1991; Cooper, 1936; Freestone and Nordstrom, 2001; Judd et al., 1977; Lubke, 2004; Moreno-Casasola, 1986; Moreno-Casasola and Espejel, 1986; Moreno-Casasola and Vasquez, 1999;

Tobias, 2014), and each will somewhat function differently in trapping and retaining sand (García-Mora et al., 1999; Novo et al., 2004; Stallins, 2003; Tobias, 2014). Hence, this study examined the effects of wind on plant morphology for specimens with three different morphology types – tall grass, short grass, and shrub. These vegetation morphologies were chosen as representative of plant morphologies commonly found at the seaward edge of the coastal embryo dunes in a wide range of geographic locations.

3.3 Methodology

Field research was conducted at Padre Island National Seashore (PINS), Texas. PINS is located in the northwestern portion of the Gulf of Mexico, approximately 160 km from the United States – Mexico border (Figure 3.2). In the northern portion of the park where the study sites were located, there is a 7.25 km section of beach on which driving is prohibited. The beach at PINS is dissipative and the foredune ridge is continuous, with very few and minor blowouts.

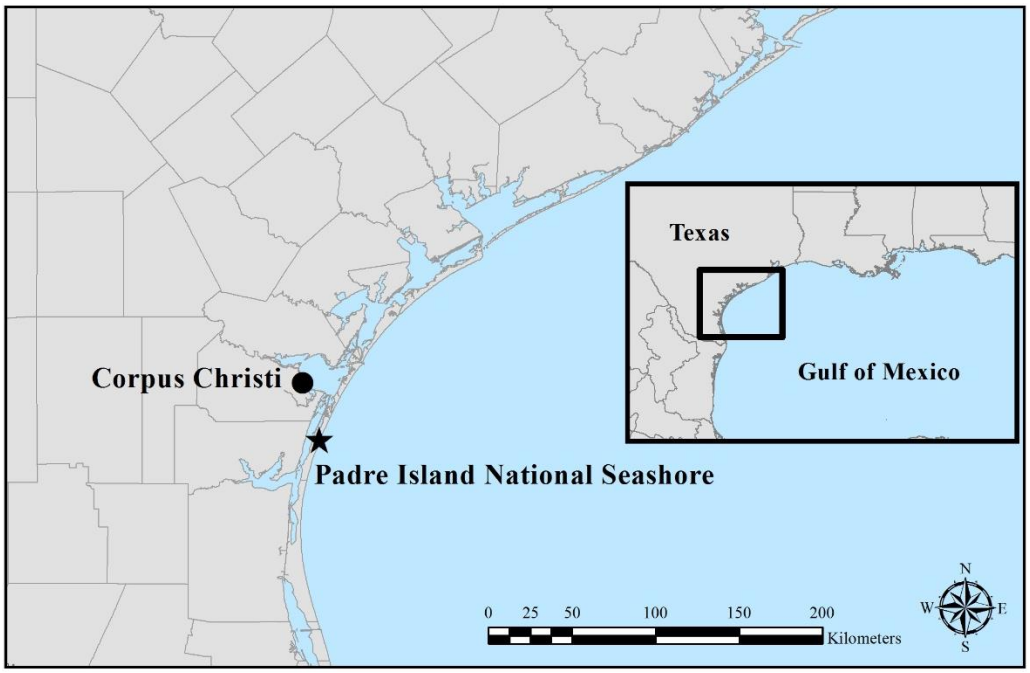

Figure 3.2. Location of Padre Island National Seashore.

Shoreward of the foredune ridge is a very wide, partially vegetated, hummocky embryo dune zone that ranges from about 30 to 40 m in width (Figure 3.3). The plants examined were at the shoreward edge of this embryo dune zone. Sediment is predominantly very-well sorted, fine to very-fine quartz sand with a mean diameter of about 0.15 mm (Schmutz, 2007). PINS is located in a subtropical and semi-arid climate region. The average temperature in winter is 14°C, in spring is 21°C, in summer is 28°C, and in fall is 23°C; while the mean annual rainfall is 81 cm (SRCC, 2015). During summer, when the field research was conducted, winds are commonly generated by sea breeze conditions, so that the dominant wind direction is from the southeast (Weise and White, 1980). During the winter, passage of cold polar frontal systems through the area generates northerly winds (Weise and White, 1980).

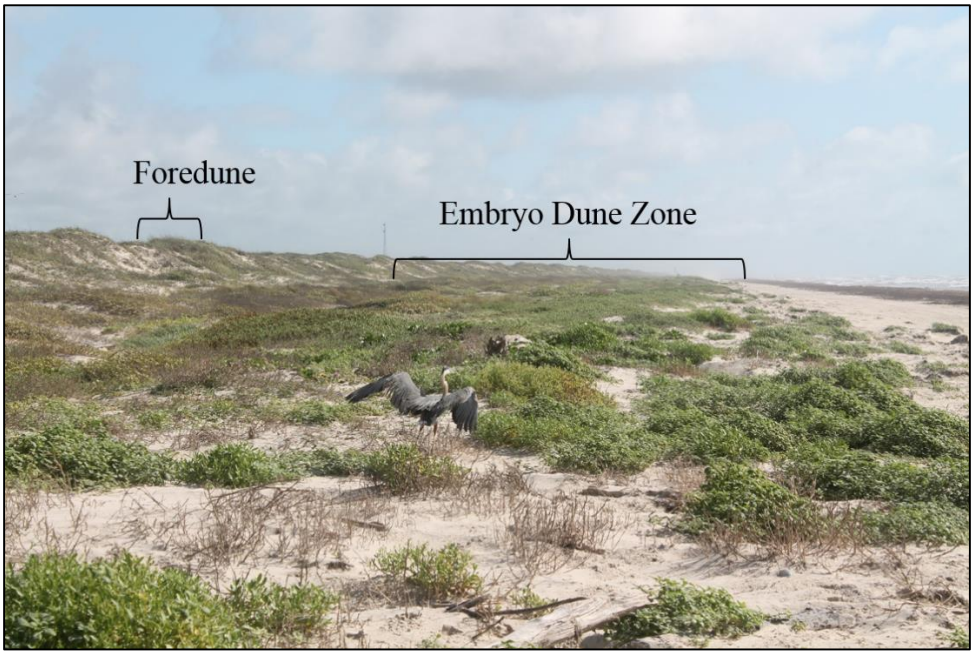

Figure 3.3. Image of the study site from the crest of the foredune, looking to the northeast so that the Gulf of Mexico is to the right.

3.3.1 Data Collection

Two isolated clumps of each vegetation morphology type were studied, creating a database that comprised of six specimens - two specimens of short grass, *Sporobolus virginicus* (Figure 3.4A; one in each of 2013 and 2014), two specimens of tall grass, *Uniola paniculata* (Figure 3.4B; one in each of 2013 and 2014), and two specimens of shrub (*Tidestromia lanuginosa (*Figure 3.4C) *in* 2013, and *Amaranthus greggii (*Figure 3.4D) *in* 2014). A suitable specimen of *Tidestromia* was not present at the seaward edge of the embryo dune zone in 2014 so a specimen of *Amaranthus*, which has a similar growth habit to *Tidestromia*, was chosen. The shrubs and tall grasses existed as discrete clumps naturally. The short grass occurred in large extensive mats and was trimmed down to roughly the same footprint as the tall grasses and shrubs.

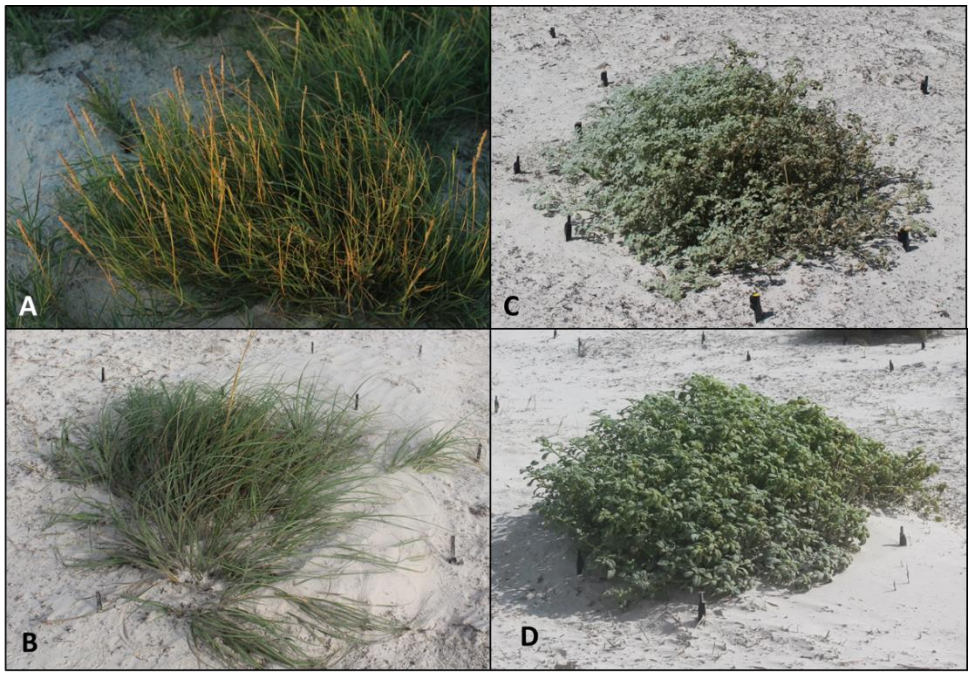

Figure 3.4. Vegetation observed – A) *Sporobolus virginicus*, B) *Uniola paniculata*, and C) *Tidestromia lanuginosa*, and D) *Amaranthus greggii*.

Digital images of isolated specimens were obtained during either three observations in 2013 or five observations in 2014. During an observation, images were collected from three different perspectives – upwind of the stand (“front”), from the side of the stand perpendicular to the front, and from overhead of the stand (“top”) (Figure 3.5).

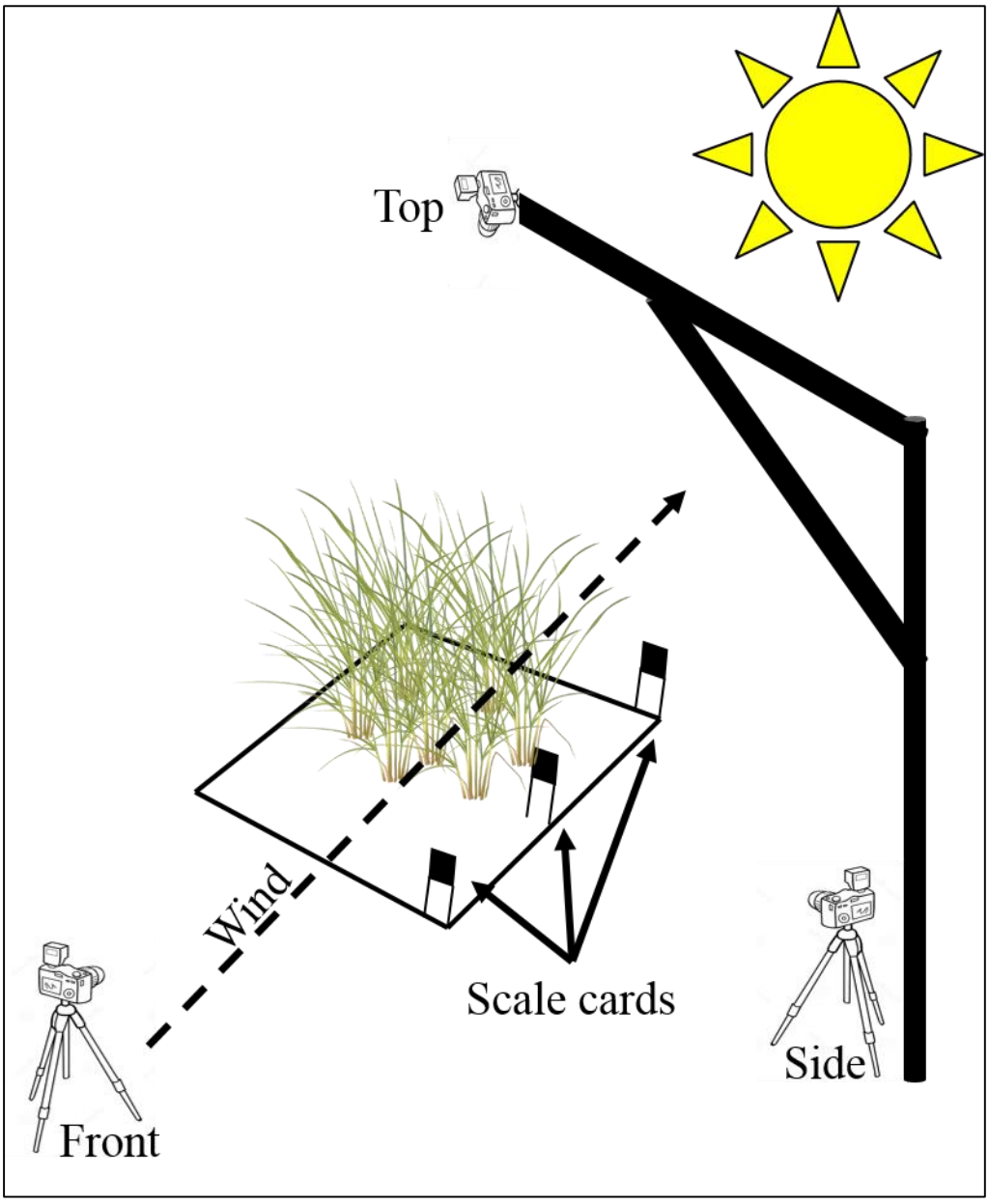

Figure 3.5. Image depicting the placement of the camera in the front, side, and top perspectives.

For the front and side images the camera was placed on a tripod. The camera sensor was horizontally positioned 3 m from the center of the plant clump, and vertically positioned so that it was level with the middle of the mass of the clump. For overhead imagery the camera was placed on a boom made of PVC pipe so that the sensor was located at 4.5 m above the ground surface and directly above the plant. Images were collected in JPEG format using a Canon Rebel T3 at the highest resolution possible for the camera, 4272 x 2848 pixels for all perspectives except the top perspective in 2013. In 2013 the overhead images were obtained in the MOV format (1280 x 720 pixels) as the equipment was not available to take still images from overhead at that time.

From each perspective, 13 total images were collected during a one-minute period at five second intervals in order to encapsulate the natural variability of vegetation morphology for a given wind regime. In order to analyze the effect of velocity on vegetation morphology, wind velocities were measured contemporaneously with image collection. Wind velocities were measured at 1 Hz using RM Young Gill 3-cup anemometers at 0.25 m, 0.75 m, and 1.5 m height on a mast located on the open beach five to eight m upwind of each plant clump on the un-vegetated backbeach. Images were processed in a GIS to determine PLA, POA, total area, and OP for each image.

3.3.2 Image Processing

Image processing was performed in ERDAS Imagine 2011 and 2013 and in ArcGIS 10.1 and 10.2.2. The following steps were required in order to calculate the plant morphology variables: 1) pixel size calculation; 2) cropping; 3) iterative self-organizing data (i.e., isodata) unsupervised classification; 4) reclassification; and 5) classification accuracy assessment.

In order to calculate pixel area of each set of images, three "scale cards" (i.e., black squares of dimension 0.1 m x 0.1 m) were placed within the frame of each image – one at the front of the plant mass, one in the middle of the plant mass, and one at the rear of the plant mass (see Figure 3.5). For the overhead perspective, the scale blocks were located on the ground surface. Pixel area was determined by measuring the number of pixels occupied by the scale blocks in the image and then dividing the actual area of each block (0.01 m^2) by the number of pixels representing that block. In order to account for image depth and distortion in pixel resolution from the front of the plant to the rear of the plant, the calculated pixel area at the front, middle, and back of the plant were averaged, based on the fact that the majority of the vegetation mass was located near the middle of the field of depth. Pixel area ranged from 0.5 to 0.6 mm^2 in all front and side images, from 0.9-1.0 mm^2 for 2014 top images, and 10-11 mm^2 for 2013 top images. Each image was then cropped at the outer perimeter of the vegetation (Figure 3.6).

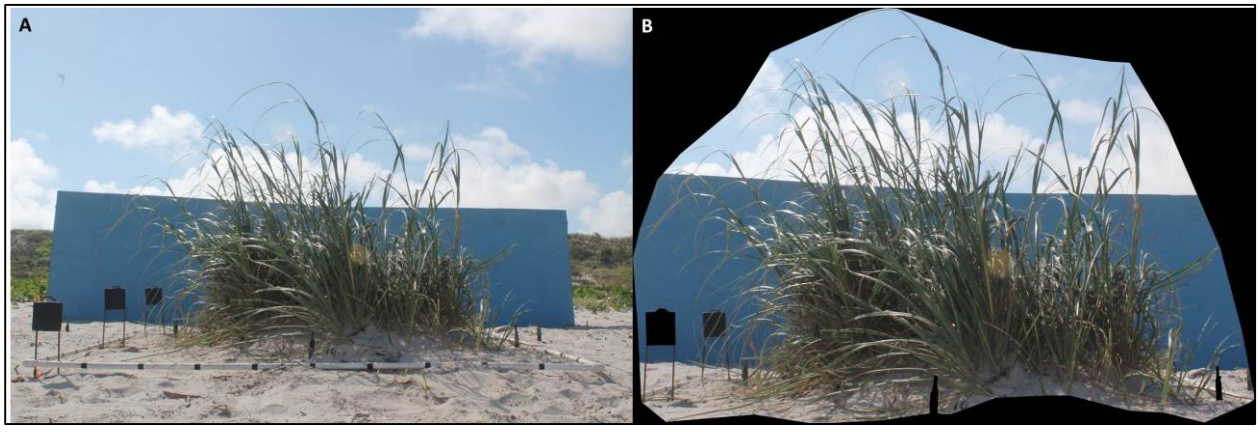

Figure 3.6. Image of a clump of *Uniola paniculata* before cropping (A) and after cropping (B).

In order to determine PLA and POA in each image, isodata unsupervised classifications were performed. The isodata analysis technique uses an algorithm that splits and merges clusters of pixels based on their RGB values. In isodata classification multiple iterations are performed to

find the best fit for the data. The isodata approach is very effective at identifying spectral clusters specific to the data being analyzed (Sciandrello et al., 2015). It also has the advantage of requiring little preliminary knowledge of the data (i.e., there is no requirement to produce individual histograms for each image to model the spectral signature of the images). Thus, this method of classification is efficient for data such as this one consisting of 936 images and including multiple image sets with different spectral signatures.

The timing of imagery collection varied throughout the day and thus the spectral signature of each image set varied based on lighting and exposure so that clustering of pixels was unique and different for each image set. All images within a given set had similar spectral properties because they were taken within a one-minute time period without sensor movement, so that it was appropriate to apply the spectral signature generated by isodata classification of the first image to the other twelve images comprising the set. Within images in a set, differences in lighting were caused by overexposure, high albedo caused by reflection of the sun by grass blades, and shadow effects occurring in early morning and late afternoon. For example, pixels in shadows on the sand on one side of the image were placed in the same class as pixels representing brightly lit vegetation on the other side of the image. As a result of this misclassification in the original image, several sets of images were subset for classification and outputs were combined for analysis.

Using the signature file created by the isodata classification, a maximum likelihood classification was performed on the remaining 12 images in the set. Output classes were visually scrutinized and re-classed as plant (1) or non-plant (0). The total number of pixels in each category was determined and converted to an area using the pixel area calculated in the first step of image processing. PLA and POA were direct outputs from the image classification. Total area was calculated as the sum of PLA and POA. OP was calculated as the ratio of POA to total area.

3.3.4 Accuracy Assessment

Accuracy of classification schemes was assessed on a representative image from each image set in order to determine how well classifications distinguished between plant and non-plant pixels in images. To compare classified images to unclassified images, error matrices were compiled from random sets of 100 points. These points were individually evaluated in both unclassified and classified images as either falling on plant- or non-plant-occupied pixels. From these error matrices, overall accuracy and Cohen's kappa coefficients were calculated. Overall accuracy is the percentage of points which were classified in the correct class. Cohen's kappa coefficient indicates how well the classification process produced results compared to random chance. Kappa ranges from -1, indicating perfect disagreement below chance, to +1, indicating perfect agreement above chance. A kappa value of 0 indicates agreement equal to chance. Results from the accuracy assessment are listed in Table 3.2. In general, the classifications performed well, with an average overall accuracy of 93% and a kappa of 0.813 for all 72 classification schemes, signifying that the classifications performed on average 81.3% better than if they occurred merely by chance.

Table 3.2. Overall accuracy percentage and Cohen's kappa coefficient for all image sets.

perspective	image set	*Uniola* 2013		*Sporobolus* 2013		*Tidestromia* 2013	
		overall accuracy	kappa	overall accuracy	kappa	overall accuracy	kappa
front	high	85	0.680	94	0.637	92	0.777
side	high	92	0.843	90	0.732	93	0.673
top	high	89	0.783	93	0.775	92	0.786
front	low	91	0.808	92	0.758	95	0.836
side	low	90	0.788	96	0.882	97	0.911
top	low	96	0.925	86	0.421	83	0.465
front	middle	84	0.664	91	0.746	92	0.781
side	middle	89	0.768	97	0.913	96	0.806
top	middle	94	0.885	91	0.634	88	0.642

Table 3.2 continued. Overall accuracy percentage and Cohen's kappa coefficient for all image sets.

perspective	image set	*Uniola* 2014		*Sporobolus* 2014		*Amaranthus* 2014	
		overall accuracy	kappa	overall accuracy	kappa	overall accuracy	kappa
front	a	95	0.891	96	1.898	97	0.852
side	a	92	0.838	96	0.906	93	0.689
top	a	95	0.898	95	0.897	95	0.825
front	b	92	0.837	93	0.877	95	0.807
side	b	91	0.828	84	0.630	96	0.853
top	b	91	0.800	94	0.873	84	0.493
front	c	88	0.762	98	0.948	94	0.813
side	c	97	0.935	94	0.864	99	0.966
top	c	93	0.854	87	0.735	94	0.821
front	d	92	0.836	88	0.745	95	0.839
side	d	97	0.946	93	0.808	95	0.849
top	d	88	0.771	98	0.958	88	0.368
front	e	95	0.895	95	0.869	97	0.851
side	e	93	0.854	93	0.802	95	0.855
top	e	92	0.826	93	0.841	96	0.898

3.4 Results

Three sets of imagery and wind velocity data were collected for each of the three specimens in 2013, and 5 sets were collected for each of the three specimens in 2014. In 2013 velocities at 0.25 m height ranged from 2.5 to 7.2 m/s during data collection, while in 2014 velocities at 0.25 m height ranged from 1. 95 to 5.7 m/s (Table 3.3). No data were collected at zero wind flow because calm conditions did not occur during the study period. However, 2 m/s can be considered calm conditions in the present context because no sediment transport occurred when the velocity at 0.25 m height was 2 m/s.

Table 3.3. One-minute average of velocity at anemometers during image collection.

perspective	image set	*Uniola* 2013			*Sporobolus* 2013			*Tidestromia* 2013		
		0.25 m	0.75 m	1.5 m	0.25 m	0.75 m	1.5 m	0.25 m	0.75 m	1.5 m
front	high	6.56	8.04	9.13	2.64	6.80	7.69	7.06	8.00	9.00
side	high	7.10	8.65	10.09	2.48	6.95	7.85	7.24	8.52	9.60
top	high	6.94	8.52	9.70	6.83	7.78	8.65	6.86	7.97	9.00
front	low	3.27	4.18	4.58	3.37	4.15	4.60	4.05	4.82	5.30
side	low	2.82	3.63	4.03	3.11	3.83	4.25	3.31	4.19	4.72
top	low	2.97	3.71	4.09	3.17	3.88	4.26	3.17	3.97	4.37
front	middle	4.84	6.09	7.02	5.44	6.64	7.41	5.44	6.60	7.18
side	middle	5.19	6.51	7.28	5.54	6.66	7.32	4.82	5.91	6.62
top	middle	4.93	6.31	7.11	5.42	6.51	7.37	5.43	6.55	7.31
perspective	image set	*Uniola* 2014			*Sporobolus* 2014			*Amaranthus* 2014		
		0.25 m	0.75 m	1.5 m	0.25 m	0.75 m	1.5 m	0.25 m	0.75 m	1.5 m
front	a	3.48	3.95	4.69	2.05	2.28	2.67	2.22	2.58	3.03
side	a	3.39	3.73	4.45	2.66	2.98	3.39	2.07	2.35	2.77
top	a	3.41	3.80	4.45	2.66	2.91	3.26	2.06	2.32	2.65
front	b	4.02	4.66	5.44	3.16	3.69	4.33	3.20	3.69	4.08
side	b	3.85	4.26	5.07	3.08	3.61	4.11	3.31	3.95	4.43
top	b	3.97	4.44	5.09	3.46	4.08	4.68	3.17	3.60	4.22
front	c	1.89	2.13	2.53	4.16	4.96	5.59	4.58	5.42	6.26
side	c	2.18	2.52	2.96	4.91	5.90	6.70	4.51	5.08	5.70
top	c	1.88	2.13	2.57	4.46	5.40	6.08	4.82	5.52	6.41
front	d	2.32	2.65	3.16	5.00	5.86	6.56	1.90	2.16	2.49
side	d	2.48	2.77	3.22	4.79	5.69	6.33	2.00	2.23	2.48
top	d	2.51	2.80	3.31	4.51	5.36	6.10	1.85	2.03	2.29
front	e	3.90	4.40	5.06	4.85	5.72	6.53	5.22	5.92	6.64
side	e	3.90	4.42	5.07	5.68	6.70	7.55	5.10	5.78	6.63
top	e	4.04	4.58	5.36	4.67	5.36	6.05	5.37	6.28	7.15

3.4.1 Wind Velocity Assessment

The purpose of this study was to determine whether the vegetation morphology parameters examined herein correlated to wind velocity. In order to evaluate the relationships between vegetation morphology parameters and wind velocity, it was necessary to determine which of the

available wind velocity measures to use. There were three options from which to choose. Average velocity was calculated for anemometers at all three heights on the anemometer mast. Average velocity was the simplest measure of wind and hence preferred. However, instantaneous velocity, which was the velocity at the moment of image capture, might improve the strength of correlations. Time-lagged velocities, which account for the time required for wind to travel the distance between the anemometer mast and vegetation, might also improve the strength of correlations. The velocity measured at one-second before image collection was used for this dataset because the mast was located at a distance of five to eight m upwind of vegetation.

A correlation analysis was performed in SAS between the three different velocity measures at 0.25 m, 0.75 m, and 1.5 m heights on the anemometer mast. There was no statistical difference between average velocity and instantaneous velocity ($R=0.989$, $p<0.0001$), between average velocity and time-lagged velocity ($R=0.970$, $p<0.0001$), or between instantaneous and time-lagged velocity ($R=0.971$, $p<0.0001$). The fact that Pearson correlation coefficients exceed 0.97 means that these measures are highly correlated to each other and the use of any one of these measures in analysis would produce the same results as the other two. Therefore, the average velocity was utilized to determine the effect of wind on vegetation morphology as it inherently incorporates the natural variability of wind.

Next, a representative anemometer elevation had to be chosen. A correlation analysis was performed in SAS between average velocities at the three anemometer heights. Average velocities at 0.25 m, 0.75 m, and 1.5 m height on the anemometer mast were highly correlated to each other (0.25 m to 0.75 m: $R=0.929$, $p<0.0001$; 0.25 m to 1.5 m: $R=0.929$, $p<0.0001$; 0.75 m to 1.5m: $R=0.998$, $p<0.0001$). As a result, velocity at any height produced the same results as the other two heights in further statistical analysis. The short grass grew no taller than 0.25 m and the shrubs no

taller than 0.5 m, while the tall grasses grew to 0.75-1 m height. Because a majority of the plant mass was below the 0.75 m anemometer, velocity recorded by the anemometer at 0.25 m height was selected for use in further analysis.

3.4.2 Wind Velocity and Plant Morphology

For the purpose of determining the relationships between vegetation morphology and velocity general linear mixed models (Proc Glimmix) were used in SAS. The use of Proc Glimmix for this data is appropriate because the data are unbalanced across specimen (66% more observations for specimens in 2014 than 2013), and because a mixed model is most appropriate when there are both random effects (specimen, velocity), which are the source of variability in the data, and fixed effects (perspective, morphology type), which are controlled in the experiment.

3.4.2.3 Wind Velocity and Total Area

The first step was to determine differences in total area between specimens of the same morphology type from the different perspectives. Total area from the front perspective was the equivalent of the frontal area variable used in other studies. Total area from the side and top perspectives were new measures that provided a more three-dimensional look at plant morphology. A general linear mixed model was used to determine the effect of type*perspective, the independent interactive variable, on total area, the dependent variable. There were significant differences in the total area of the different vegetation morphology types based on the perspective from which it was measured ($p<0.0001$). The results are shown in Table 3.4.

Table 3.4. Average total area (m^2) by type and perspective.

	Front	Side	Top
Shrub	0.72	0.66	1.98
Short grass	0.73	0.76	3.53
Tall grass	1.51	1.89	3.52

Shrub specimens were nearly the same size as the short grass specimens from the front and side perspectives and substantially smaller than short grass and tall grass specimens from the top perspectives. Tall grass specimens were roughly twice the size of the shrub and short grass specimens from front and side perspectives. The larger plant area from the front and side perspectives of the tall grass specimens indicates that the tall grass occupied the greatest volume, extending higher into the boundary layer and presenting a greater obstruction to flow. The short grass, which was trimmed to match the size of the tall grass and fit within a 2 m by 2 m quadrat, had a large total area from the top perspective because it naturally grows in dense blankets covering the sand.

The next objective was to determine the change in total area as function of wind velocity. For this purpose, a general linear mixed model tested the effects of the following independent variables on the dependent variable total area: velocity*perspective, velocity*type, and velocity*type*perspective. The * signifies that the terms were interactive. Only the effect of velocity by perspective on total area was significant ($p=0.0004$). For all morphology types, total area from the front and side perspectives increased as a function of velocity (0.051 $m^2/m/s$ for front; 0.001 $m^2/m/s$ from side) while total area from the top perspective decreased as a function of wind velocity (-0.085 $m^2/m/s$). Changes in total area as a function of wind velocity indicate that live plants indeed change shape in response to increasing wind velocity. From the front perspective, total area increased when blades at the top of the plants were pushed down while blades at side of the plants were pushed out laterally by increased turbulence that accompanies

higher velocities. Walter et al. (2012a) observed the same phenomenon in their study of *Lolium perenne*, a non-native perennial rye-grass used for lawns and pastures, in a wind tunnel. Minor increases in side total area occurred when blades at the front of the plants were pushed into the main mass of the plants but blades at the rear of the plants were pushed down and out to extend behind the main mass of the plants. From the top perspective, total area decreased because blades at the front of the plants bent toward the main mass of the plants, resulting in overlap of blades. Any extension of blades at the rear or side of the plants did not increase the area here substantially because blades overlapped each other from the top perspective.

3.4.2.2 Wind Velocity and Plant Area

The next step was to distinguish between the plant area and pore area within the total area and to determine how these differ for the different morphology types. Plant area is the area occupied by the plant within the perimeter of the plant. It does not include pore space. A general linear mixed model in SAS was used to determine differences in PLA between morphology types based on perspective. Plant area was significantly different between the tall grasses, the short grasses, and the shrubs, depending on the perspective from which it was measured ($p<0.0001$). Results are shown in Table 3.5.

Table 3.5. Average PLA (m^2) by type and perspective.

	Front	Side	Top
Shrub	0.61	0.55	1.59
Short grass	0.55	0.59	2.51
Tall grass	0.76	0.99	1.94

The shrub specimens and the short grass specimens occupied roughly the same area from the front and side perspectives while the tall grass specimens were larger from front and side

perspectives. The shrubs were substantially smaller than the short grass specimens and slightly smaller than the tall grass specimens from the top perspective. Differences in PLA between morphology types were similar to total area for each specimen, in that the tall grass had the highest PLA from the front and side perspectives, signifying that this morphology type presents a greater obstruction to wind flow than the other morphology types. The short grass had a larger plant area from the top perspective due to its natural growth habit, which was low and dense.

Next to be examined was the relationship between velocity and PLA. A general linear mixed model tested the effects of the following independent variables on the dependent variable PLA: velocity*perspective, velocity*type, and velocity*type*perspective. The * signifies that the terms were interactive. Only the effect of velocity by perspective on PLA was significant ($p=0.0104$). For all morphology types, both front PLA and side PLA increased as a function of wind velocity (0.038 $m^2/m/s$ for front; 0.002 $m^2/m/s$ from side) while top PLA decreased as a function of wind velocity (-0.045 $m^2/m/s$). Changes in PLA as a function of wind velocity were similar to changes in total area. PLA from the front increased when blades at the top of the plants bent to become more streamlined while blades extended to the side as more turbulence affected the plants at higher velocity. From the side perspective, decreases in PLA at the front of the plant as a result of blades being pushed toward the main mass of the plant were offset by extension of blades downwind of the plant. Plant area decreased from the top perspective as blades on all sides of the plant realigned parallel to the wind and overlapped the main mass of the plant.

3.4.2.3 Wind Velocity and Pore Area

Pore area is a measure the available space through which wind can flow within the structure of the plant. A general linear mixed model was used to determine the effect of type*perspective,

the independent interactive variable, on the dependent variable POA. There were significant differences in the amount of pore area of the different vegetation morphology types based on the perspective (p=0.0002). The results are shown in Table 3.6.

Table 3.6. Average POA (m^2) by type and perspective.

	Front	Side	Top
Shrub	0.11	0.11	0.39
Short grass	0.18	0.17	1.02
Tall grass	0.75	0.90	1.59

Shrub specimens by far had the least amount of pore area from all perspectives while tall grass specimens were the most porous. The short grass specimens had slightly larger POA than shrub specimens from the front and side perspective and much greater POA than shrub specimens from the top perspective. Shrub specimens were denser than any other species, with the lower pore area than short grass specimens, which had less pore area than tall grass specimens. This finding is significant because plants which are denser are more capable of extracting energy from the fluid flow, promoting deposition and reducing erosion, than plants that naturally are less dense (Arens et al., 2001; Bouma et al., 2009; Gillies et al., 2002; Leonard and Luther, 1995; Neumeier, 2005; Neumeier and Amos, 2006).

A general linear mixed model was used to test the effects of the following independent variables on the dependent variable POA: velocity, velocity*perspective, velocity*type, and velocity*type*perspective. The * signifies that the terms were interactive. None of these independent variables had a significant effect on POA (p=0.4709, p=0.7950, p=0.2562, and p=0.8294, respectively). It was expected that pore area would decrease as plants bent and became more streamlined in higher velocities. Instead, there was not a significant relationship between

POA and wind velocity. This was likely a result of changes in the configuration of three-dimensional pore space not being detectable on two-dimensional projected images because of optical overlap of blades and leaves. Instead, POA measured pore area around the outer perimeter of vegetation.

3.4.2.4 Wind Velocity and Optical Porosity

The final step was to analyze the differences between the OP of different morphology types as well as the effect of velocity on OP. Because it is a ratio, OP reduced the emphasis on the actual size of the specimens chosen for examination. A general linear mixed model was used to determine the effect of morphology type on OP. There were significant differences in OP between the different morphology types ($p=0.0222$). Shrub specimens had a lower optical porosity (average=0.17) than short grass specimens (average=0.26) and tall grass specimens (average=0.46). The tall grass had nearly twice the OP of the short grass, which in turn had nearly twice the OP of the shrubs. There was no significant difference in OP of the different morphology types from the different perspectives ($p=0.2249$). These findings reinforce those related to POA, wherein the shrub was found to be denser than the short grass, with the tall grass as the least dense. The tall grass specimens had long blades which spread out away from the main mass of the plant, resulting in large pore spaces near the periphery of the plants.

A general linear mixed model was used to test the effects of the following independent variables on the dependent variable OP: velocity*perspective, velocity*type, and velocity*type*perspective. The * signifies that the terms were interactive. None of these independent variables had a significant effect on OP ($p=0.4145$, $p=0.4086$, $p=0.2561$, and $p=0.2991$, respectively). Again, it was expected that OP would decrease as velocity increased,

causing plants to bend and become more aerodynamic. However, this phenomenon was not observed. OP does not correspond directly to aerodynamic porosity. Pore space was visible in imagery, but was not distinguishable in classification due to visual overlap of blades and leaves in a two-dimensional projected image.

3.5 Summary and Conclusions

The first goal of this study was to evaluate several measures of vegetation morphology and to quantify differences between vegetation morphology types. Three types of vegetation morphology common to coastal dune systems were examined herein – shrub, short grass, and tall grass – in terms of their total area, plant area, pore area, and optical porosity.

There were significant differences in the morphology of the different types of vegetation. The tall grasses were the largest in terms of total area, plant area, and pore area. Shrubs had the smallest total area, plant area, and pore area from all perspectives. Short grasses fell in the middle of the spectrum. The variation in total area, plant area, and pore area between morphology types was dependent upon the individual specimens chosen for examination. To account for natural variability in specimen size, OP, which normalized the amount of pore area by the total area of the vegetation, was also evaluated. Unlike plant area and pore area, which varied significantly for each morphology type dependent upon the direction from which images were taken, OP was not different from the different perspectives of the same morphology type. It did however, differ between morphology types. The shrubs had the lowest OP The short grasses had roughly twice the OP of the shrubs, and the tall grasses had roughly twice the OP of the short grasses. Loeffler et al. (1992) and Gillies et al. (2002) found also found differences in OP between species, emphasizing the need to investigate species-specific differences in response to wind velocity. OP can be used

to predict the degree of sheltering which vegetation provides against erosion (Leenders et al., 2011; Loeffler et al., 1992; Musick et al., 1996). Objects with higher OPs shelter downstream areas to a lesser degree and therefore greater erosion or less deposition occurs downwind of more porous objects.

The second objective of this study was to quantify the response of different vegetation morphologies to wind velocity in an attempt to develop a more appropriate method for incorporating roughness object size into shear stress partitioning models for use in the coastal embryo dune environment, where roughness objects come in a wide range of sizes and growth habits. This research found that total area and plant area of live plants from all perspectives indeed change as a function of wind velocity as blades of live grass and shrubs bend and flex in response to increasing fluid forces on them. Changes in plant area and total area as a function of wind velocity were the same magnitude for all vegetation morphology types. Either the method for measuring plant response to wind velocity is inappropriate or too little data were collected to substantiate any relationship between velocity and plant area or total area based on morphology type. In the future it will be necessary to expand the data set by collecting imagery from a greater number of specimens of each type of vegetation morphology at a larger sample of wind velocities.

In the range of velocities observed in this study, total area from the front increased as a function of wind velocity. In contrast, Walter et al. (2012b) found that total area from the front and roughness density decrease with increasing wind velocity. As Walter et al. (2012b) further explained, frontal area increased at lower velocities as plants flutter and expand, but decreased at higher velocities. The natural range of wind observed in the field during this study did not reach the velocities that Walter et al. (2012b) generated in their wind tunnel study.

Pore area and OP did not change as a function of wind velocity. These two measures of pore space are inappropriate for quantification of the response of vegetation to wind velocity because they do not equate to three-dimensional aerodynamic porosity. Three-dimensional pore spaces "disappear" in two-dimensional projections of vegetation. In the future, it is worth exploring the applicability of a relatively new technology, terrestrial laser scanning, to produce a three-dimensional digital model of vegetation morphology in order to assess the effect of velocity on aerodynamic porosity.

In conclusion, findings indicate that natural growth habits, in terms of blade density and height, of the various species in the coastal embryo dune zone may be more important in relation to their ability to influence and alter aeolian processes than previous research has indicated. This research emphasizes the importance of incorporating the three-dimensional response of vegetation, which was also suggested by Musick et al. (1996) in their investigation of the influence of vegetation structure on saltation. Furthermore, this research emphasizes the need to develop a more appropriate measure of aerodynamic porosity. The effect of velocity on vegetation porosity is still unclear, and so it remains difficult to model how porosity influences surface shear stress distributions and sediment transport thresholds (Brown et al., 2008; Crawley and Nickling, 2003; Gillies et al., 2007). The next phase in investigations of the complex interaction between biological elements and geomorphic processes necessitates examination of the influence of different vegetation morphology types on fluid flow patterns as well as patterns of sediment erosion and deposition surrounding the vegetation. The next chapter delves into this topic in greater depth.

3.6 References

Agır, S., Kutbay, H., Karaer, F., Surmen, B., 2014. The classification of coastal dune vegetation in Central Black Sea Region of Turkey by numerical methods and EU habitat types. Rend. Fis. Acc. Lincei, 25(4), 453-460.

Arens, S.M., Baas, A.C.W., Van Boxel, J.H., Kalkman, C., 2001. Influence of reed stem density on foredune development. Earth Surface Processes and Landforms, 26(11), 1161-1176.

Baas, A.C.W., Nield, J.M., 2007. Modelling vegetated dune landscapes. Geophysical Research Letters, 34(6).

Barbour, M., De Jong, T., Pavlik, B., 1985. Marine beach and dune plant communities. In: B. Chabot, H. Mooney (Eds.), Physiological Ecology of North American Plant Communities. Springer Netherlands, pp. 296-322.

Bouma, T.J., Friedrichs, M., van Wesenbeeck, B.K., Temmerman, S., Graf, G., Herman, P.M.J., 2009. Density-dependent linkage of scale-dependent feedbacks: a flume study on the intertidal macrophyte Spartina anglica. Oikos, 118(2), 260-268.

Brown, S., Nickling, W.G., Gillies, J.A., 2008. A wind tunnel examination of shear stress partitioning for an assortment of surface roughness distributions. Journal of Geophysical Research-Earth Surface, 113(F2).

Buckley, R., 1987. The effect of sparse vegetation on the transport of dune sand by wind. Nature, 325(6103), 426-428.

Burri, K., Gromke, C., Lehning, M., Graf, F., 2011. Aeolian sediment transport over vegetation canopies: A wind tunnel study with live plants. Aeolian Research, 3(2), 205-213.

Carls, E.G., Lonard, R.I., Fenn, D.B., 1991. Notes on the vegetation and flora of North Padre Island, Texas. The Southwestern Naturalist, 36(1), 121-125.

Cooper, W.S., 1936. The strand and dune flora of the Pacific Coast of North America: a geographic study. University of California Press.

Crawley, D.M., Nickling, W.G., 2003. Drag partition for regularly-arrayed rough surfaces. Boundary-Layer Meteorology, 107(2), 445-468.

Dallavis, K.C., Henderson, S.M., Mullarney, J.C., 2011. Wave dissipation by flexible vegetation. Geophysical Research Letters.

de Langre, E., 2008. Effects of wind on plants. Annual Review of Fluid Mechanics, 40(1), 141-168.

Dijkstra, J.T., Uittenbogaard, R.E., 2010. Modeling the interaction between flow and highly flexible aquatic vegetation. Water Resources Research, 46(12), W12547.

Dong, Z.B., Luo, W.Y., Qian, G.Q., Lu, P., 2008. Wind tunnel simulation of the three-dimensional airflow patterns around shrubs. Journal of Geophysical Research-Earth Surface, 113(F2).

Freestone, A.L., Nordstrom, K.F., 2001. Early development of vegetation in restored dune plant microhabitats on a dourished beach at Ocean City, New Jersey. J Coast Conserv, 7(2), 105-116.

García-Mora, M.R., Gallego-Fernández, J.B., García-Novo, F., 1999. Plant functional types in coastal foredunes in relation to environmental stress and disturbance. Journal of Vegetation Science, 10(1), 27-34.

Gillette, D.A., Stockton, P.H., 1989. The effect of nonerodible particles on wind erosion of erodible surfaces. Journal of Geophysical Research: Atmospheres, 94(D10), 12885-12893.

Gillies, J.A., Lancaster, N., Nickling, W.G., Crawley, D.M., 2000. Field determination of drag forces and shear stress partitioning effects for a desert shrub (Sarcobatus vermiculatus, greasewood). J. Geophys. Res.-Atmos., 105(D20), 24871-24880.

Gillies, J.A., Nickling, W.G., King, J., 2002. Drag coefficient and plant form response to wind speed in three plant species: Burning Bush (Euonymus alatus), Colorado Blue Spruce (Picea pungens glauca.), and Fountain Grass (Pennisetum setaceum). J. Geophys. Res.-Atmos., 107(D24).

Gillies, J.A., Nickling, W.G., King, J., 2007. Shear stress partitioning in large patches of roughness in the atmospheric inertial sublayer. Boundary-Layer Meteorology, 122(2), 367-396.

Grant, P.F., Nickling, W.G., 1998. Direct field measurement of wind drag on vegetation for application to windbreak design and modelling. Land Degradation & Development, 9(1), 57-66.

Guan, D., Zhong, Y., Jin, C., Wang, A., Wu, J., Shi, T., Zhu, T., 2009. Variation in wind speed and surface shear stress from open floor to porous parallel windbreaks: A wind tunnel study. J. Geophys. Res., 114(D15), D15106.

Jia, Y., Sill, B.L., Reinhold, T.A., 1998. Effects of surface roughness element spacing on boundary-layer velocity profile parameters. Journal of Wind Engineering and Industrial Aerodynamics, 73(3), 215-230.

Judd, F.W., Lonard, R.I., Sides, S.L., 1977. The vegetation of South Padre Island, Texas in relation to topography. The Southwestern Naturalist, 22(1), 31-48.

Kenney, W.A., 1987. A method for estimating windbreak porosity using digitized photographic silhouettes. Agricultural and Forest Meteorology, 39(2–3), 91-94.

Kim, S.J., Stoesser, T., 2011. Closure modeling and direct simulation of vegetation drag in flow through emergent vegetation. Water Resources Research, 47(10), W10511.

King, J., Nickling, W.G., Gillies, J.A., 2005. Representation of vegetation and other nonerodible elements in aeolian shear stress partitioning models for predicting transport threshold. Journal of Geophysical Research-Earth Surface, 110(F4).

Kuriyama, Y., Mochizuki, N., Nakashima, T., 2005. Influence of vegetation on aeolian sand transport rate from a backshore to a foredune at Hasaki, Japan. Sedimentology, 52(5), 1123-1132.

Lancaster, N., Baas, A., 1998. Influence of vegetation cover on sand transport by wind: Field studies at Owens Lake, California. Earth Surface Processes and Landforms, 23(1), 69-82.

Leenders, J.K., Sterk, G., Van Boxel, J.H., 2011. Modelling wind-blown sediment transport around single vegetation elements. Earth Surface Processes and Landforms, 36(9), 1218-1229.

Leenders, J.K., van Boxel, J.H., Sterk, G., 2007. The effect of single vegetation elements on wind speed and sediment transport in the Sahelian zone of Burkina Faso. Earth Surface Processes and Landforms, 32(10), 1454-1474.

Leonard, L.A., Croft, A.L., 2006. The effect of standing biomass on flow velocity and turbulence in Spartina alterniflora canopies. Estuar. Coast. Shelf Sci., 69(3-4), 325-336.

Leonard, L.A., Luther, M.E., 1995. Flow hydrodynamics in tidal marsh canopies. Limnology and Oceanography, 40(8), 1474-1484.

Lightbody, A.F., Nepf, H.M., 2006. Prediction of velocity profiles and longitudinal dispersion in emergent salt marsh vegetation. Limnology and Oceanography, 51(1), 218-228.

Loeffler, A.E., Gordon, A.M., Gillespie, T.J., 1992. Optical porosity and windspeed reduction by coniferous windbreaks in Southern Ontario. Agroforest Syst, 17(2), 119-133.

Lubke, R.A., 2004. Vegetation dynamics and succession on sand dunes of the eastern coasts of Africa. In: M.L. Martínez, N. Psuty (Eds.), Coastal Dunes. Ecological Studies. Springer Berlin Heidelberg, pp. 67-84.

Luhar, M., Rominger, J., Nepf, H., 2008. Interaction between flow, transport and vegetation spatial structure. Environ. Fluid Mech., 8(5-6), 423-439.

Marshall, J.K., 1971. Drag measurements in roughness arrays of varying density and distribution. Agricultural Meteorology, 8(4-5), 269-&.

Martinez, M.L., Vasquez, G., Sanchez, C.S., Colon, S., 2001. Spatial and temporal variability during primary succession on tropical coastal sand dunes. Journal of Vegetation Science, 12, 361-372.

Maun, M.A., 2009. The Biology of Coastal Sand Dunes. Oxford University Press, Oxford, UK.

Moller, I., 2006. Quantifying saltmarsh vegetation and its effect on wave height dissipation: Results from a UK East coast saltmarsh. Estuar. Coast. Shelf Sci., 69(3-4), 337-351.

Moreno-Casasola, P., 1986. Sand movement as a factor in the distribution of plant communities in a coastal dune system. Vegetatio, 65, 67-76.

Moreno-Casasola, P., Espejel, I., 1986. Classification and ordination of coastal sand dune vegetation along the Gulf and Caribbean Sea of Mexico. Vegetatio, 66(3), 147-182.

Moreno-Casasola, P., Vasquez, G., 1999. Succession in tropical dune slacks after disturbance by water-table dynamics. Journal of Vegetation Science, 10, 515-524.

Musick, H.B., Gillette, D.A., 1990. Field evaluation of relationships between a vegetation structural parameter and sheltering against wind erosion. Land Degradation and Rehabilitation, 2, 87-94.

Musick, H.B., Trujillo, S.M., Truman, C.R., 1996. Wind-tunnel modelling of the influence of vegetation structure on saltation threshold. Earth Surface Processes and Landforms, 21(7), 589-605.

Nepf, H.M., 1999. Drag, turbulence, and diffusion in flow through emergent vegetation. Water Resources Research, 35(2), 479-489.

Neumeier, U., 2005. Quantification of vertical density variations of salt-marsh vegetation. Estuar. Coast. Shelf Sci., 63(4), 489-496.

Neumeier, U., 2007. Velocity and turbulence variations at the edge of saltmarshes. Cont. Shelf Res., 27(8), 1046-1059.

Neumeier, U., Amos, C.L., 2006. The influence of vegetation on turbulence and flow velocities in European salt-marshes. Sedimentology, 53(2), 259-277.

Neumeier, U., Ciavola, P., 2004. Flow resistance and associated sedimentary processes in a Spartina maritima salt-marsh. Journal of Coastal Research, 20(2), 435-447.

Nilsson, S.B., Hertz, C.H., Falk, S., 1958. On the relation between turgor pressure and tissue rigidity. II. Physiologia Plantarum, 11(4), 818-837.

Nordstrom, K.F., 2008. Beach and Dune Restoration. Cambridge University Press.

Novo, F.G., Barradas, M.C.D., Zunzunegui, M., Mora, R.G., Fernández, J.B.G., 2004. Plant functional types in coastal dune habitats. In: M.L. Martínez, N. Psuty (Eds.), Coastal Dunes. Ecological Studies. Springer Berlin Heidelberg, pp. 155-169.

Okin, G.S., 2008. A new model of wind erosion in the presence of vegetation. Journal of Geophysical Research-Earth Surface, 113(F2).

Pavlik, B.M., 1984. Seasonal changes of osmotic pressure, symplasmic water content and tissue elasticity in the blades of dune grasses growing in situ along the coast of Oregon. Plant, Cell & Environment, 7(7), 531-539.

Raupach, M.R., 1992. Drag and drag partition on rough surfaces. Boundary-Layer Meteorology, 60(4), 375-395.

Raupach, M.R., Gillette, D.A., Leys, J.F., 1993. The effect of roughness elements on wind erosion threshold. J. Geophys. Res.-Atmos., 98(D2), 3023-3029.

Schmutz, P., 2007. Investigation of utility of delta-t thetaprobe for obtaining surficial moisture measurements on beaches. M.S., Louisiana State University, Baton Rouge, 114 pp.

Sciandrello, S., Tomaselli, G., Minissale, P., 2015. The role of natural vegetation in the analysis of the spatio-temporal changes of coastal dune system: a case study in Sicily. J Coast Conserv, 1-14.

SRCC, 2015. Southern Regional Climate Center: 1981 - 2010 NCDC Monthly Normals.

Stallins, J.A., 2003. Dune plant species diversity and function in two barrier island biogeomorphic systems. Plant Ecology, 165(2), 183-196.

Steudle, E., Zimmermann, U., Lüttge, U., 1977. Effect of turgor pressure and cell size on the wall elasticity of plant cells. Plant Physiology, 59(2), 285-289.

Suter-Burri, K., Gromke, C., Leonard, K.C., Graf, F., 2013. Spatial patterns of aeolian sediment deposition in vegetation canopies: Observations from wind tunnel experiments using colored sand. Aeolian Research, 8(0), 65-73.

Sutton, S.L.F., McKenna-Neuman, C., 2008. Variation in bed level shear stress on surfaces sheltered by nonerodible roughness elements. Journal of Geophysical Research-Earth Surface, 113(F3).

Tobias, M.M., 2014. California foredune plant biogeomorphology. Physical Geography, 36(1), 19-33.

Udo, K., Takewaka, S., 2007. Experimental study of blown sand in a vegetated area. Journal of Coastal Research, 23(5), 1175-1182.

Walter, B., Gromke, C., Lehning, M., 2012a. Shear-stress partitioning in live plant canopies and modifications to Raupach's model. Boundary-Layer Meteorology, 144(2), 217-241.

Walter, B., Gromke, C., Leonard, K.C., Manes, C., Lehning, M., 2012b. Spatio-temporal surface shear-stress variability in live plant canopies and cube arrays. Boundary-Layer Meteorology, 143(2), 337-356.

Weise, B.R., White, W.A., 1980. Padre Island National Seashore: a guide to the geology, natural environments, and history of a Texas barrier island. Bureau of Economic Geology, Austin, Texas.

Wolfe, S.A., Nickling, W.G., 1993. The protective role of sparge vegetation in wind erosion. Progress in Physical Geography, 17(1), 50-68.

Wolfe, S.A., Nickling, W.G., 1996. Shear stress partitioning in sparsely vegetated desert canopies. Earth Surface Processes and Landforms, 21(7), 607-619.

Woodhouse, W.W., 1978. Dune building and stabilization with vegetation. US Army, Corps of Engineers, Coastal Engineering Research Center.

Wyatt, V.E., Nickling, W.G., 1997. Drag and shear stress partitioning in sparse desert creosote communities. Can. J. Earth Sci., 34(11), 1486-1498.

Zong, L., Nepf, H., 2010. Flow and deposition in and around a finite patch of vegetation. Geomorphology, 116(3–4), 363-372.

Chapter 4. The Effect of Vegetation on the Spatial Distribution of Aeolian Fluid Flow and Sediment Deposition and Erosion in Coastal Embryo Dunes

4.1 Introduction

Vegetation behaves as a roughness element in aeolian environments, increasing drag on fluid flow, altering shear stress, and influencing patterns of sediment transport (Buckley, 1987; Crawley and Nickling, 2003; Dong et al., 2008; Gillies et al., 2000; Gillies et al., 2002; Gillies et al., 2006; Grant and Nickling, 1998; Lancaster and Baas, 1998; Leenders et al., 2011; Leenders et al., 2007; Leonard and Croft, 2006; Luhar and Nepf, 2013; Luhar et al., 2008; Mattis et al., 2012; Nepf, 1999; Neumeier, 2007; Neumeier and Amos, 2006; Okin, 2008; Pasquill, 1950; Siniscalchi et al., 2012; Suter-Burri et al., 2013; Wolfe and Nickling, 1993; Wyatt and Nickling, 1997; Zong and Nepf, 2010). Shear stress is the driving force of sediment transport (Bagnold, 1941). Currently, it is not possible to model wind flow and sediment deposition within the coastal embryo dune environment because the distribution and morphology of vegetation in this environments has a high degree of variability, with vegetation growing in non-systematic and unpredictable spatial arrangements and producing hummocky terrain.

Modeling shear stress distribution around roughness elements provides a means to predict sediment transport patterns that lead to dune formation and evolution. The predominant shear stress partitioning model used for aeolian environments, which allows the prediction of the total shear stress on the entire canopy as well as the peak and the average shear-stress ratios, was derived around solid, rigid roughness elements (Raupach et al., 1993). Recent work has shown that this model does not perform well in environments where there is live, non-rigid vegetation (Gillies et al., 2002; Grant and Nickling, 1998; Okin, 2008; Walter et al., 2012a; Walter et al., 2012b; Wolfe and Nickling, 1996; Wyatt and Nickling, 1997). This is due in large part to the fact that porous elements behave very differently than solid objects (Gillies et al., 2000; Grant and Nickling, 1998;

Okin, 2008; Walter et al., 2012a) and to the fact that live vegetation has dynamic morphology so that the morphology and drag coefficients of individual elements changes as function of wind velocity (Gillies et al., 2000; Gillies et al., 2002). Before a shear stress partitioning model applicable to live, natural vegetation can be developed, it is necessary to first examine the influence of different vegetation morphology types on spatial patterns of flow and sediment transport.

The goal of this chapter was to investigate spatial patterns of aeolian fluid flow as well as sediment deposition and erosion around live, native species of different morphology – a short grass, a tall grass, and a shrub. Analyzing differences in flow and transport between species with different morphologies is necessary as the first step in building the framework for a shear stress partitioning which will be applicable within a natural environment. This research will enhance our understanding of aeolian ecogeomorphodynamics in a highly complex coastal embryo dune environment.

4.2 Background

4.2.1 Modeling Shear Stress

The shear stress partitioning model most commonly used in the context of terrestrial vegetation in aeolian environments is that of Raupach et al. (1993). Conceptually, shear stress can be subdivided into components of shear force that act on each of the different elements that comprise the ground surface in a given location (e.g., sand grains, bed forms, vegetation, etc.), and a remainder that is left to drive sediment transport (Marshall, 1971; Raupach, 1992; Raupach et al., 1993; Schlichting, 1936). Raupach et al. (1993) proposed the following definition for the threshold friction velocity ratio, R_t:

$$R_t = \frac{u_{*S}}{u_{*R}} = \sqrt{\frac{\tau_S''}{\tau_R}} = \sqrt{\frac{1}{(1-m\sigma\lambda)(1+m\beta\lambda)}} \quad (1)$$

where u_{*S} is the threshold shear velocity on the surface with no roughness elements present, u_{*R} is threshold shear velocity on the surface with roughness elements present, τ_s'' is the maximum stress on the ground surface at any point, τ_R is the shear stress acting on the roughness elements, σ is the ratio of basal area (ground area occupied by the plant) to frontal area, m is an empirical parameter between 0 and 1 that accounts for spatial and temporal variations in shear stress on intervening surface, λ is roughness density ($\lambda=nbh/S$, where n is number of elements, b is element width, h is element height, and S is surface area occupied by elements), and β is the ratio of drag coefficient of isolated roughness element to the drag coefficient of the surface itself (or C_R/C_S, where C_R is the drag coefficient of the element and C_S is the drag coefficient of the surface). The Raupach et al. (1993) model was developed using solid, rigid elements with uniform spatial distribution and stable object morphology and has been evaluated with successful results for either solid, rigid objects or rigid desert shrubs (Brown et al., 2008; Crawley and Nickling, 2003; Gillies et al., 2000; Gillies et al., 2006; Gillies et al., 2007; Jia et al., 1998; King et al., 2005; Leenders et al., 2011; Leenders et al., 2007; Luo et al., 2012; Musick et al., 1996; Raupach, 1992; Raupach et al., 1993; Sutton and McKenna-Neuman, 2008; Wolfe and Nickling, 1996).

However, considerable limitations arise when applying this shear stress partitioning model to coastal dune environments. First of all, the Raupach et al. (1993) model emphasizes the effect of the spatial distribution of roughness elements, which was based on the findings of Marshall (1971). In fact, several studies have evaluated the effect of roughness density on shear stress partitioning and found that the measured partitioning of shear stress validated the model, regardless of their spatial configuration (Brown et al., 2008; Crawley and Nickling, 2003; Gillies et al., 2006; Gillies et al., 2007; King et al., 2005). These studies used artificial elements to represent vegetation and thus roughness element size was held constant. However, recent research has shown that

object height plays a significant role in influencing the spatial distribution of wind velocity and shear stress partitioning (Leenders et al., 2011; Webb et al., 2014), with taller elements causing greater magnitude of deceleration in their lee. Vegetation in embryo dune environment comes in many different shapes and size and therefore, it is necessary to investigate spatial patterns of aeolian processes around natural vegetation of different size in an embryo dune environment.

Furthermore, live vegetation has very different effects on flow dynamics as a result of being porous and flexible. A limited number of studies have shown distinct differences in aeolian flow and shear stress distribution around solid, rigid roughness elements and live, flexible grasses (Burri et al., 2011; Gillies et al., 2002; Walter et al., 2012a; Walter et al., 2012b). Gillies et al. (2002) showed that drag of certain vegetation species changes as plants become more streamlined in response to higher velocity. Therefore, there is a compelling need to examine the dynamics of aeolian flow and sediment transport around flexible grasses, which are the most common species type found in coastal dunes, to incorporate these in shear stress partitioning models.

Finally, it is worth noting that a majority of studies examining shear stress partitioning models have been conducted in wind tunnels (Brown et al., 2008; Buckley, 1987; Burri et al., 2011; Crawley and Nickling, 2003; Dong et al., 2008; Gillies et al., 2002; Jia et al., 1998; Luo et al., 2012; Marshall, 1971; Musick et al., 1996; Raupach, 1992; Raupach et al., 1993; Suter-Burri et al., 2013; Sutton and McKenna-Neuman, 2008; Udo and Takewaka, 2007; Walter et al., 2012a; Walter et al., 2012b). The handful of studies which have been conducted in the field have examined flow around either artificial roughness elements (Gillies et al., 2006; Gillies et al., 2007) or shrubs (Gillies et al., 2000; Grant and Nickling, 1998; Leenders et al., 2011; Leenders et al., 2007; Wyatt and Nickling, 1997). Wind dynamics within wind tunnels are greatly simplified in comparison to nature due unsteadiness in wind velocity and direction and uneven surfaces. Thus there exists an

inherent need to examine flow around *in situ* coastal dune grass and sediment transport dynamics as the first step toward understanding how these plants control shear stress and sediment transport.

Ideally, bed shear stress would be measured directly. However, this is not practicable in the context of the present study due to instrument limitations in natural environments. Instruments capable of measuring surface shear stress that are: a) small enough to avoid interfering with the behavior of the vegetation or be interrupted by vegetation, b) robust enough to operate consistently and accurately when exposed to blowing sand, and c) inexpensive enough to allow simultaneous deployment of a dozen or more units to capture spatial variability (within practical budget constraints), simply do not exist. Moreover, surface shear stresses cannot be predicted using velocity at some height above the bed because the law of the wall does not apply when sparsely distributed roughness elements are present in the flow field (King et al., 2008). Instead, near-surface wind velocities were measured to document and analyze differences in the extent and magnitude of the influence of various plant species on aeolian fluid flow.

4.2.2 Patterns of Sediment Transport around Vegetation

The Raupach et al. (1993) model, while capable of predicting values of average and peak shear stresses within an area of study, is neither useful for predicting spatial patterns of flow around vegetation nor how these patterns correlate to zones of erosion and deposition. Wolfe and Nickling (1993) published a widely used conceptual model for aeolian flow patterns and wake development around roughness elements based on roughness element concentration. Leenders et al. (2011) generated a model to predict spatial patterns of sediment transport around vegetation (Figure 4.1). The impact of vegetation on aeolian flow and shear stress distribution is more localized than previously thought (Ghisalberti and Nepf, 2006). Vegetation decreases velocity and shear stress in

a localized area in the immediate lee of the plant instead of affecting shear stress across the entire surface where vegetation is present.

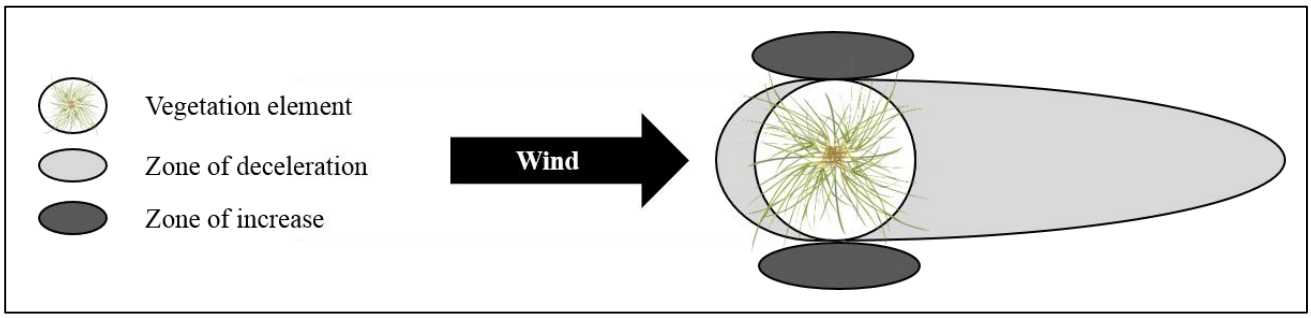

Figure 4.1. Depiction zones of acceleration and deceleration around vegetation. Image taken from Leenders et al. (2011).

Echo dunes form upwind of roughness elements as a result of the formation of reversed flow caused by flow interaction with the roughness object (Qian et al., 2012). As wind steers around vegetation there are small localized areas of accelerated wind velocity located directly to the sides of the element coinciding with areas of erosion (Dong et al., 2008; Leenders et al., 2011; Leenders et al., 2007; Sutton and McKenna-Neuman, 2008). In the lee of vegetation, flow separation and decreased turbulence lead to deposition in features called shadow dunes in aeolian environments (Gillies et al., 2014; Gunatilaka and Mwango, 1989; Luo et al., 2012).

Since different species and different vegetation densities alter fluid flow and shear stress distribution in different ways in aeolian environments (Gillies et al., 2002) as well as in aquatic environments (Ghisalberti and Nepf, 2006; Leonard and Croft, 2006; Luhar et al., 2008; Neumeier, 2005; Neumeier, 2007; Neumeier and Amos, 2006; Siniscalchi and Nikora, 2012), it follows that patterns of deposition and erosion will differ among vegetation morphology types. However, the influence of vegetation on patterns of aeolian processes in the embryo dune zone are poorly understood. The purposes of this study were to 1) quantify and map the near-surface aeolian fluid

flow around different types of *in situ* vegetation, 2) differentiate flow modification patterns between vegetation morphology types, and 3) differentiate sediment deposition and erosion patterns to vegetation morphology type.

4.3 Methodology

4.3.1 Study Site

A series of experiments were conducted at Padre Island National Seashore (PINS), Texas. The field site at Padre Island National Seashore is located in the northwestern Gulf of Mexico, approximately 160 km north of the United States – Mexico border (Figure 4.2). The shoreline is

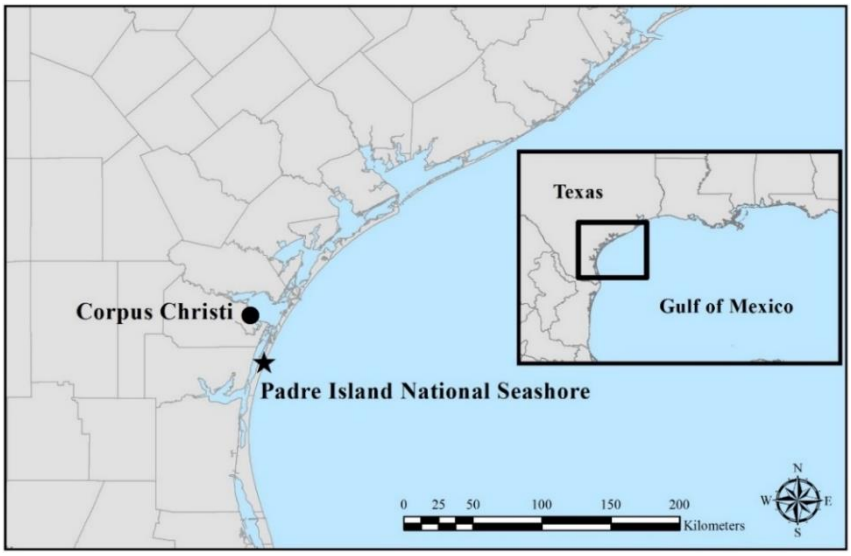

Figure 4.2. Location of Padre Island National Seashore.

oriented SSW to NNE (220°-20°) and the dominant wind direction in summer is from the southeast (135°). The beach at PINS is dissipative with a wide, well-established, partially vegetated, and hummocky embryo dune zone which was approximately 40 m wide during the study period. Beach sediment is predominately very-well sorted, fine to very-fine quartz sand with a mean diameter of

about 0.15 mm (Schmutz, 2007). Dune vegetation was fairly typical of northern and western Gulf of Mexico barrier islands and beaches.

4.3.2 Site Preparation

Three vegetation morphology types were chosen for examination - 1) a short, rhizomatous grass that grows in dense blankets up to approximately 0.25 m in height with thin blades *(Sporobolus virginicus*; Figure 4.3A); 2) a tall, rhizomatous grass that grows up to 2 m in height with thin (<0.6 cm in width) blades (*Uniola paniculata*; Figure 4.3B); and 3) a short, rigid shrub that grows up to approximately 0.5 m in height in the embryo dune environment, with either erect or ascending stems that were no more than 2 cm in diameter, and with leaves circular and obovate up to 0.5 cm in thickness and 4 cm in length (*Tidestromia lanuginosa* – Figure 4.3C, *Amaranthus greggii* – Figure 4.3D).

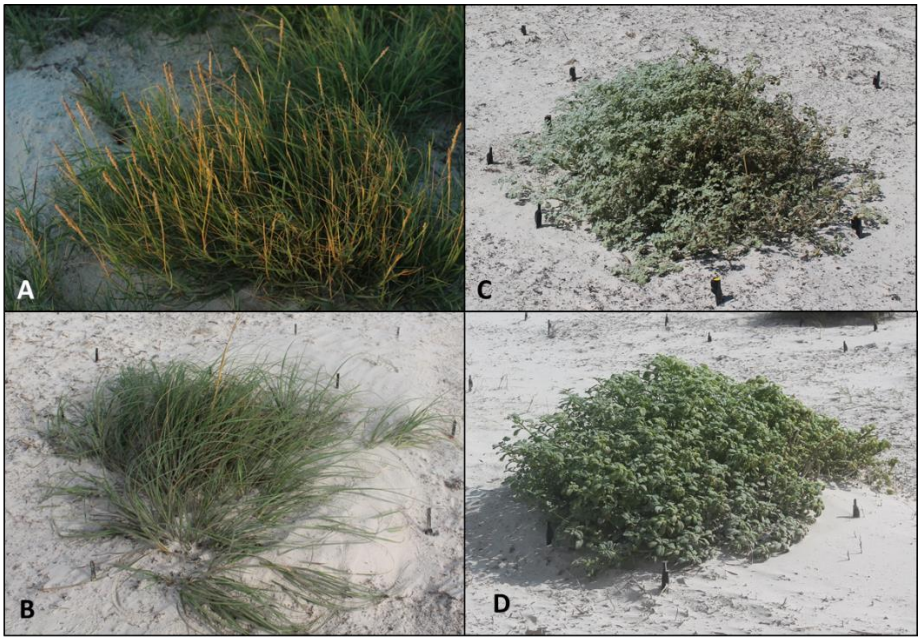

Figure 4.3. Images of each of the plant species examined herein. A) The short grass, *Sporobolus*, B) The tall grass, *Uniola*, C) a shrub, *Tidestromia*, and D) a shrub, *Amaranthus*.

Finite patches of each of these morphology types were selected based on meeting several criteria – a) only a single species occupied a patch; b) vegetation was located near the seaward edge of the embryo dune zone so that approaching winds were not altered by other vegetation; and c) surrounding terrain was generally flat to reduce variability in wind flow caused by a sloped surface.

Preparation of the specimen sites for data collection consisted of the following steps. First, other vegetation and debris within a 5 to 10 m radius around the clump were removed to reduce the effect of any surrounding vegetation on the airflow. For the purpose of measuring wind velocity approaching vegetation and determining upwind, lateral, and down-stream effects of vegetation on the flow field, 16-32 tent stakes, or erosion pins, were emplaced in a grid (Figure 4.4). These pins marked the location of the anemometers used to measure near-surface wind velocities and surface elevation changes.

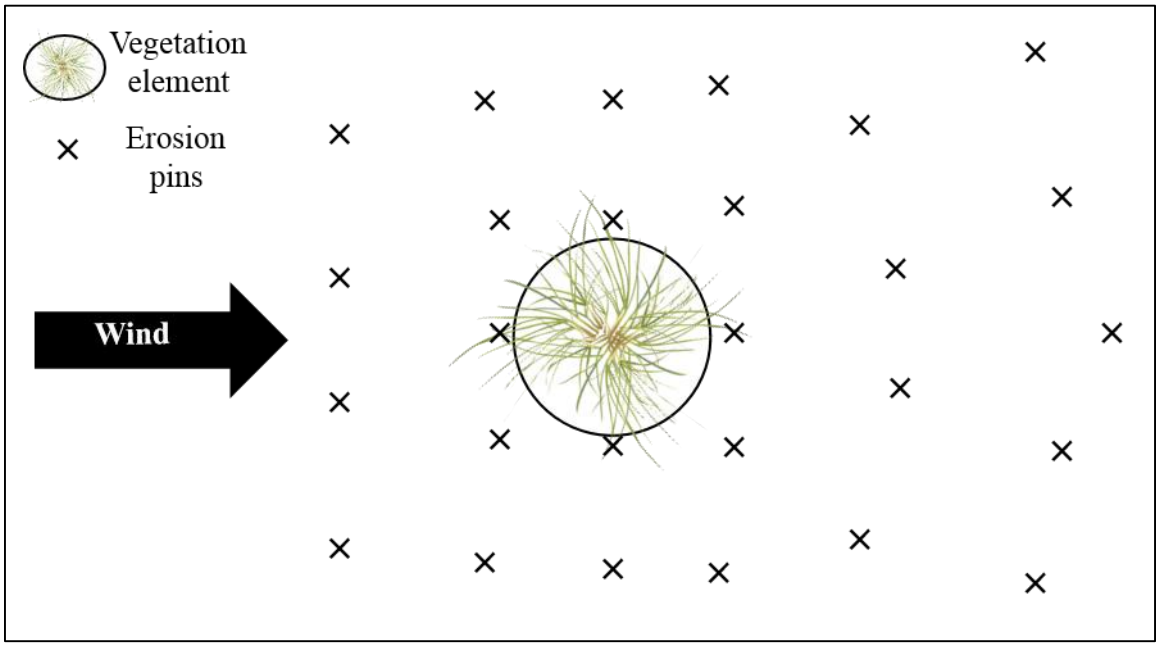

Figure 4.4. Example of arrangement of stakes around a finite patch of vegetation.

Rows of 3-5 pins were oriented perpendicular to the dominant wind direction at distances 1) 1.5-2 m upwind of the edge of vegetation clump; 2) touching the upwind edge of the clump; 3) at the middle of the clump with stakes on either side of the clump; 4) touching the downwind edge of the clump; 5) 2 m downwind of the clump; and 6) 4-5 m downwind of the clump. An anemometer mast was installed on the open beach within 10 m of the vegetation clump of interest, with anemometers at 0.25 m, 0.75 m, and 1.5 m heights. The locations of stakes, masts, and perimeters of vegetation clumps were recorded with a total station.

Data were collected around three specimens of short grass (8 runs for 2012 specimen, 9 runs for 2013 specimen, 13 runs for 2014 specimen), four specimens of tall grass (9 runs for 2012 specimen, 10 runs for 2013 specimen, 16 runs for first 2014 specimen, and 12 runs for second 2014 specimen), and two specimens of shrubs (9 runs for 2013 specimen, 12 runs for 2014 specimen). In total, 98 runs of near-surface flow data were collected and analyzed for all specimens at a range of wind velocities (Table 4.1, Figure 4.5). The wind direction during each run was observed using a flag located at 1 m height on the anemometer mast, measured with a compass, and recorded in a field notebook (Table 4.2, Figure 4.6).

Table 4.1. Average velocity in m/s at 0.25 m height on anemometer mast for each run.

Obs.	2012 *Sporobolus*	2013 *Sporobolus*	2014 *Sporobolus*	2012 *Uniola*	2013 *Uniola*	2014 *Uniola* 1	2014 *Uniola* 2	2013 *Tidestromia*	2014 *Amaranthus*
A	1.98	3.75	2.53	1.61	2.16	2.17	2.39	3.59	2.37
B	2.44	4.18	2.82	1.99	2.54	2.62	2.79	3.69	2.96
C	2.63	4.24	3.19	2.54	2.91	2.77	2.92	3.82	3.15
D	3.49	4.52	3.67	3.59	3.09	3.13	3.16	3.87	3.20
E	4.03	5.05	3.82	4.20	3.63	3.33	3.66	4.03	3.39
F	4.37	5.43	4.22	4.35	4.05	3.37	3.71	4.47	3.59
G	4.48	5.54	4.75	4.59	4.06	3.57	3.95	4.61	3.94
H	4.62	5.80	4.80	4.74	4.17	3.69	4.31	4.66	4.05

Table 4.1 continued. Average velocity in m/s at 0.25 m height on anemometer mast for each run.

Obs.	2012 *Sporobolus*	2013 *Sporobolus*	2014 *Sporobolus*	2012 *Uniola*	2013 *Uniola*	2014 *Uniola* 1	2014 *Uniola* 2	2013 *Tidestromia*	2014 *Amaranthus*
J		6.14	5.01	4.82	4.18	4.01	4.75	4.78	4.99
K			5.13		4.55	4.18	4.80		5.13
L			5.22			4.34	5.33		5.27
M			5.28			5.38	5.57		5.51
N			5.28			5.60			
P						5.71			
Q						5.79			
R						5.79			

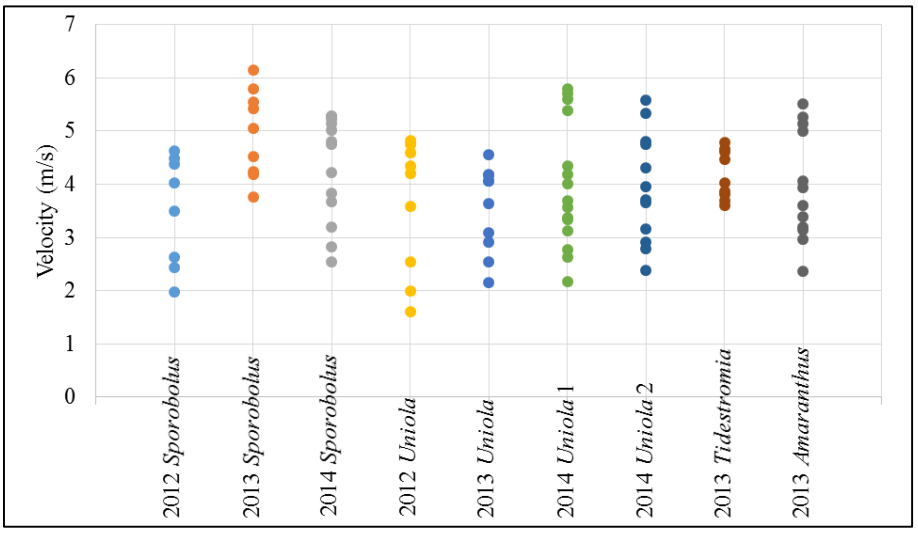

Figure 4.5. Average velocity (m/s) at 0.25 m height on anemometer mast for each run.

Table 4.2. Wind direction in degrees from which wind blew for each run. Due onshore was 110°.

Obs.	2012 *Sporobolus*	2013 *Sporobolus*	2014 *Sporobolus*	2012 *Uniola*	2013 *Uniola*	2014 *Uniola* 1	2014 *Uniola* 2	2013 *Tidestromia*	2014 *Amaranthus*
A	171	150	187	115	146	141	105	152	113
B	170	162	181	90	148	140	112	153	107
C	136	149	188	82	140	140	95	151	93
D	153	156	180	138	138	145	114	150	105
E	122	156	188	140	133	140	113	150	106
F	135	153	189	122	120	144	135	130	129

Table 4.2 continued. Wind direction in degrees from which wind blew for each run. Due onshore was 110°.

Obs.	2012 *Sporobolus*	2013 *Sporobolus*	2014 *Sporobolus*	2012 *Uniola*	2013 *Uniola*	2014 *Uniola* 1	2014 *Uniola* 2	2013 *Tidestromia*	2014 *Amaranthus*
G	127	144	196	137	129	160	123	147	130
H	137	143	187	240	131	140	135	135	135
J		134	195	236	131	149	120	142	115
K			195		140	125	160		143
L			187			125	150		151
M			198			197	150		160
N			185			162			
P						162			
Q						172			
R						165			

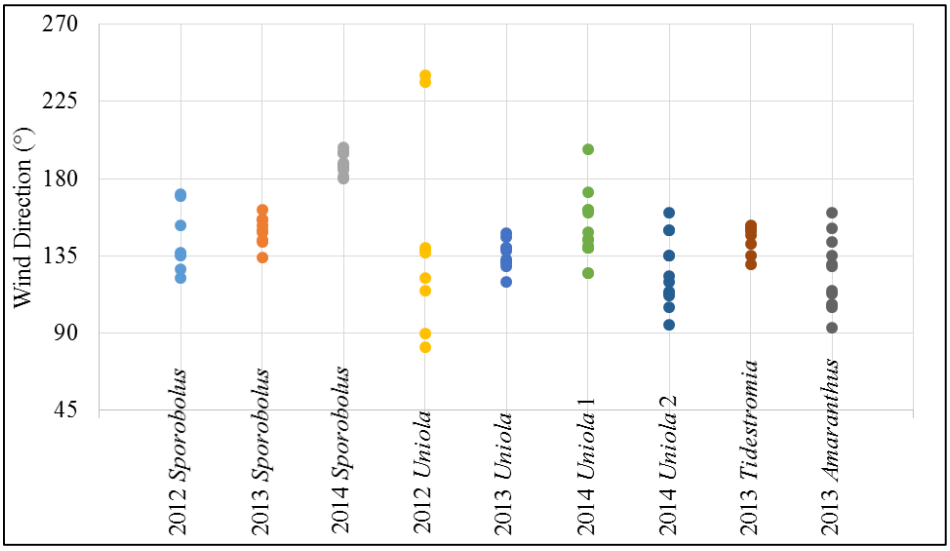

Figure 4.6. Wind direction for each run.

4.3.3 Near-surface Flow Data Collection

All wind velocity data were collected with RM Young Gill 3-cup anemometers at 1 Hz. Velocity was measured continuously at the mast for the duration of a run. Velocity was measured at each pin within the grid array at 0.25 m height for a 3-minute interval. The 3-minute sampling duration was selected because it was deemed sufficient to allow averaging of wind unsteadiness

cause by turbulence but not so long that velocity changed substantially during an entire run cycle. Wind velocity was averaged for each 3-minute sampling interval. For the purpose of determining the effect of vegetation on velocity three-minute average velocities at pins were normalized by dividing by average velocity recorded at 0.25 m height on the mast for the same time interval. Raster maps depicting normalized velocities for each run were interpolated using the kriging method. Raster maps were included in Appendix B. Four runs (2spa, 2spb, 2unh, and 2unj) were removed from all further analysis because the wind direction was not from the open beach but instead from over surrounding vegetation.

4.3.4 Surface Elevation Data Collection and Analysis

In order to analyze patterns of sediment transport around vegetation, surface elevation change was measured during the 2013 and 2014 field seasons at the erosion pins in the grid surrounding each specimen. The initial heights of the erosion pins above the surface were recorded at the onset of the experiments. Heights of erosion pins were subsequently recorded at daily intervals for the duration of each set of experiments, and changes were calculated for the entire study period. During the 2013 field season, elevation data were collected for a 6-day period from 1100 hours on July 23 to 1000 hours on July 29. During the 2014 field season surface elevation data were collected for a 9-day period starting at 0900 hours on June 2 and ending at 0900 hours on June 11. Elevation change was determined by subtracting the initial elevation values from the final elevation values. Raster maps showing elevation change for the entirety of each study period were generated in Surfer 8 by interpolating change at each grid location using the kriging method.

4.3.5 Wind Data for Surface Elevation Change

Since anemometers were not deployed continuously at all clumps for the duration of field work, wind direction and velocity data were acquired from the National Buoy Data Center at Bob Hall Pier located approximately 15 km north-northeast from the study site. These data were averaged for 1-hour periods for input into the Lakes Environmental WRPlot Freeware program. Wind roses were produced for each study period to determine the dominant velocity and resultant direction of wind during the time over which elevation data were recorded. While the WRPlot program adjusts for the 360 degree compass, so that winds from 355° and 5° do not produce an average of 180°. However, this was not significant because winds during the 2013 study period ranged from 119° to 177°and during the 2014 field season ranged from 68° to 196°.

Wind directions and wind velocities measured at the Bob Hall Pier buoy had minor differences between the 2013 and 2014 study periods (Figure 4.7). Due onshore was 110°. During both study periods, there were diurnal patterns in wind direction. Wind direction shifted approximately 40-50° throughout each day. During the night, the wind had a stronger easterly component than during the day, when winds were more southerly. The average wind direction during 2013 was 153° (Figure 4.7C) and during 2014 was 128° (Figure 4.7F). Diurnal patterns in wind direction were consistent throughout the 2013 field season. On the other hand wind direction shifted during the 9-day 2014 field season, from more easterly during the first 3 days and more southeasterly during the last 3 days. The average wind velocity for the 2013 study period was 10 m/s with 0% calm winds (<1 m/s). The average wind velocity for the 2014 study period was 8 m/s with 0% calm winds. Wind velocities were lower during the first three days of the 2014 season than the latter half of the 2014 season.

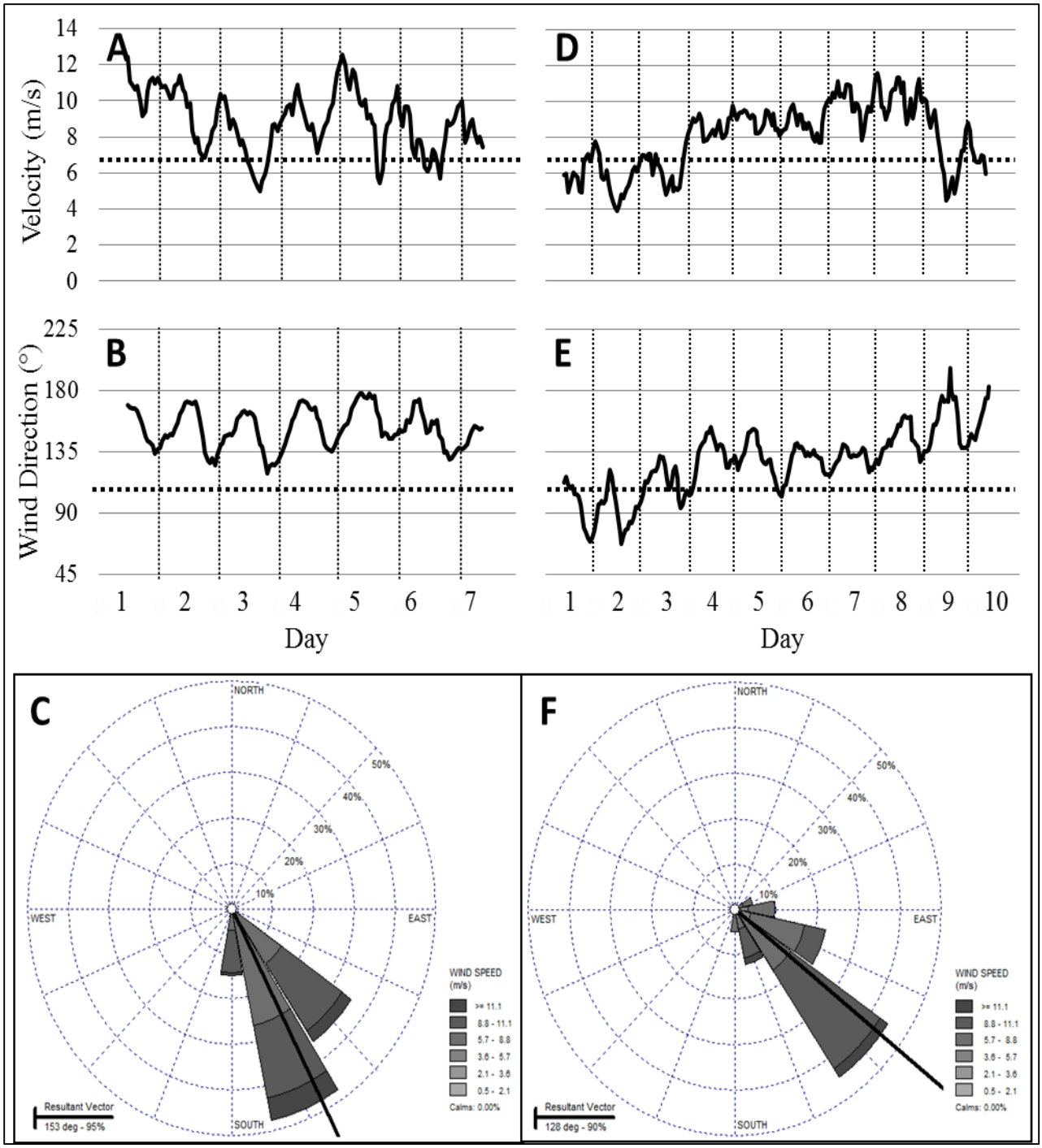

Figure 4.7. Wind data for the two study periods – A) 2013 wind velocity, B) 2013 wind direction, C) 2013 wind rose, D) 2014 wind velocity, E) 2014 wind direction, and F) 2014 wind rose. Vertical lines indicate midnight. Dashed lines on A and D indicate the threshold velocity for sediment transport (u=6.24 m/s at 7.92 m height of buoy) Dashed lines on B and E indicate due onshore (110°).

4.4 Results

4.4.1 Near-surface Flow Patterns

For the purpose of determining the effect of vegetation on spatial patterns of flow it was necessary to analyze flow patterns around the different vegetation morphology types. Interpolated raster maps of normalized velocity were not directly comparable and could not be overlaid in a GIS because wind direction varied substantially between the different specimens. Therefore, another approach was adopted. Values of normalized velocities were extracted from interpolated rasters in ArcGIS 10.2.2 3D Analyst along 3 lines (Figure 4.8).

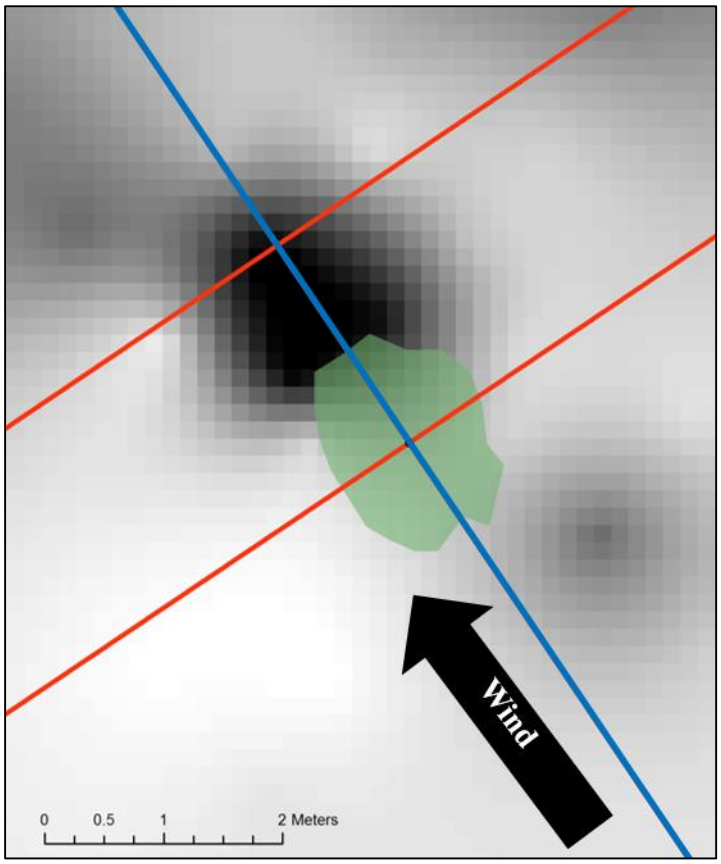

Figure 4.8. Example of lines of extraction from interpolated raster of normalized velocity in ArcGIS 10.2.2 for analysis (specimen: 4u1a). The blue line is parallel to wind direction through the center; the other two lines are lines perpendicular to wind direction – one through the center of the vegetation and the other 2 m downwind of vegetation center; green polygon indicates the outline of perimeter of specimen.

One line was parallel to wind direction through plant centers to provide insight into stream-wise differences in velocity between morphology types. The second line was perpendicular to wind direction through plant centers in order to investigate the lateral effects of vegetation on velocity. The third line was perpendicular to wind direction 2 m downwind from plant centers so that the cross stream influence on the flow downwind of vegetation could be examined. Data were referenced to the center of each specimen.

4.4.1.1 Streamwise Variation in Velocity

The first step in this analysis was examining normalized velocities along flow parallel to the wind direction through the center of specimens and comparing flow patterns around different morphology types. Normalized velocity for each morphology type was averaged for all runs for each morphology type and shown in Figure 4.9.

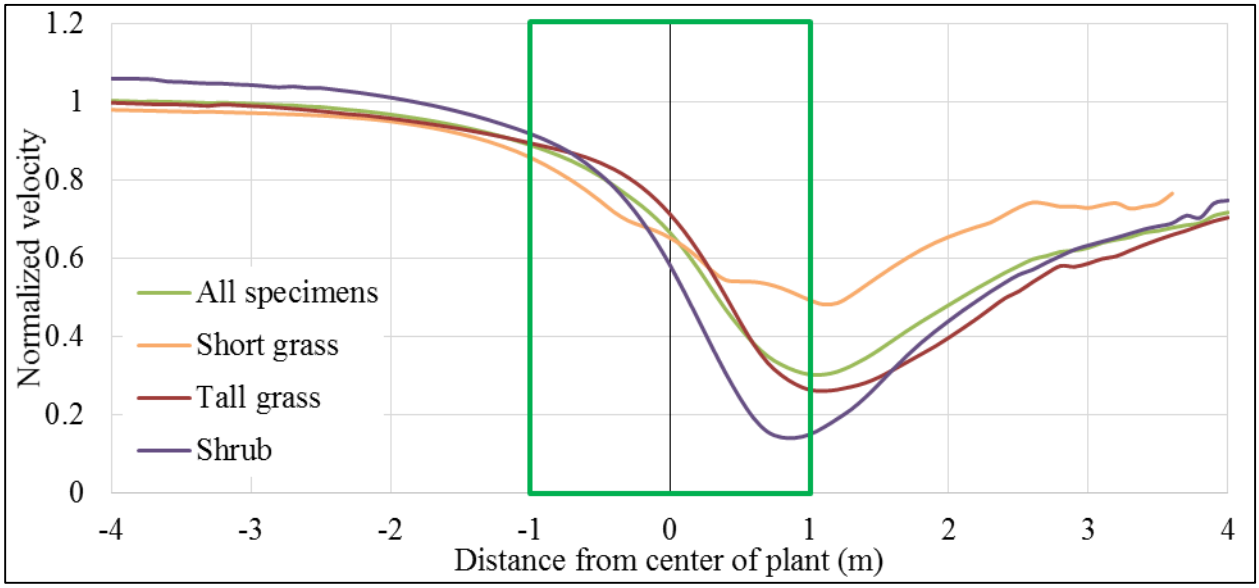

Figure 4.9. Normalized velocity along lines parallel to wind direction averaged for each morphology type. Negative x values indicate distance upwind while positive x values indicate distance downwind of the specimen center; and the green boxes indicate the approximate locations of specimen perimeters.

The different morphology types had different effects on velocity in the lee of the vegetation. The upwind influence of vegetation on velocity was alike for all morphology types. Flow was not altered by the vegetation at a distance of 1 m upstream of the leading edge of all specimens. At 0.5 m upstream of the leading edge of all specimens, velocity was decreased to an average of approximately 90% that of open beach velocity. Short grasses were the least effective at reducing velocity within and immediately downwind of the vegetation. Shrubs were most effective at reducing velocity downwind and therefore the greatest amount of deposition was expected in this area. Tall grasses reduced velocity by a lesser magnitude than shrubs but in a zone extending farther downwind. Consequently, it was expected that low amounts of deposition occurred downwind of short grasses and greater amounts of deposition were expected downwind of shrubs. Accordingly, deposition downwind of the tall grass was expected to be of lower magnitude than for the shrub, but covering a larger area. In order to examine differences in the influence on flow between specimens, all runs for each specimen are shown in Figure 4.10.

Both shrub specimens were consistently effective at reducing velocity directly in the lee of the vegetation, with velocity at this location averaging 15% of open beach velocity. Trends in normalized flow around tall grass specimens had a wide range of variability. The tall grass specimen from 2012 and the first specimen from 2014 had similar impacts on flow, with longer zones of deceleration downwind of the vegetation. The zone of deceleration downwind of the second 2014 tall grass specimen was smaller than the 2012 or first 2014 specimen. The 2013 tall grass specimen was much less effective at reducing velocity downwind than the other tall grass specimens, with a velocity reduction of 35-60% of open beach velocity at the lowest.

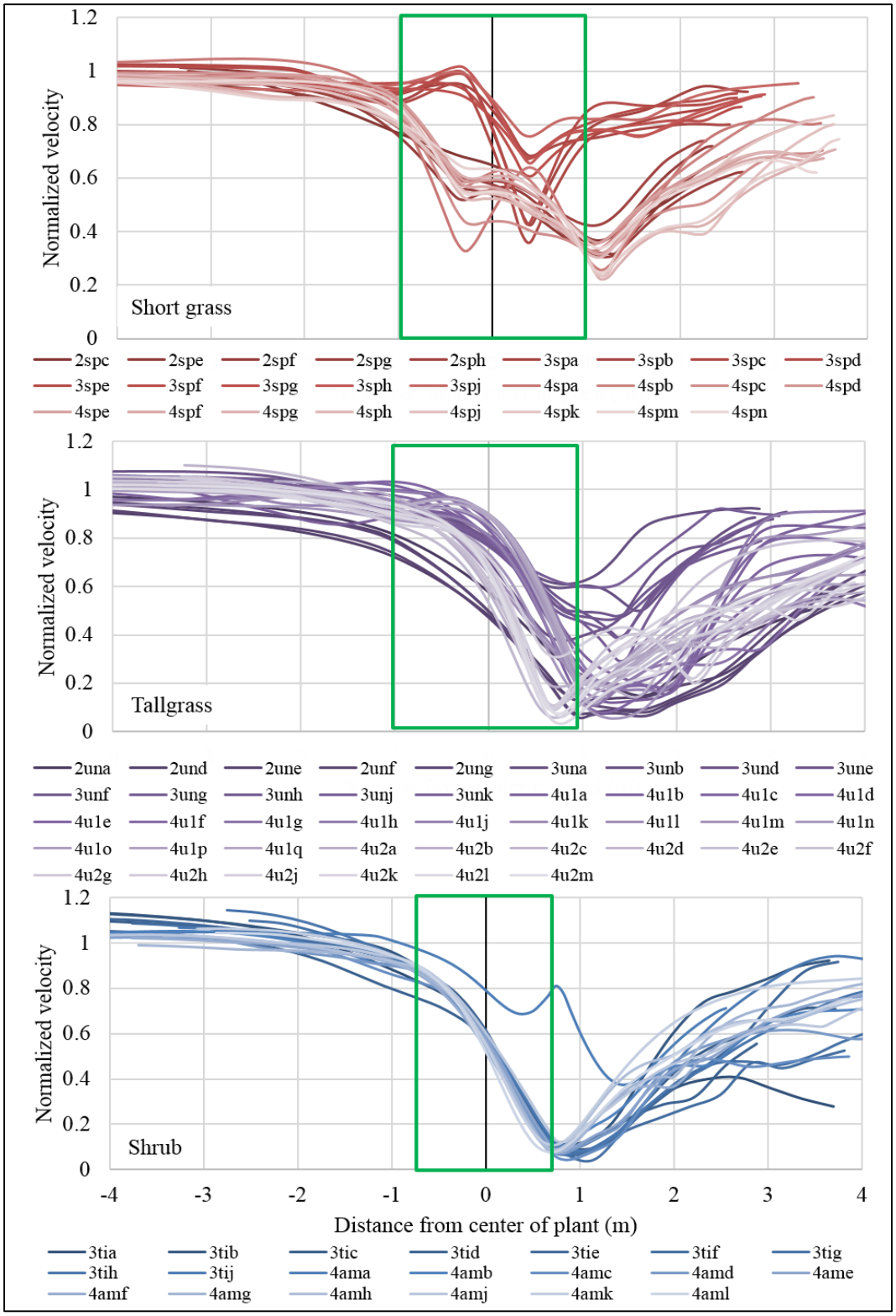

Figure 4.10. Normalized velocities parallel to wind direction through the center of specimens. Negative x values indicate distance upwind while positive x values indicate distance downwind of the specimen center; and the green boxes indicate the approximate locations of specimen perimeters.

There were substantial differences in the effect of flow caused by short grass specimens from 2012 and 2014 than the short grass specimen from 2013. The 2012 and 2014 specimens caused a 50-60% decrease in velocity in the first third of the plant and a minor increase in velocity (up 5%) at the second third of the plant. Velocity directly in the lee of these two specimens was 40% of open beach velocity. In contrast, the 2013 specimen had nearly the opposite influence on flow velocities in the streamwise direction. Velocity remained the same as or actually increased by 5-10% of open beach velocity in the first third of the specimen, decreased to 40-80% of open beach velocity in second third of specimen, and increased to 80% of open beach velocity directly in lee of the specimen. At 0.5 m downwind of the 2013 shot grass specimen, velocity was no less than 80% of open beach flow.

Leenders et al. (2007) found that near-surface wind velocity was reduced by 15% on average in an area downwind extending to 7 times the height of an isolated shrub. For the tall grass, this would be approximately 5.25-7 m downwind of the edge of vegetation 0.75-1 m high, 1.75 m downwind of the edge of the short grass (0.25 high), and 3.5 m downwind of the edge of the shrubs (0.5 m high). These findings did not hold for the short grass specimens of 2012 and 2014, which had velocities at 60-80% of open beach flow at 1.75 m downwind of the edge of vegetation, and they could not be evaluated for tall grass and shrub specimens because velocity data did not extend to this distance.

4.4.1.2 Lateral Impact of Vegetation on Flow

In order to evaluate the cross-stream effect of the presence of vegetation to the sides of a finite patch of vegetation, normalized velocity was extrapolated from interpolated rasters along lines perpendicular to the wind direction through the center of the plant. The first step was

comparing flow patterns between the different morphology types. Normalized velocity for each morphology type was averaged for all runs for each morphology type and shown in Figure 4.11.

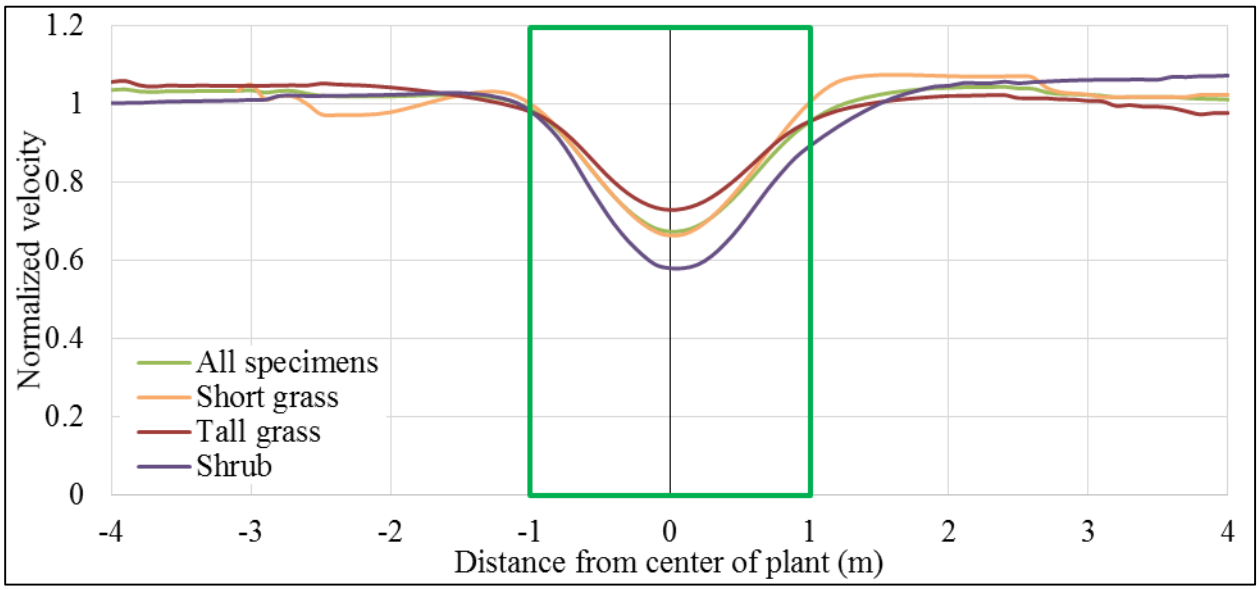

Figure 4.11. Average normalized velocity along lines perpendicular to wind direction through the center of vegetation for each morphology type. Negative x values indicate distance to the left of the specimen based on wind direction, and green boxes indicate the approximate locations of specimen perimeters.

Generally, vegetation did not alter fluid flow at a distance of 1.5 m from the center of the vegetation for all morphology types. Minor flow acceleration occurred immediately to the sides of the short grass. Acceleration did not occur immediately to the sides of tall grass or shrub morphology types. Flow reduction in the middle of the plant was less for the tall grass than the short grass. The shrub morphology was most effective at reducing velocity within the plant. Therefore, minor amounts of erosion were expected on the lateral edges of the short grass but not of the tall grass or shrub. A comparison of all runs for each specimen showed different effects on flow of the individual specimens (Figure 4.12).

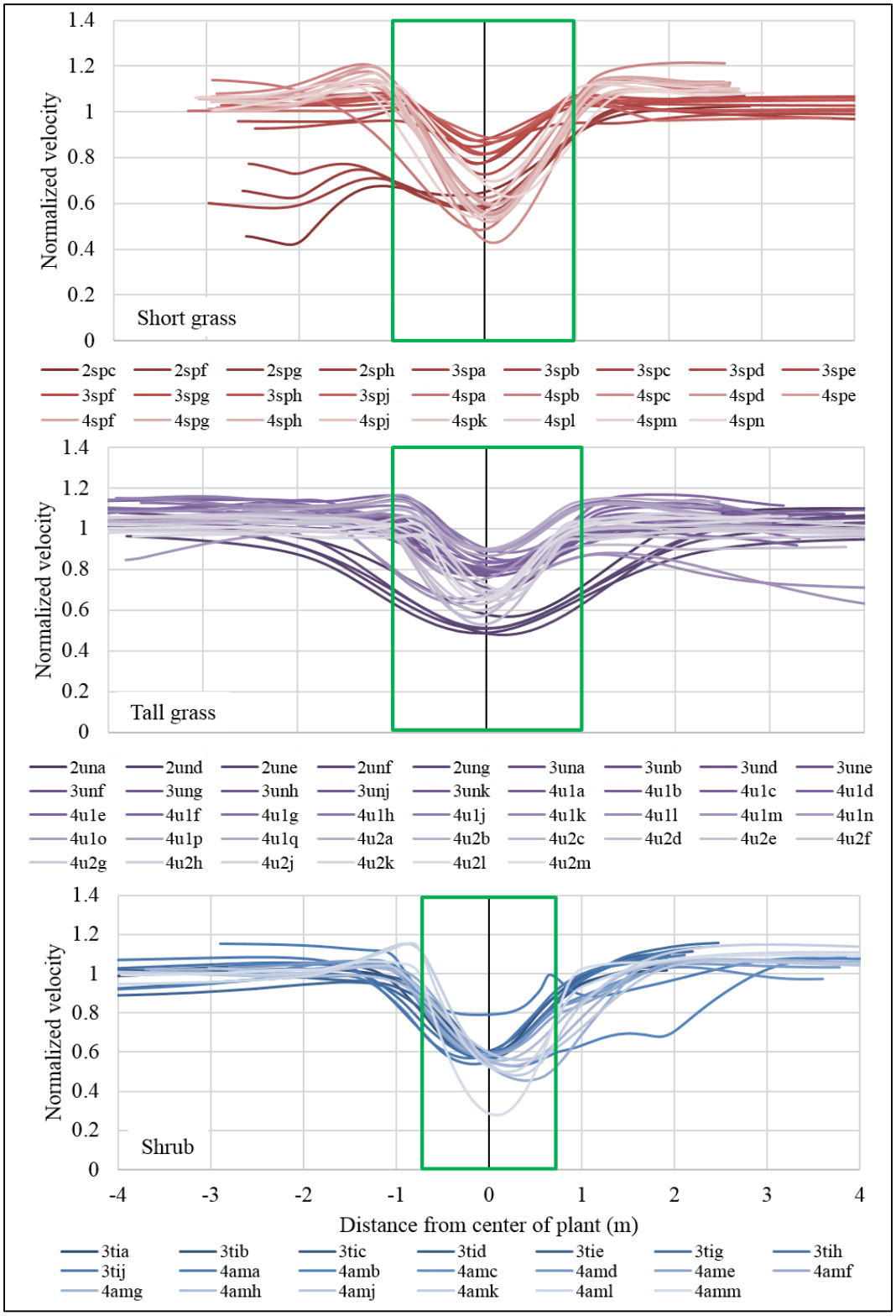

Figure 4.12. Normalized velocities along lines perpendicular to wind through the center of specimens. Negative x values indicate distance to the left of the specimen based on wind direction, and green boxes indicate the approximate locations of specimen perimeters.

This comparison revealed that greater velocity acceleration occurred on the lateral edges of the 2014 short grass specimen than for the other two short grass specimens. Also, flow acceleration occurred on the lateral edges of both 2014 tall grass specimens, but not on the 2012 or 2013 tall grass specimen. Flow patterns to the sides of the 2012 tall grass specimen were unlike the other three specimens for this morphology type in that flow was reduced up to 2 m away from the center of vegetation. Both shrubs exhibited similar influences on flow along lines perpendicular to the wind velocity through the center of vegetation, with flow reduction at the edges of this morphology type. As a result of these flow patterns, it was expected that greater erosion would occur to the sides of the 2014 short grass and both 2014 tall grass specimens.

4.4.1.3 Cross-stream Variation in Velocity Downwind of Vegetation

In order to examine the effect that vegetation had on downstream velocity, normalized velocity along lines perpendicular to wind direction 2 m downwind of specimen centers were extrapolated from interpolated rasters. Normalized velocity was averaged for all specimens of each type along these lines (Figure 4.13)

The short grass morphology produced a narrower zone of deceleration downwind of the plant than the other two morphology types. In fact, flow acceleration occurred downwind and to the sides of the short grass morphology type. The effect of the tall grass morphology and the shrub morphology were similar at this location, with reductions to 40-50% of open beach flow. A comparison of all runs for each specimen showed that flow downwind of the individual specimens had the greatest variability of any dataset (Figure 4.14).

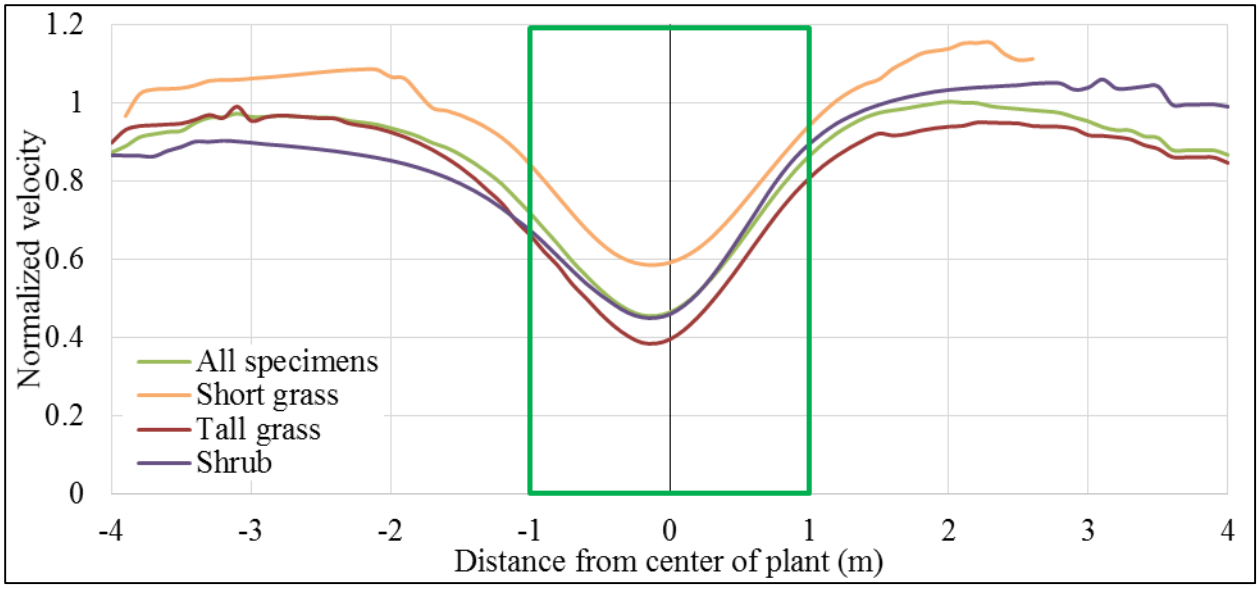

Figure 4.13. Average normalized velocity along lines perpendicular to wind direction 2 m downwind of the center of vegetation for each morphology type. Negative x values indicate distance to the left of the specimen based on wind direction, and green boxes indicate the approximate locations of specimen perimeters.

At the center line, the short grass specimens were less consistent and effective at reducing velocity (25-90% of open beach velocity) than shrub specimens (40-60% of open beach velocity) or tall grass specimens (40-50% of open beach velocity for 2012 and 2014 specimens, 60-80% of open beach velocity for 2013 specimen). The lowest proportional velocity was not always found at the centerline, where the line parallel through the center of vegetation intersected the cross-stream line. Instead, the location of the lowest velocity was often found within 1 m on either side of the centerline, indicating the tendency for the zone of deceleration to have an asymmetrical shape as the result of non-uniform wind and non-uniform vegetation morphology in the field. These data indicate the great deal of spatial variability in flow around specimens of similar morphology type and as well as between specimens of different morphology type, confirming the inherent variability of flow around live vegetation in a field setting.

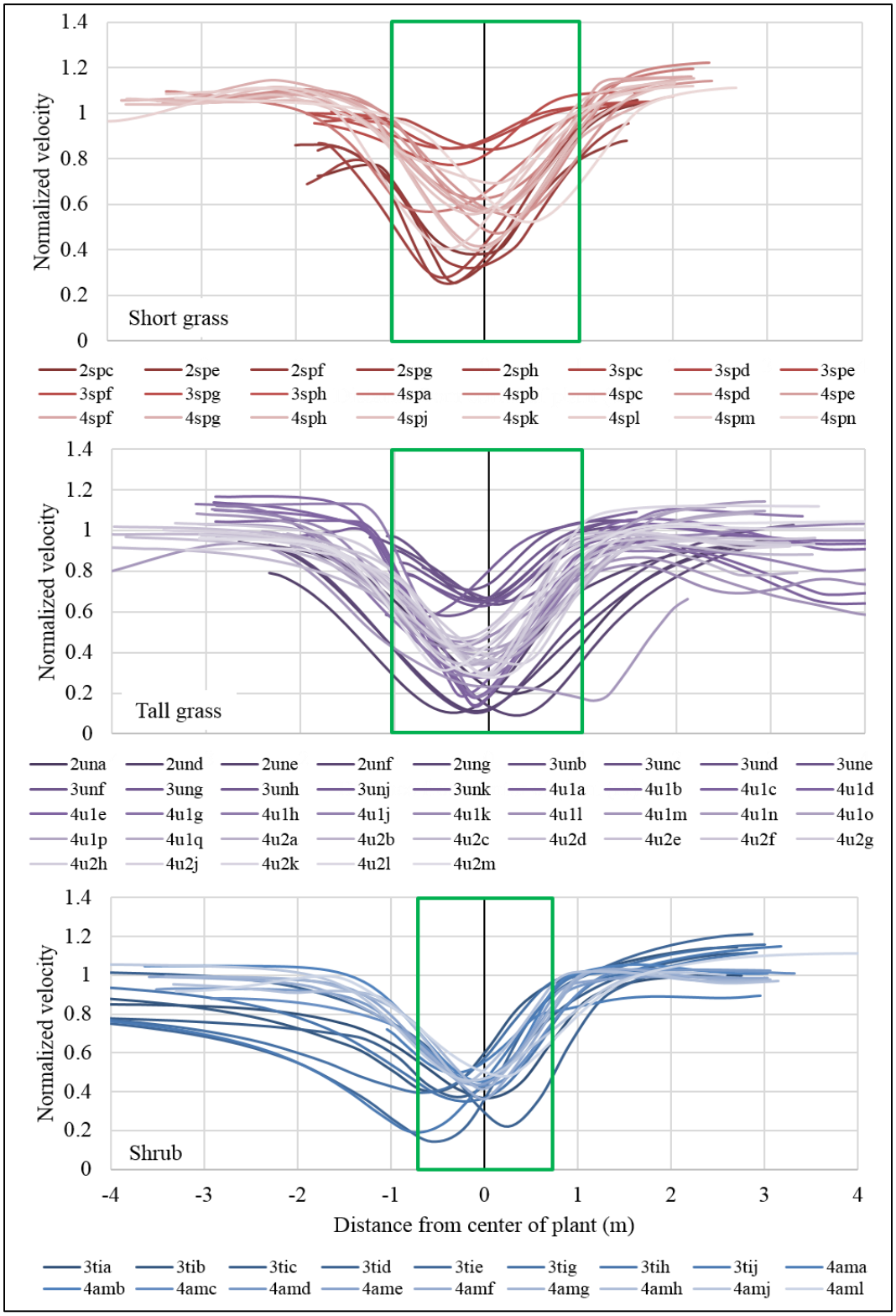

Figure 4.14. Normalized velocities along lines perpendicular to wind 2 m downwind of center of specimens. Negative x values indicate distance to the left of the specimen based on wind direction, and green boxes indicate the approximate locations of specimen perimeters.

4.4.2 Surface Elevation Changes

In order to assess the influence of vegetation morphology type on sediment transport patterns, changes in surface elevation were measured and analyzed surrounding short grass, tall grass, and shrub specimens. There were substantial differences in the spatial patterns of elevation change around the different species as well as between study periods for the same morphology type (Figure 4.15).

In 2013 minor deposition was concentrated in small areas directly in the lee of the tall grass (20-25 mm), within the perimeter of the short grass (20-25 mm), and in two areas to the side of the shrub (10-15 mm). The remainder of the study sites experienced erosion, which was typically concentrated on the lateral edges of specimens (40-45 mm for tall grass, 30 mm for short grass, and 20-25 mm for shrub).

In contrast, greater amounts of erosion and deposition occurred around specimens in 2014. In 2014 the greatest deposition around each specimen occurred on an axis which did not match the mean wind direction for the entire study period. The axis of greatest deposition for each specimen had a more north-south component than the mean wind direction. During the study period, wind direction shifts from southeasterly to more southerly so that the last half of the study period (days 6-10) was dominated by winds approaching from 125-155° (Figure 4.7E). These winds were also of higher velocity (8-12 m/s with the exception of half of day 9) than the rest of the study period (Figure 4.7D). Mean wind was determined using all winds during the study period with equal emphasis on winds during the first half and the second half of the study period. It is highly likely that winds during days 6-9 of 2014 field season had a stronger influence on sediment transport than winds during days 1-3. Even so, the greatest deposition occurred at the edges of the short grass (75 mm), with slightly less deposition measured within the shrub (35-40 mm) and directly

adjacent to both tall grass specimens (each with 40-45 mm). The isolated deposition at pin 19 for the 2014 shrub was an artifact of the edge effect of surrounding vegetation.

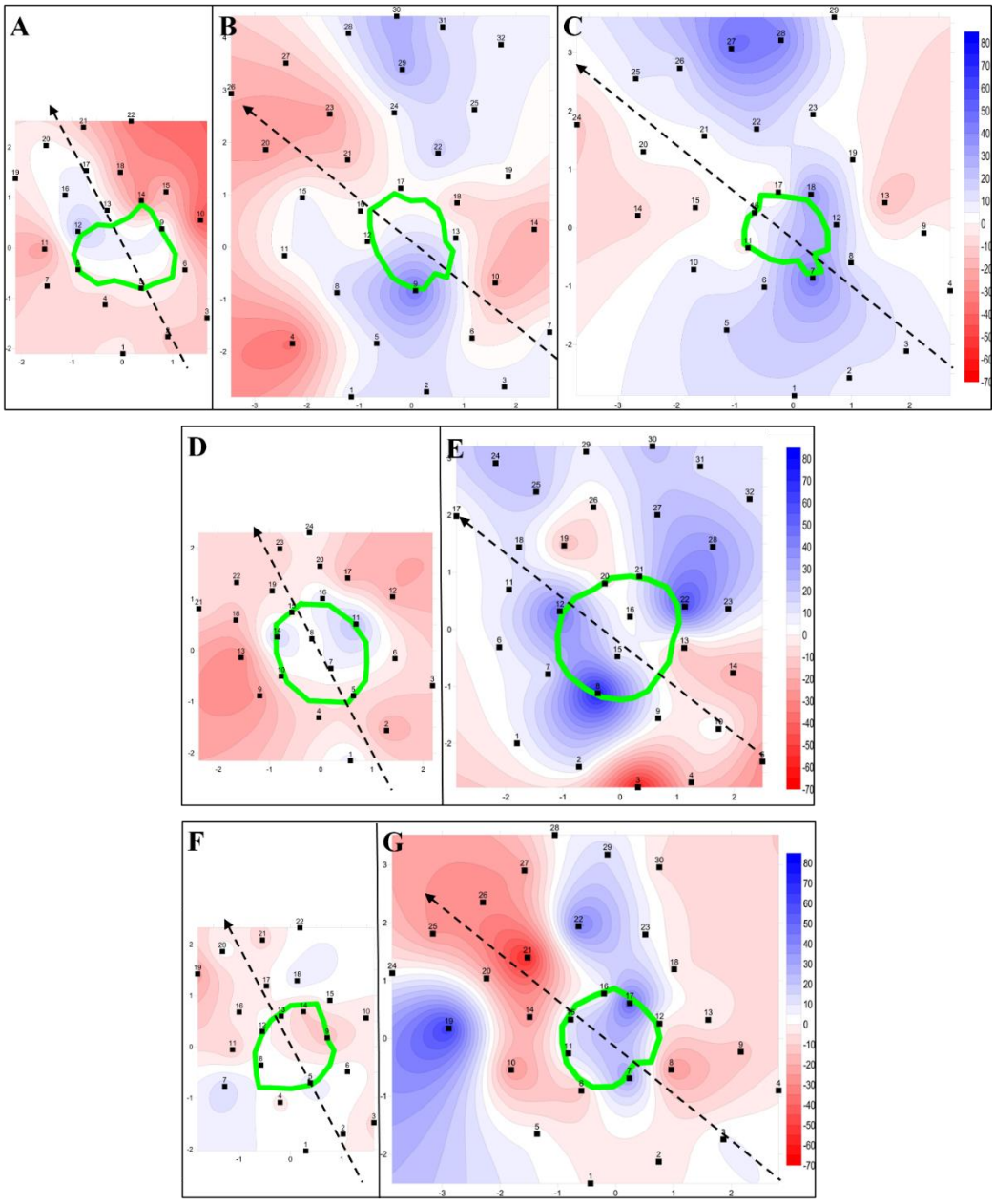

Figure 4.15. Surface elevation changes in mm for A) 2013 *Uniola*, B) 2014 *Uniola* 1, and C) 2014 *Uniola* 2, D) 2013 *Sporobolus*, E) 2014 *Sporobolus*, F) 2013 *Tidestromia*, and G) 2014 *Amaranthus*. Plant footprint denoted by green line. Erosion pin location signified by numbered squares. Dashed lines indicate average wind direction for study period.

In 2013 the areas surrounding the plants were dominated by erosion while deposition dominated the areas surrounding vegetation in 2014. This was likely a result of the characteristics of the beach surface. In 2013 dead Sargasso was pervasive and covered a majority of the entire beach, whereas Sargasso only covered the seaward portion of the dry beach (Figure 4.16). This clearly limited the supply of sediment from the beach, leading to a negative sediment budget and transportation out of the vegetation plots.

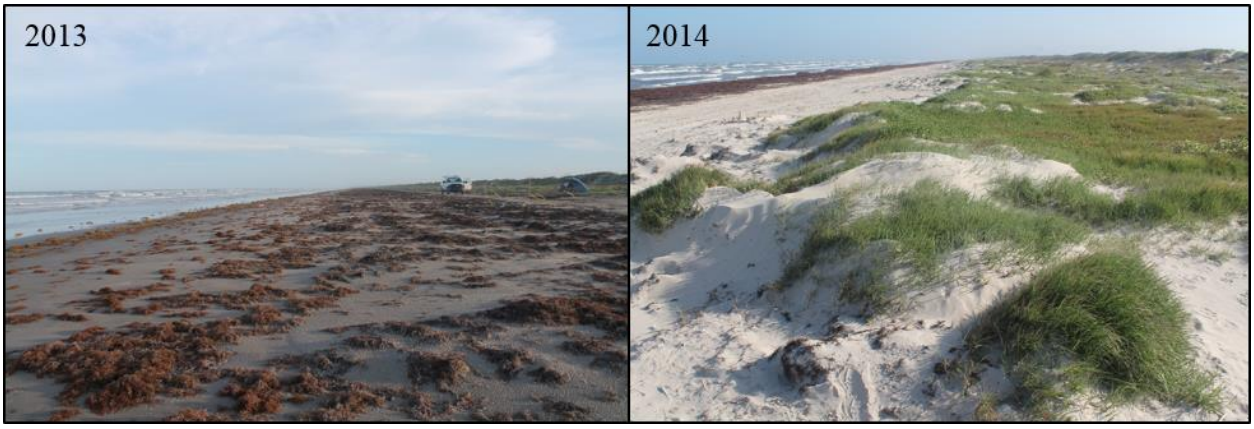

Figure 4.16 Cover and distribution of Sargasso in 2013 and 2014.

4.4.3 Comparison of Flow and Surface Elevation Change Patterns

The final step was comparing the distribution of zones of acceleration and deceleration around specimens to spatial patterns of deposition and erosion around specimens. Patterns of flow more closely correspond to zones of sediment deposition and erosion around specimens in 2013 than in 2014. Patterns in wind direction were more consistent throughout the study period in 2013 than 2014. Spatial patterns of erosion and deposition agree with patterns of wind velocity for the 2013 tall grass. Erosion occurred to the lateral sides of the vegetation, where wind velocity was slightly accelerated, and deposition occurred immediately in the lee where velocity was greatly reduced by the vegetation. Patterns of erosion and deposition deviated slightly from expected

patterns based on flow distribution around the short grass in 2013. Minor amounts of deposition occurred within and immediately to the side of the vegetation, with erosion higher at distances farther from the sides of the vegetation.

There was an incongruity between spatial patterns of normalized velocity and observed patterns of sediment deposition and erosion with respect to wind direction around specimens in 2014. The cause of this incongruity lies in the temporal resolution of the two datasets. Velocity for runs was recorded over a short period of time (3-minute intervals during a 40-minute run period) whereas wind data utilized in surface elevation change analysis were averaged over a 6-day or 9-day period. It is likely that a majority of the winds which caused the patterns of erosion and deposition seen in 2014 occurred in the latter half of the study period, during which time wind was stronger and had a more southerly component, than the first half of the 2014 study period.

4.5 Summary and Conclusions

The goal of this study was to document the spatial distribution of the aeolian flow field as well as sediment deposition and erosion around different species in the coastal embryo dune zone to identify the effects of different vegetation morphology types on these processes. There were considerable differences in spatial patterns of aeolian flow and of surface elevation change around the different species morphology types.

First, greater magnitude of total elevation change, both erosion and deposition, occurred around the two grasses in both years than around the shrubs. This suggests that natural coastal dune grasses have larger influences on aeolian processes than shrubs in this environment. More sediment deposition occurred because grasses were more effective at reducing shear stress than shrubs, indicating that grasses have higher drag coefficients than shrubs. This contrasts with the

work of Gillies et al. (2002), who found that the ornamental grass that they examined had lower drag coefficients at a range of velocities than the shrub and tree that they examined. It is difficult to extend their findings to the species examined herein, because species should have different drag coefficients based on density of blades and leaves (Dallavis et al., 2011; Leonard and Croft, 2006; Marshall, 1971; Neumeier, 2005; Neumeier and Amos, 2006), which is controlled by both biotic and abiotic factors. More research is needed concerning the range of drag coefficients for different species. It cannot be assumed that all grasses behave the same way with regard to drag, because species differ in blade/leaf size, shape, rigidity (i.e., ability to flex based on cell structure and water pressure within the blades/leaves/stems) (de Langre, 2008; Nilsson et al., 1958; Pavlik, 1984; Steudle et al., 1977) and stem and blade density of individuals (Arens et al., 2001; Moller, 2006; Neumeier, 2005).

Second, with regard to the effects of vegetation on flow, nearly all specimens altered flow upwind of the plant, decreasing velocity by as much as 20% within 0.5 m upwind of the edge of vegetation. This phenomenon has been observed in aeolian environments (Qian et al., 2012) as well as aquatic marsh environments, where velocity decreases upstream of the vegetation due to a high-pressure region generated by the leading edge of the vegetation (Chen et al., 2013). Essentially, the wind "feels" the vegetation before it actually touches the vegetation. As expected based on previous research (Dong et al., 2008; Zong and Nepf, 2010), flow was diverted around the sides of the vegetation and acceleration occurred. These zones of flow acceleration extended farther from the edges of the tall grass than the short grass or shrubs. In the lee of vegetation, the shrub and tall grass were both effective at reducing velocity, whereas the short grass was the least effective at reducing velocity downstream. The zone of deceleration downwind of tall grass

extended farther downwind and was larger than the shrubs, likely because the shrubs were 0.5 m high and ~0.5 m narrower than the tall grasses, which were 0.75-1 m high.

The short grass, *Sporobolus*, was the least effective at reducing velocity in the lee of the plant. In contrast, this short grass was the most effective at retaining sediment in 2013 and trapping sediment in 2014 in the area around the plant. Although the blades and inflorescences of the short grass do not protrude into the boundary layer by more than 0.25 m, the high density of blades of these short grasses decreased sediment transport and increased sediment capture, as Neumeier and Amos (2006) found with salt marsh vegetation.

Patterns in velocity and sediment transport around vegetation are likely dependent upon the specimens chosen for examination. There was considerable variability in the normalized velocities between specimens of the same morphology type. It is highly likely that blade/leaf density played a significant role in flow dynamics around specimens. A concurrent research experiment found that the 2013 short grass had a lower optical porosity at a range of wind velocity, which is related to flow permeability through the vegetation, than the 2014 short grass in 2-dimensional images of the 2013 and 2014 specimens from upwind (2013=0.0030, 2014=0.0054), perpendicular to the wind (2013=0.0054, 2014=0.0079), and overhead (2013=0.0093, 2014=0.0160). In the future, flow and deposition patterns should be recorded around a variety of specimens of the same species (therefore holding constant the biotic factors controlling rigidity of blades) with the same height but different blade densities in order to determine whether density or height is the dominant variable controlling the spatial distribution of velocity, shear stress, and sediment transport around this species.

Canopy, or roughness, density (Arens et al., 2001; Moller, 2006; Neumeier, 2005; Neumeier and Amos, 2006; Suter-Burri et al., 2013; Zarnetske et al., 2012) and height (Leenders

et al., 2011; Leenders et al., 2007; Webb et al., 2014) have separately been found to influence patterns of flow and sediment transport. In the future, it is necessary to determine how both density and height affect fluid flow and sediment transport patterns. This is achievable by documenting flow around specimens of similar height with different densities, which should be explored in future research.

In conclusion, the individual morphology of the various species examined herein had a tangible influence on aeolian fluid dynamics and associated sediment transport dynamics. Flow retardation occurred within 0.5 m of the leading edge of vegetation regardless of specimen morphology type, while flow acceleration occurred on both sides of the vegetation within 0.5 m of the edge of vegetation. In the lee of the vegetation, the tall, dense grass specimens were most effective at reducing velocity to a greater extent than the short grass, and in a larger area than the rigid shrubs. Contrary to expectations, the short grass, which reduced velocity to a much lesser extent in the lee of the plant than both tall grass and shrub specimens, caused the least amount of erosion in one study period and the greatest deposition in the area surrounding it in the other study period. The area surrounding the rigid shrub experienced the lowest magnitude of surface elevation change of all three morphology types.

Natural unsteadiness in wind direction and velocity proved to be a complicating factor in analysis. While the intention of this study was to examine *in situ* processes and dynamics, the next step must involve either significantly larger data sets collected in the field, or placement of live plants in a wind tunnel where wind is steadier and shear stress and turbulence can be measured direction without sand present.

4.6 References

Arens, S.M., Baas, A.C.W., Van Boxel, J.H., Kalkman, C., 2001. Influence of reed stem density on foredune development. Earth Surface Processes and Landforms, 26(11), 1161-1176.

Bagnold, R.A., 1941. The Physics of Blown Sand and Desert Dunes. Methuen, London.

Brown, S., Nickling, W.G., Gillies, J.A., 2008. A wind tunnel examination of shear stress partitioning for an assortment of surface roughness distributions. Journal of Geophysical Research-Earth Surface, 113(F2).

Buckley, R., 1987. The effect of sparse vegetation on the transport of dune sand by wind. Nature, 325(6103), 426-428.

Burri, K., Gromke, C., Lehning, M., Graf, F., 2011. Aeolian sediment transport over vegetation canopies: A wind tunnel study with live plants. Aeolian Research, 3(2), 205-213.

Chen, Z., Jiang, C., Nepf, H., 2013. Flow adjustment at the leading edge of a submerged aquatic canopy. Water Resources Research, 49(9), 5537-5551.

Crawley, D.M., Nickling, W.G., 2003. Drag partition for regularly-arrayed rough surfaces. Boundary-Layer Meteorology, 107(2), 445-468.

Dallavis, K.C., Henderson, S.M., Mullarney, J.C., 2011. Wave dissipation by flexible vegetation. Geophysical Research Letters.

de Langre, E., 2008. Effects of wind on plants. Annual Review of Fluid Mechanics, 40(1), 141-168.

Dong, Z.B., Luo, W.Y., Qian, G.Q., Lu, P., 2008. Wind tunnel simulation of the three-dimensional airflow patterns around shrubs. Journal of Geophysical Research-Earth Surface, 113(F2).

Ghisalberti, M., Nepf, H., 2006. The structure of the shear layer in flows over rigid and flexible canopies. Environ. Fluid Mech., 6(3), 277-301.

Gilbert, M., Pammenter, N., Ripley, B., 2008. The growth response of coastal dune species are determined by nutrient limitation and sand burial. Oecologia, 156, 169-178.

Gillies, J.A., Lancaster, N., Nickling, W.G., Crawley, D.M., 2000. Field determination of drag forces and shear stress partitioning effects for a desert shrub (Sarcobatus vermiculatus, greasewood). J. Geophys. Res.-Atmos., 105(D20), 24871-24880.

Gillies, J.A., Nickling, W.G., King, J., 2002. Drag coefficient and plant form response to wind speed in three plant species: Burning Bush (Euonymus alatus), Colorado Blue Spruce (Picea pungens glauca.), and Fountain Grass (Pennisetum setaceum). J. Geophys. Res.-Atmos., 107(D24).

Gillies, J.A., Nickling, W.G., King, J., 2006. Aeolian sediment transport through large patches of roughness in the atmospheric inertial sublayer. Journal of Geophysical Research-Earth Surface, 111(F2).

Gillies, J.A., Nickling, W.G., King, J., 2007. Shear stress partitioning in large patches of roughness in the atmospheric inertial sublayer. Boundary-Layer Meteorology, 122(2), 367-396.

Gillies, J.A., Nield, J.M., Nickling, W.G., 2014. Wind speed and sediment transport recovery in the lee of a vegetated and denuded nebkha within a nebkha dune field. Aeolian Research, 12(0), 135-141.

Grant, P.F., Nickling, W.G., 1998. Direct field measurement of wind drag on vegetation for application to windbreak design and modelling. Land Degradation & Development, 9(1), 57-66.

Gunatilaka, A., Mwango, S.B., 1989. Flow separation and the internal structure of shadow dunes. Sedimentary Geology, 61(1–2), 125-134.

Jia, Y., Sill, B.L., Reinhold, T.A., 1998. Effects of surface roughness element spacing on boundary-layer velocity profile parameters. Journal of Wind Engineering and Industrial Aerodynamics, 73(3), 215-230.

King, J., Nickling, W.G., Gillies, J.A., 2005. Representation of vegetation and other nonerodible elements in aeolian shear stress partitioning models for predicting transport threshold. Journal of Geophysical Research-Earth Surface, 110(F4).

Krebs, C.J., 1972. Ecology. The Experimental Analysis of Distribution and Abundance. Harper and Row, New York.

Lancaster, N., Baas, A., 1998. Influence of vegetation cover on sand transport by wind: Field studies at Owens Lake, California. Earth Surface Processes and Landforms, 23(1), 69-82.

Leenders, J.K., Sterk, G., Van Boxel, J.H., 2011. Modelling wind-blown sediment transport around single vegetation elements. Earth Surface Processes and Landforms, 36(9), 1218-1229.

Leenders, J.K., van Boxel, J.H., Sterk, G., 2007. The effect of single vegetation elements on wind speed and sediment transport in the Sahelian zone of Burkina Faso. Earth Surface Processes and Landforms, 32(10), 1454-1474.

Leonard, L.A., Croft, A.L., 2006. The effect of standing biomass on flow velocity and turbulence in Spartina alterniflora canopies. Estuar. Coast. Shelf Sci., 69(3-4), 325-336.

Luhar, M., Nepf, H.M., 2013. From the blade scale to the reach scale: A characterization of aquatic vegetative drag. Advances in Water Resources, 51(0), 305-316.

Luhar, M., Rominger, J., Nepf, H., 2008. Interaction between flow, transport and vegetation spatial structure. Environ. Fluid Mech., 8(5-6), 423-439.

Luo, W.Y., Dong, Z.B., Qian, G.Q., Lu, J.F., 2012. Wind tunnel simulation of the three-dimensional airflow patterns behind cuboid obstacles at different angles of wind incidence, and their significance for the formation of sand shadows. Geomorphology, 139, 258-270.

Marshall, J.K., 1971. Drag measurements in roughness arrays of varying density and distribution. Agricultural Meteorology, 8(4-5), 269-&.

Mattis, S.A., Dawson, C.N., Kees, C.E., Farthing, M.W., 2012. Numerical modeling of drag for flow through vegetated domains and porous structures. Advances in Water Resources, 39(0), 44-59.

Moller, I., 2006. Quantifying saltmarsh vegetation and its effect on wave height dissipation: Results from a UK East coast saltmarsh. Estuar. Coast. Shelf Sci., 69(3-4), 337-351.

Musick, H.B., Trujillo, S.M., Truman, C.R., 1996. Wind-tunnel modelling of the influence of vegetation structure on saltation threshold. Earth Surface Processes and Landforms, 21(7), 589-605.

Nepf, H.M., 1999. Drag, turbulence, and diffusion in flow through emergent vegetation. Water Resources Research, 35(2), 479-489.

Neumeier, U., 2005. Quantification of vertical density variations of salt-marsh vegetation. Estuar. Coast. Shelf Sci., 63(4), 489-496.

Neumeier, U., 2007. Velocity and turbulence variations at the edge of saltmarshes. Cont. Shelf Res., 27(8), 1046-1059.

Neumeier, U., Amos, C.L., 2006. The influence of vegetation on turbulence and flow velocities in European salt-marshes. Sedimentology, 53(2), 259-277.

Nilsson, S.B., Hertz, C.H., Falk, S., 1958. On the relation between turgor pressure and tissue rigidity. II. Physiologia Plantarum, 11(4), 818-837.

Okin, G.S., 2008. A new model of wind erosion in the presence of vegetation. Journal of Geophysical Research-Earth Surface, 113(F2).

Pasquill, F., 1950. The aerodynamic drag of grassland. Proceedings of the Royal Society of London Series a-Mathematical and Physical Sciences, 202(1068), 143-153.

Pavlik, B.M., 1984. Seasonal changes of osmotic pressure, symplasmic water content and tissue elasticity in the blades of dune grasses growing in situ along the coast of Oregon. Plant, Cell & Environment, 7(7), 531-539.

Qian, G.Q., Dong, Z.B., Luo, W.Y., Zhang, Z.C., Zhao, A.G., 2012. Airflow patterns upwind of obstacles and their significance for echo dune formation: A field measurement of the effects of the windward slope angle. Sci. China-Earth Sci., 55(4), 545-553.

Raupach, M.R., 1992. Drag and drag partition on rough surfaces. Boundary-Layer Meteorology, 60(4), 375-395.

Raupach, M.R., Gillette, D.A., Leys, J.F., 1993. The effect of roughness elements on wind erosion threshold. J. Geophys. Res.-Atmos., 98(D2), 3023-3029.

Schlichting, H., 1936. Experimental investigation of the problem of surface roughness. Ingeniur Archiv., 7, 1-34.

Schmutz, P., 2007. Investigation of utility of delta-t thetaprobe for obtaining surficial moisture measurements on beaches. M.S., Louisiana State University, Baton Rouge, 114 pp.

Siniscalchi, F., Nikora, V.I., 2012. Flow-plant interactions in open-channel flows: A comparative analysis of five freshwater plant species. Water Resources Research, 48(5), W05503.

Siniscalchi, F., Nikora, V.I., Aberle, J., 2012. Plant patch hydrodynamics in streams: Mean flow, turbulence, and drag forces. Water Resources Research, 48(1), W01513.

Steudle, E., Zimmermann, U., Lüttge, U., 1977. Effect of turgor pressure and cell size on the wall elasticity of plant cells. Plant Physiology, 59(2), 285-289.

Suter-Burri, K., Gromke, C., Leonard, K.C., Graf, F., 2013. Spatial patterns of aeolian sediment deposition in vegetation canopies: Observations from wind tunnel experiments using colored sand. Aeolian Research, 8(0), 65-73.

Sutton, S.L.F., McKenna-Neuman, C., 2008. Variation in bed level shear stress on surfaces sheltered by nonerodible roughness elements. Journal of Geophysical Research-Earth Surface, 113(F3).

Udo, K., Takewaka, S., 2007. Experimental study of blown sand in a vegetated area. Journal of Coastal Research, 23(5), 1175-1182.

Walter, B., Gromke, C., Lehning, M., 2012a. Shear-stress partitioning in live plant canopies and modifications to Raupach's model. Boundary-Layer Meteorology, 144(2), 217-241.

Walter, B., Gromke, C., Leonard, K.C., Manes, C., Lehning, M., 2012b. Spatio-temporal surface shear-stress variability in live plant canopies and cube arrays. Boundary-Layer Meteorology, 143(2), 337-356.

Webb, N.P., Okin, G.S., Brown, S., 2014. The effect of roughness elements on wind erosion: The importance of surface shear stress distribution.

Wolfe, S.A., Nickling, W.G., 1993. The protective role of sparge vegetation in wind erosion. Progress in Physical Geography, 17(1), 50-68.

Wolfe, S.A., Nickling, W.G., 1996. Shear stress partitioning in sparsely vegetated desert canopies. Earth Surface Processes and Landforms, 21(7), 607-619.

Wyatt, V.E., Nickling, W.G., 1997. Drag and shear stress partitioning in sparse desert creosote communities. Can. J. Earth Sci., 34(11), 1486-1498.

Zarnetske, P.L., Hacker, S.D., Seabloom, E.W., Ruggiero, P., Killian, J.R., Maddux, T.B., Cox, D., 2012. Biophysical feedback mediates effects of invasive grasses on coastal dune shape. Ecology, 93(6), 1439-1450.

Zong, L., Nepf, H., 2010. Flow and deposition in and around a finite patch of vegetation. Geomorphology, 116(3–4), 363-372.

Zuo, X., Zhao, H., Zhao, X., Guo, Y., Li, Y., Luo, Y., 2008. Plant distribution at the mobile dune scale and its relevance to soil properties and topographic features. Environmental Geology, 54, 1111-1120.

Chapter 5. Summary and Conclusions

The goal of this dissertation was to improve understanding of how vegetation influences aeolian fluid flow and sediment transport patterns in the coastal embryo dune environments. Three studies were undertaken – one to document larger-scale vegetation community dynamics, a second to investigate the morphology response of vegetation to changes in wind velocity, and a third to quantify spatial patterns of flow and deposition around vegetation. Chapters 2-4 presented empirical findings from field research conducted in 2012-2013 in an embryo dune environment along the Gulf of Mexico coast.

5.1 Empirical Findings

This section presents a summary of findings from the field experiments. The objective for Chapter 2 was to document and quantify spatiotemporal trends in vegetation community composition, including trends in species abundance and diversity. Two major findings emerged from of this chapter. First, there were significant inter-annual variations in 5 of the 12 major species, where 2 species increased cover through time and 3 species decreased cover through time. Changes in species abundance signify the active and continuing process of community succession which began following the establishment of the national seashore in 1962 and the subsequent cessation of cattle ranching practices which had severely disturbed the landscape. The second important finding from chapter 2 is that the embryo dune zone, which has previously been considered as one environment, is in fact divisible into sub-environments as determined by community assemblage. The foredune slope and rear of the embryo dune zone, which were the most stable sub-environments, were occupied by *Croton punctatus*, *Panicum amarum*, *Atriplex acanthocarpa*, *Oenethera drumondii*, and *Ipomoea imperati* as well as two rare species

Chamaecrista spp. and *Hydrocotile bonariensis*. In contrast, the seaward edge of the embryo dune zone was colonized by *Tidestromia lanuginosa*, *Sesuvium portulacastrum*, and *Amaranthus* greggii. These pioneer species promoted deposition of sand transported from the beach by wind.

Chapters 3 and 4 focused on distinctions between three different vegetation morphology types which naturally occur in the embryo dune environment – tall grass, short grass, and shrub. Chapter 3 was designed to evaluate the applicability of several different parameters to measure morphology changes of different species as a function of wind velocity. There were significant differences in plant area, pore area, and optical porosity of the different morphology types, with the latter presenting the greatest implication for flow. The tall grass, the morphology type which occupied the largest volume, also had the largest optical porosity. The short grass, which occupied a smaller area, had 56% of the optical porosity of the tall grass. The shrubs were the densest morphology type, with 65% the optical porosity of the short grass, and also occupied the smallest volume.

Most importantly Chapter 3 explored the three-dimensional nature of vegetation response to wind flow. Findings demonstrated that vegetation morphology indeed changed as a result of wind velocity, where plant area from the front increased as a function of velocity while plant area from the top decreased. As plants became more streamlined in higher velocities, compression occurred in the vertical dimension with blades bending and aligning parallel to wind direction. At the same time, extension of the plant shape occurred in the horizontal dimension, as the blades and leaves of plants flattened out in response to greater wind velocities. Pore area and optical porosity are not appropriate measures for the purpose of analyzing the effect of velocity on plant on aerodynamic porosity. Three-dimensional pore spaces were not detectable in two-dimensional

projections of vegetation. Further research should include exploring other technologies for measuring aerodynamic porosity.

Chapter 4 sought to document and analyze spatial patterns of fluid flow and sediment erosion and deposition around species with different morphologies. While all examined species generated a zone of deceleration and deposition within 0.5 m upwind, results showed considerable differences in patterns of flow and sediment deposition in the lee of different morphology types. Tall grasses, such as *Uniola paniculata*, develop shadow dunes that cover large areas because they obtrude higher into the boundary layer flow and develop a large, intense deceleration zone in their lee. On the other hand, short grasses, such as *Sporobolus virginicus*, do not reduce velocity in their lee to the same extent as large grasses but are effective at trapping saltating grains, causing large magnitude of deposition within and directly around the edges of a finite patch. Shrubs, while most effective at reducing the velocity, only reduce flow in a small area in their lee as a result of their compact and dense nature. Thus findings presented in Chapter 4 indicate that the role of vegetation in aeolian processes is dependent upon the morphology of a given species.

Chapters 3 and 4 demonstrate that there is a tradeoff between overall size and optical porosity. While the tall grass had the largest size and thus should have been the most effective at trapping sediment, it also had the highest optical porosity and thus greatest turbulence behind the plant, reducing the amount of deposition. The short grass was of a smaller size, particularly shorter height than the other species, and thus less effective at reducing velocity downstream. However, the short grass had roughly half the optical porosity of the tall grass, and thus it was more effective at trapping larger amounts of sediment than the other two morphology types. The shrub, which had lowest optical porosity, also occupied the smallest total volume and so the area where it

effectively reduced velocity was limited to a small zone directly in the lee of the plant, and consequently the least amount of deposition was observed around this type of vegetation.

Currently it is not feasible to apply shear stress partitioning models in real world environments where roughness element morphology is neither static nor the same for all roughness elements. The findings of chapter 3 and 4 have significant ramifications in terms of modeling shear stress and sediment transport in highly complex coastal embryo dune environments. Results demonstrate that species in the coastal embryo dune environment interact with aeolian processes in different manners depending on their morphology. The findings of this dissertation reinforce the need to develop parameters that allow for incorporations of variable roughness object morphology into shear stress partitioning models.

Furthermore, the findings of this research show that management of coastal dune restoration projects can be enhanced by including a multi-species approach to dune restoration projects, wherein species of different morphology are interspersed during planting. Each species within the coastal embryo dune and foredune environments affects wind flow differently based on morphology and growth habit. Tall grasses reduce velocity more effectively and over a larger area than shrubs, or short grasses. However, findings also indicate that short grasses, while they do not reduce velocity to as great an extent as tall grasses or shrubs, are capable of trapping larger amounts of sediment, promoting deposition and dune formation and growth.

5.2 Future Research Needs

This dissertation represents an advance in our understanding of the role of vegetation, specifically of different species, in aeolian processes within the embryo dune environment. However, additional research is essential before it will become possible to model shear stress and

sediment transport in embryo dune environments. The two avenues which will need to be explored before a model can be developed are 1) drag coefficients specific to individual species, and 2) spatial patterns of turbulence surrounding different morphology types. Once these topics have been investigated further, it will be possible to augment existing shear stress partitioning models in order to simulate dune evolution in coastal embryo dune environments.

Appendix A. Species Percent Cover

The following figure show the percent cover of each of the major species in Chapter 2, richness, and diversity in each plot along transects for the study years 2012, 2013, and 2014. In each of the following figures, the topography of each transect in each year (represented as lines) overlays the vegetation data, which are represented as bars for the plots in which they were measured, or calculated for richness and diversity. The elevation profile and the vegetation data from each year are represented by the same color.

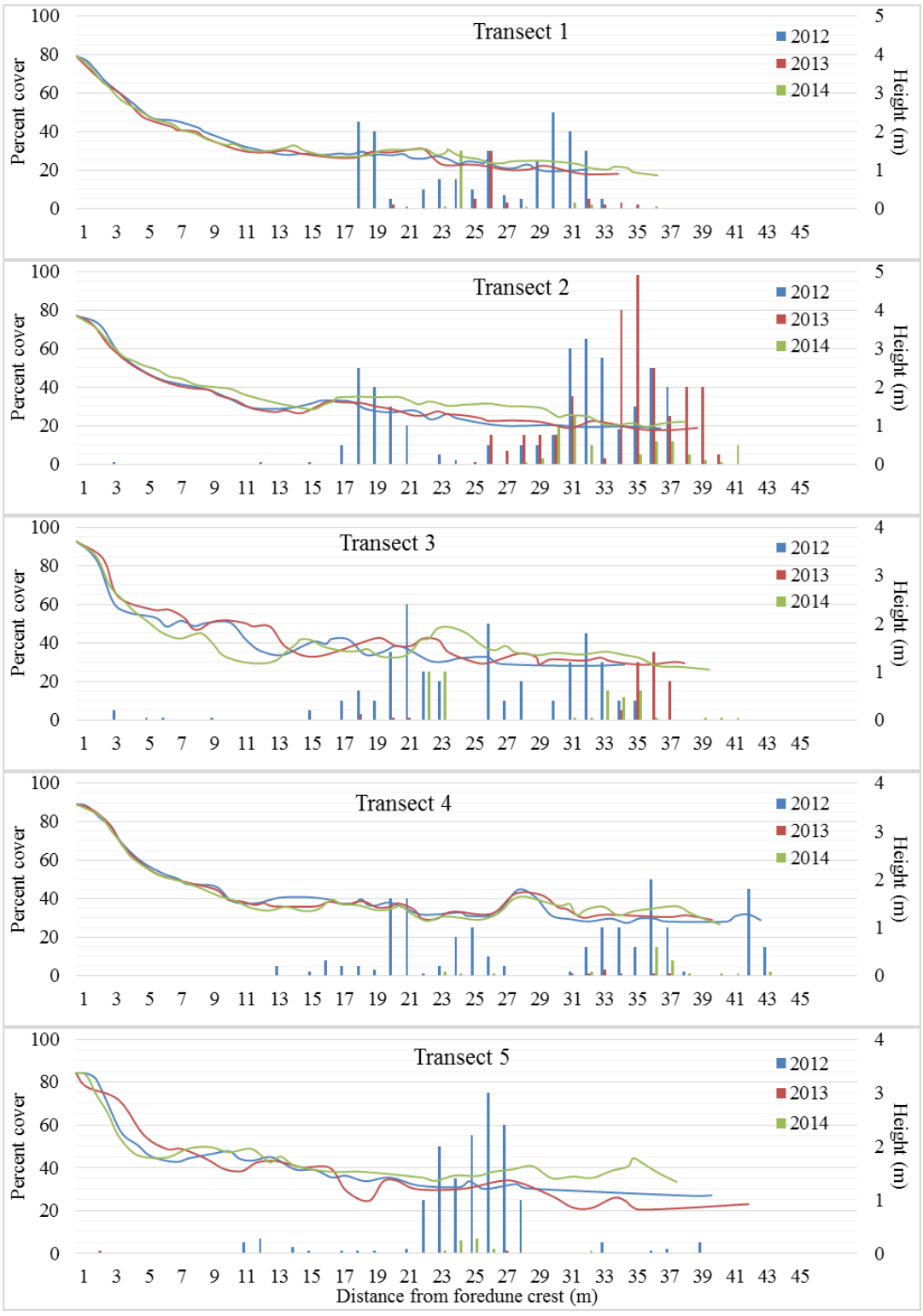

Figure A1. Percent cover of *Amaranthus* along transects.

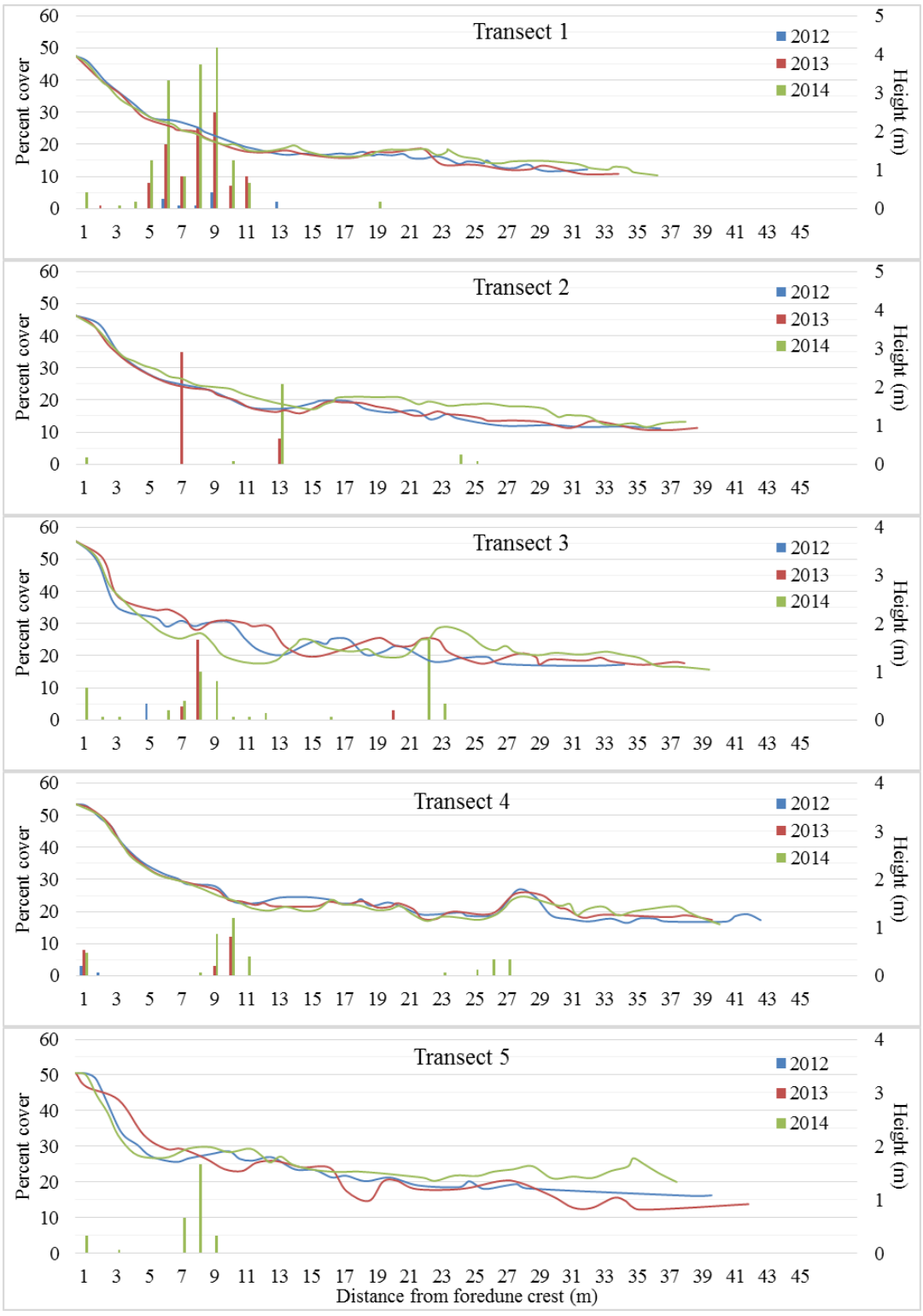

Figure A2. Percent cover of *Atriplex* along transects.

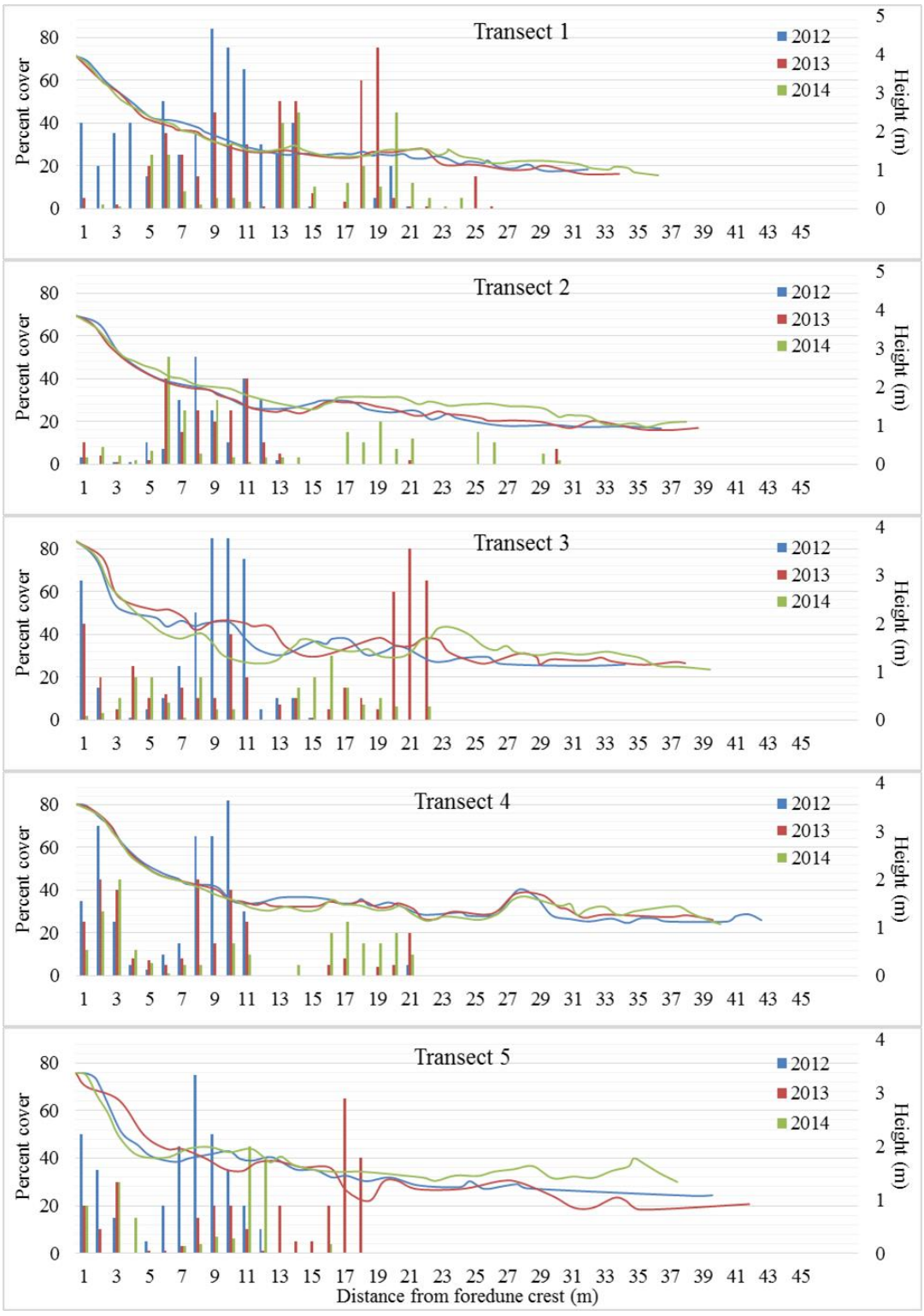

Figure A3. Percent cover of *Croton* along transects.

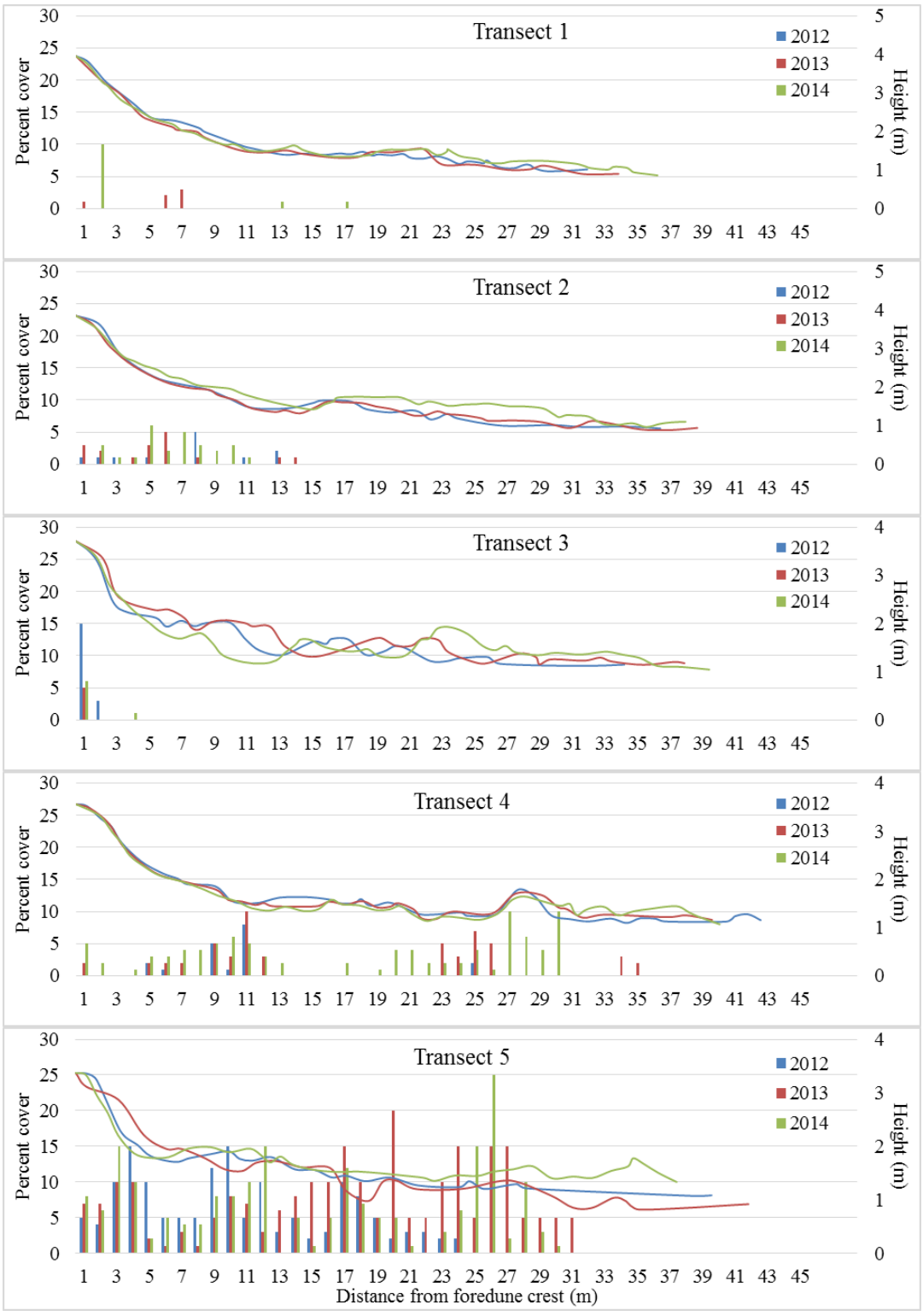

Figure A4. Percent cover of *I. imperati* along transects.

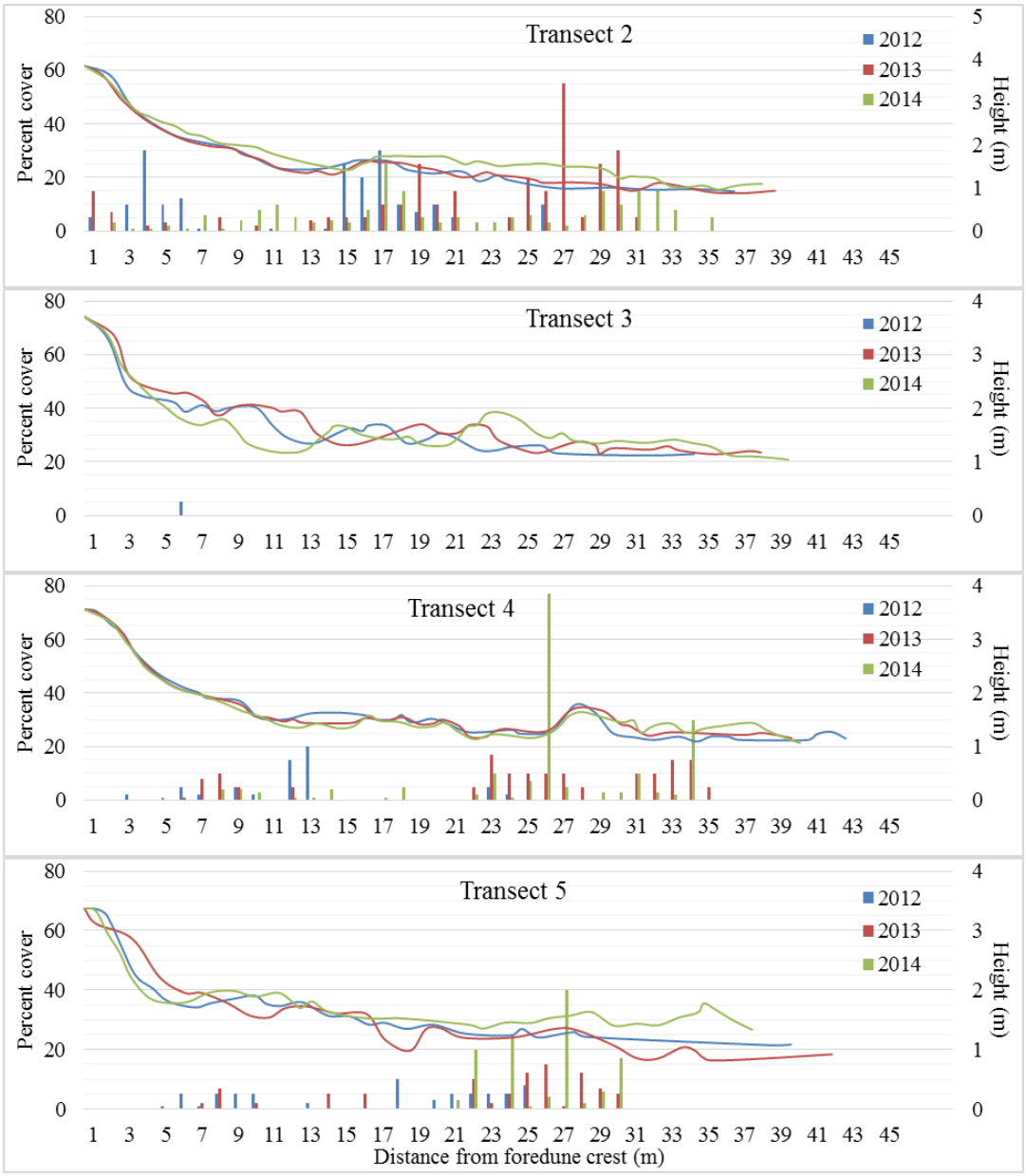

Figure A5. Percent cover of *I. pes-caprae* along transects.

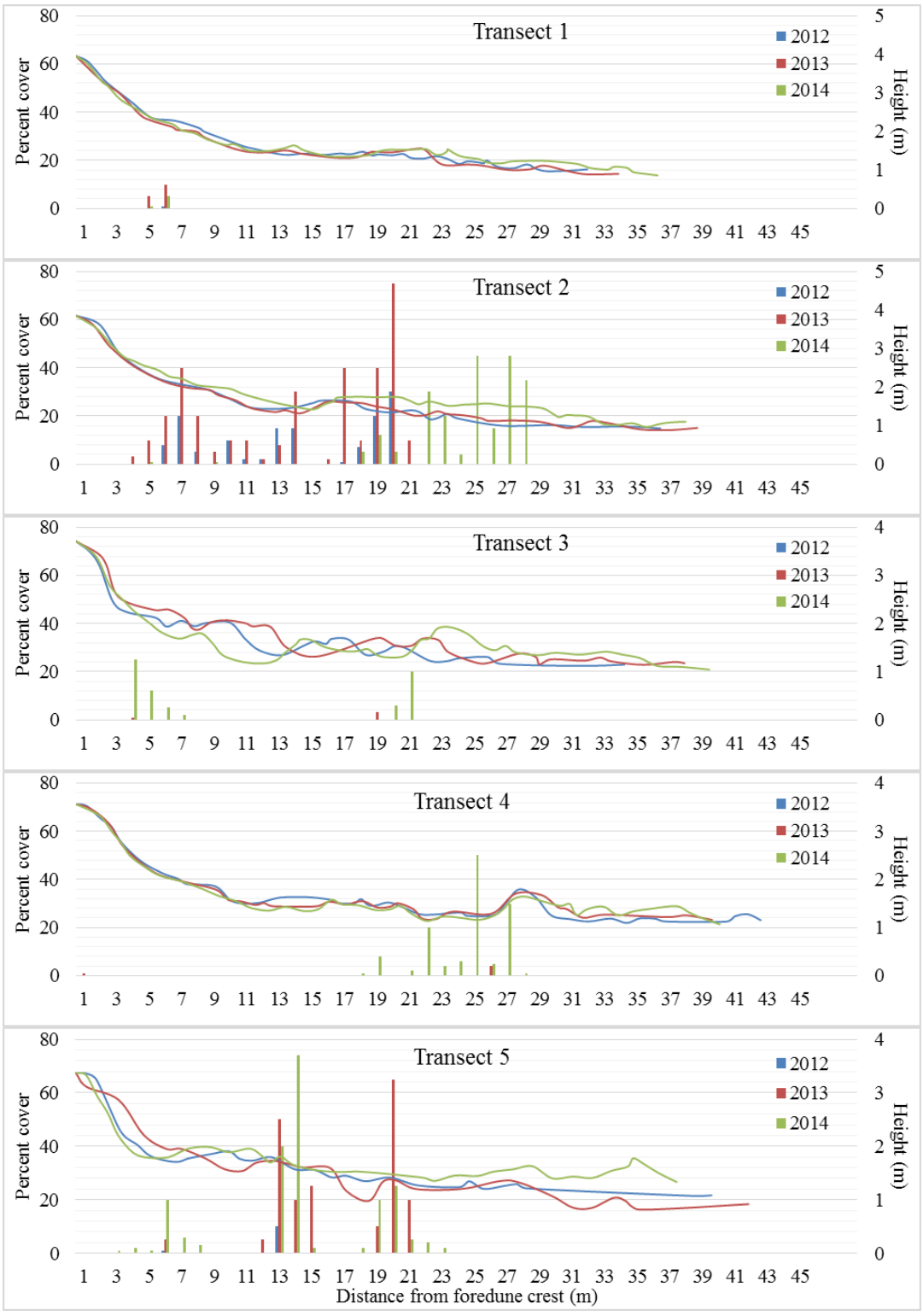

Figure A6. Percent cover of *Oenethera* along transects.

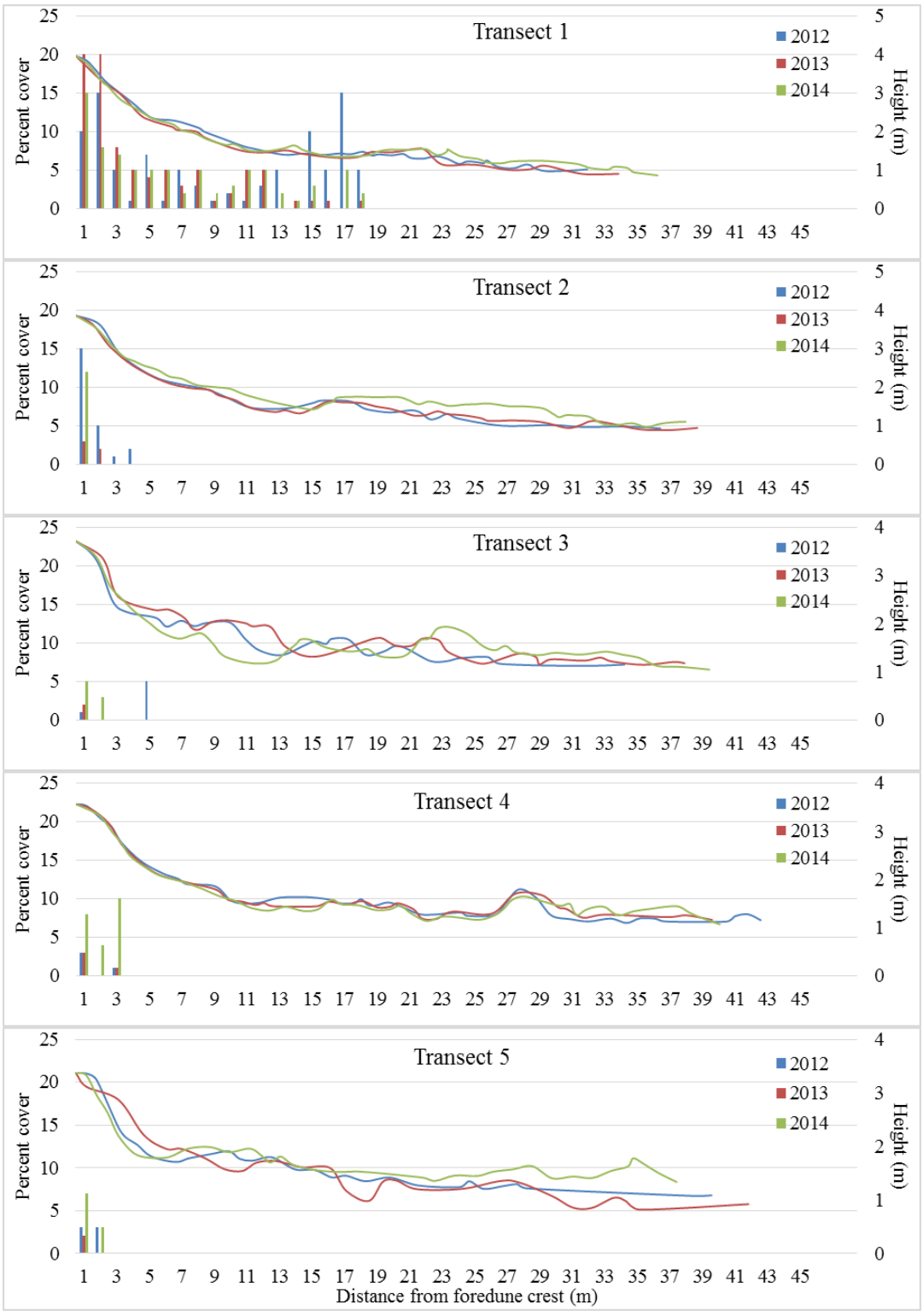

Figure A7. Percent cover of *Panicum* along transects.

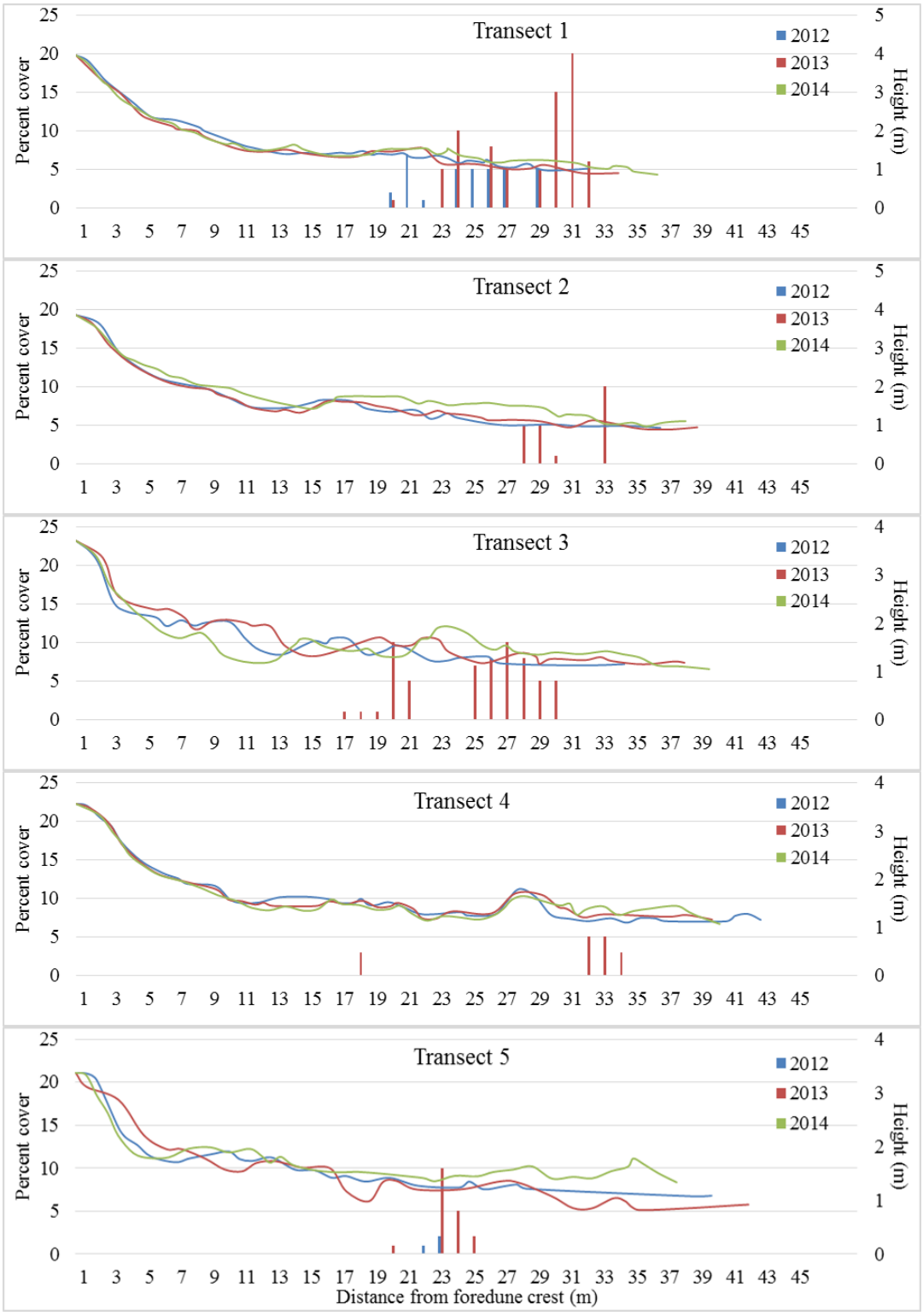

Figure A8. Percent cover of *Salicornia* along transects.

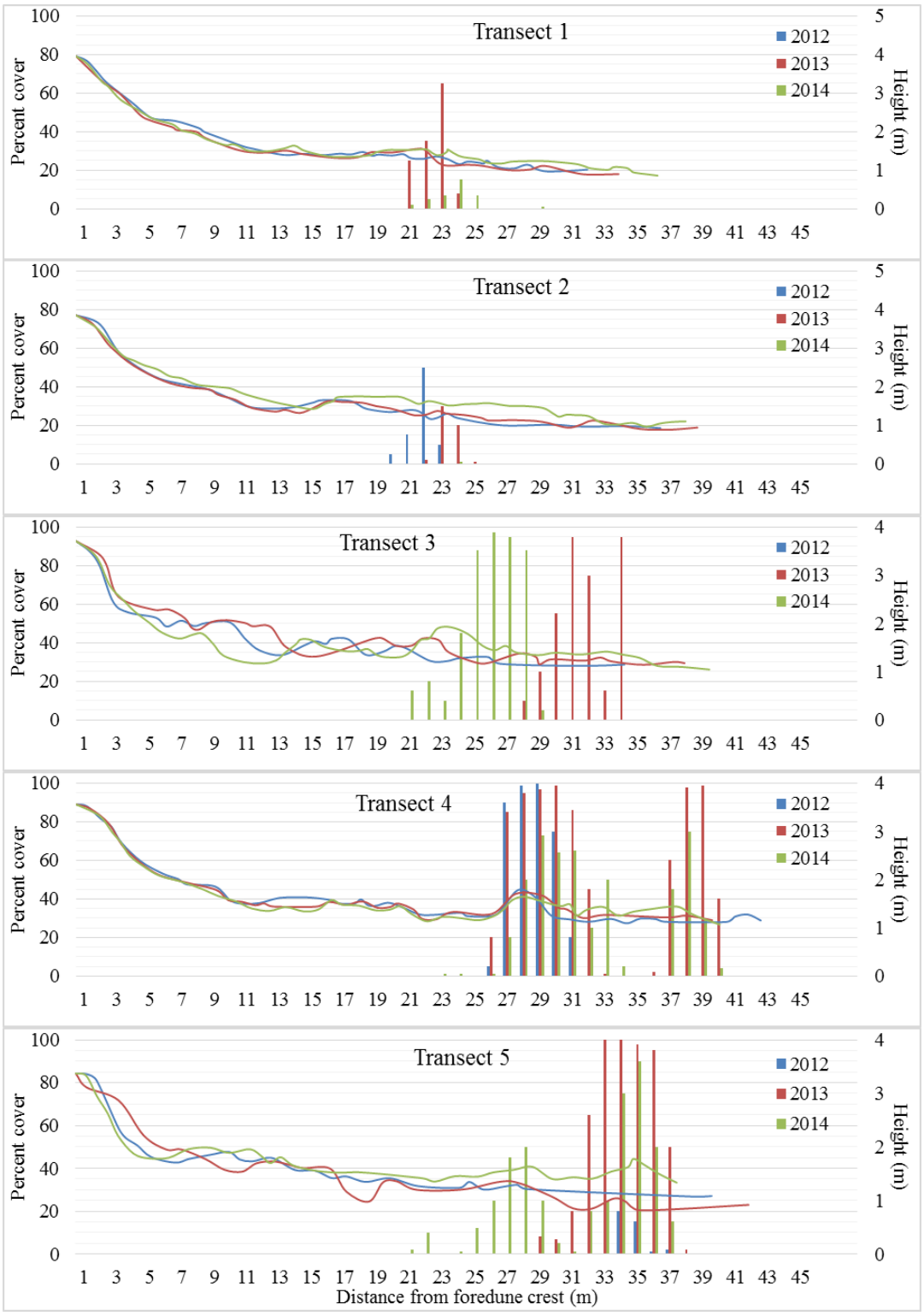

Figure A9. Percent cover of *Sesuvium* along transects.

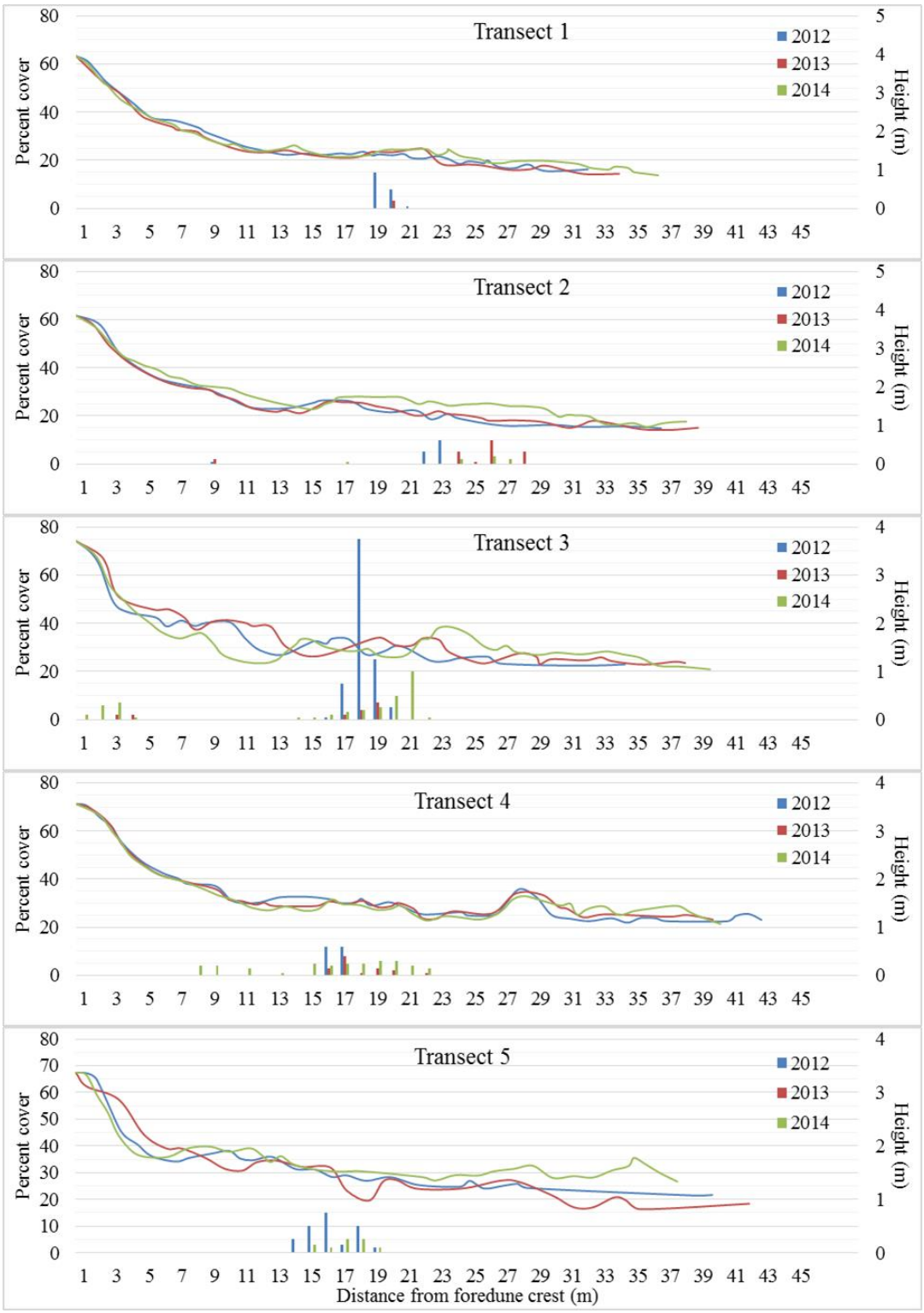

Figure A10. Percent cover of *Sporobolus* along transects.

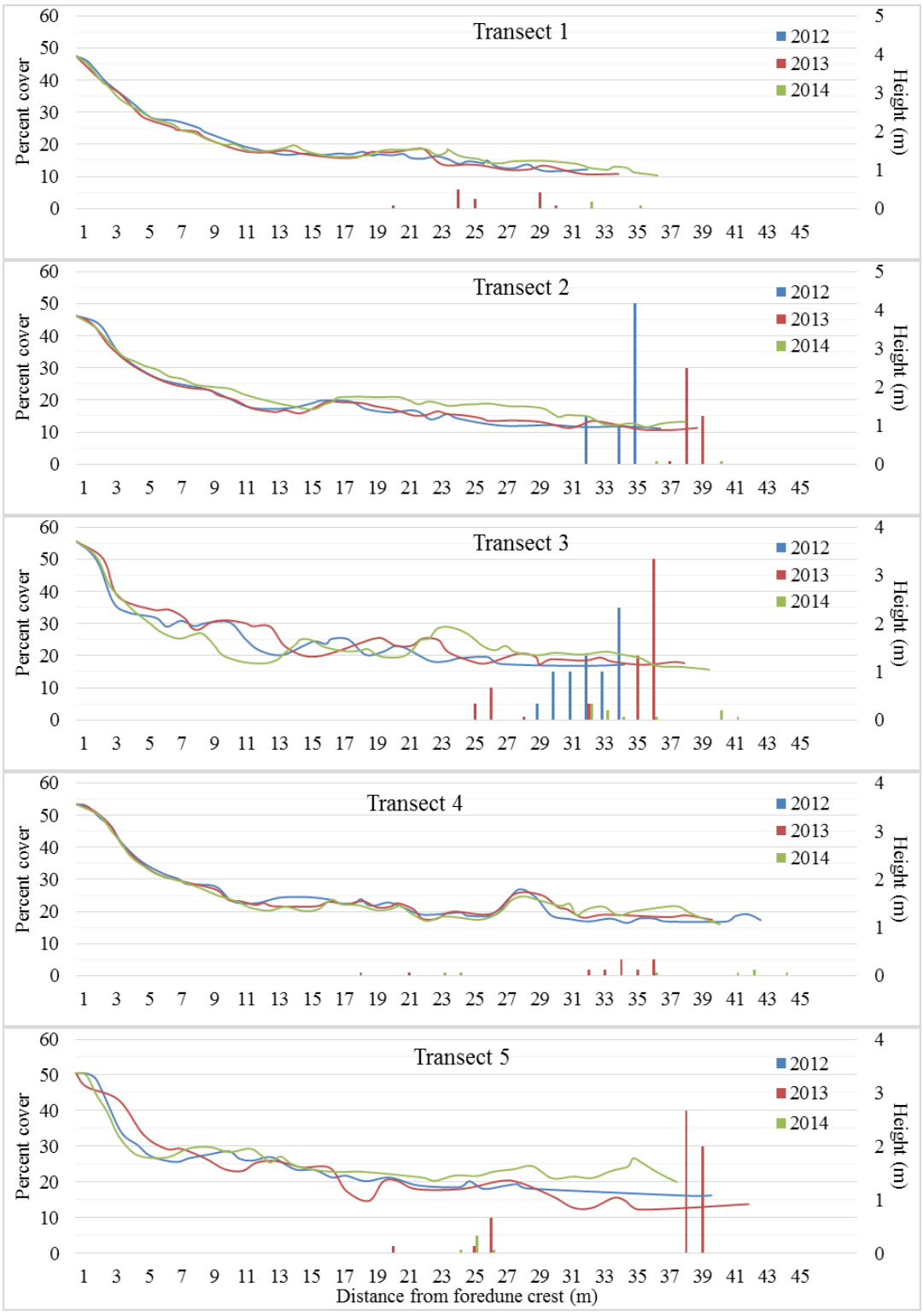

Figure A11. Percent cover of *Tidestromia* along transects.

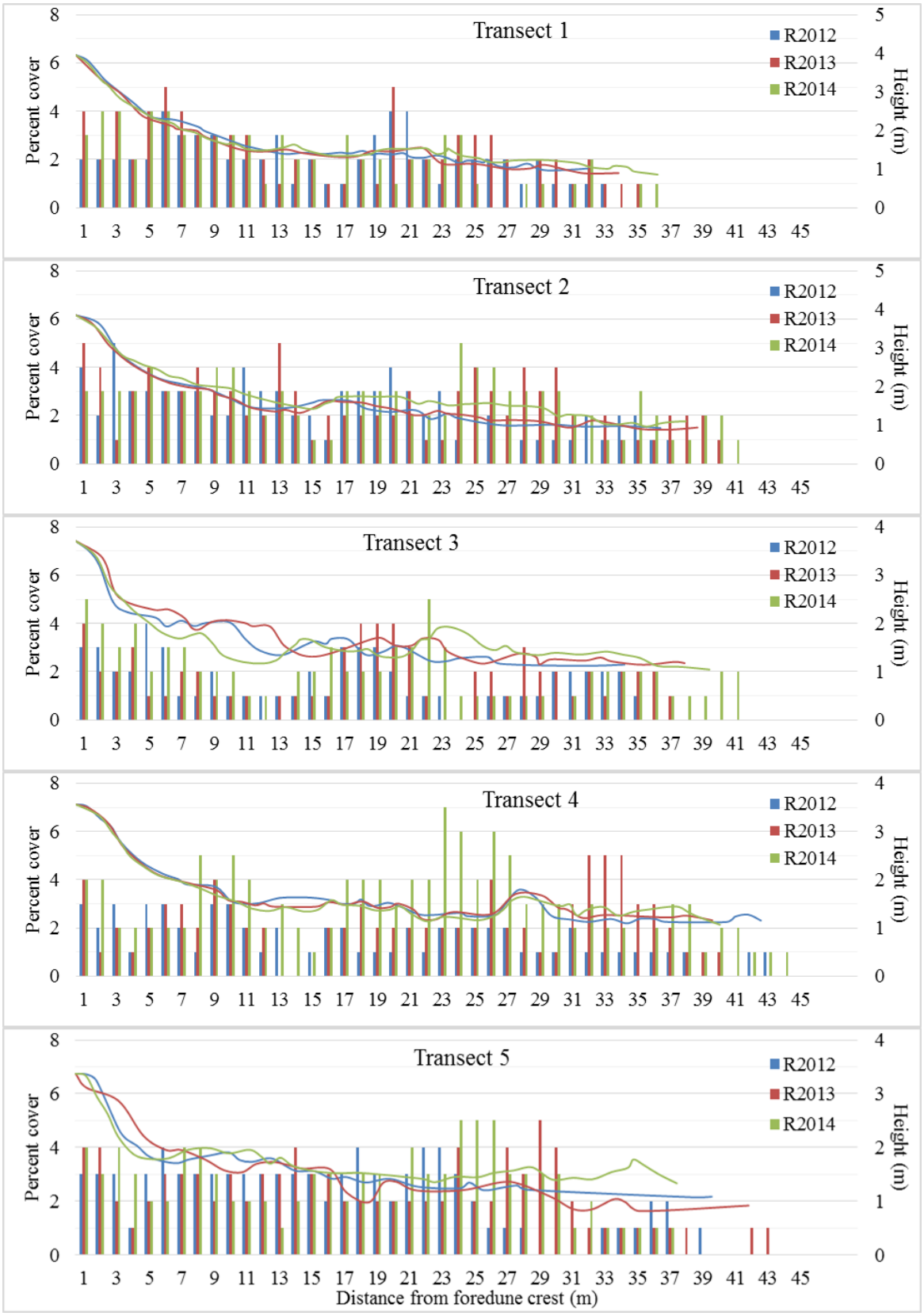

Figure A12. Species richness along transects for each year.

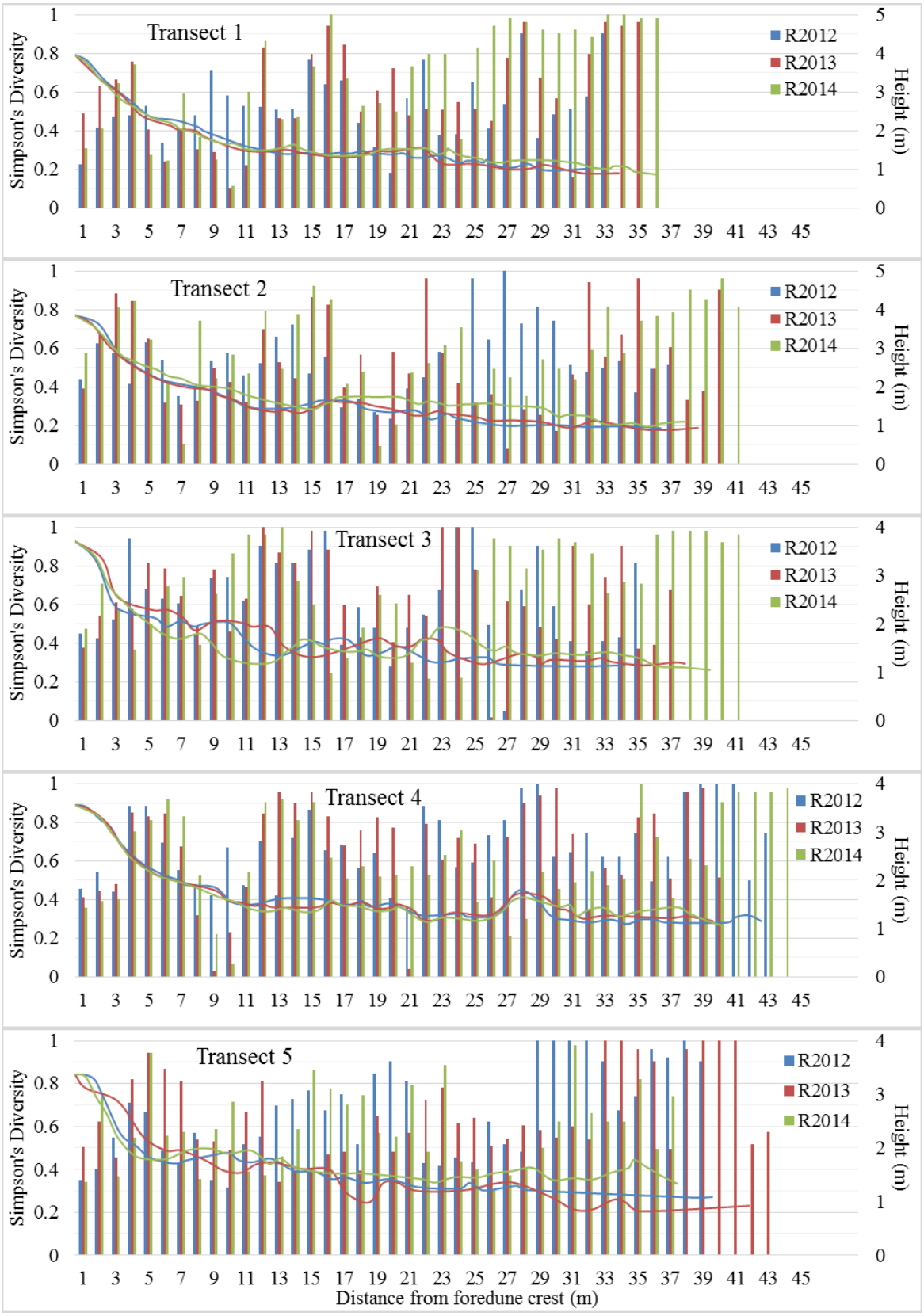

Figure A13. Simpson's Diversity Index along transects for each year.

Appendix B. Contour Maps of Normalized Velocity

The following figures are the interpolated contour maps of normalized velocity around each specimen for each data run. There exists one figure for each specimen. Within this figure are multiple contour maps. They are ordered based on increasing wind velocity, so that A is always the lowest velocity run and the final map is the highest velocity run captured for that species. The distances along the x and y axis are measured in meters. The plant is outlined in green. The scale bar to right of each contour map shows the normalized velocity, where blue indicates negative normalized velocity, or decelerated flow; white indicates no change in velocity; and red indicates accelerated velocity compared to flow on the open beach. The locations of the stakes, or erosion pins, are shown as squares with numbers identifying them. In the lower right corner of each contour map is a compass, with an arrow indicating the direction of flow during that data run.

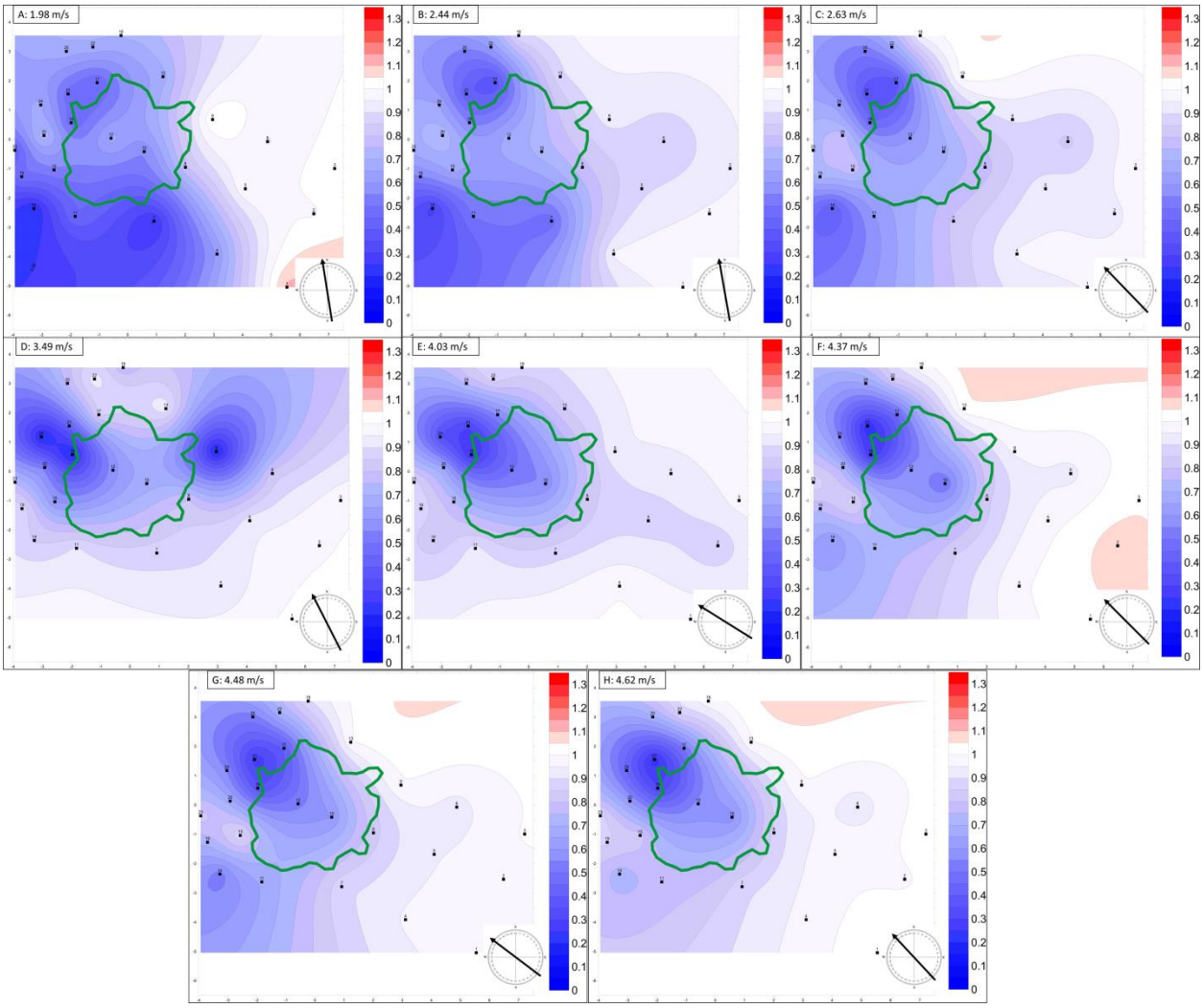

Figure B1. Flow around *Sporobolus virginicus* in 2012.

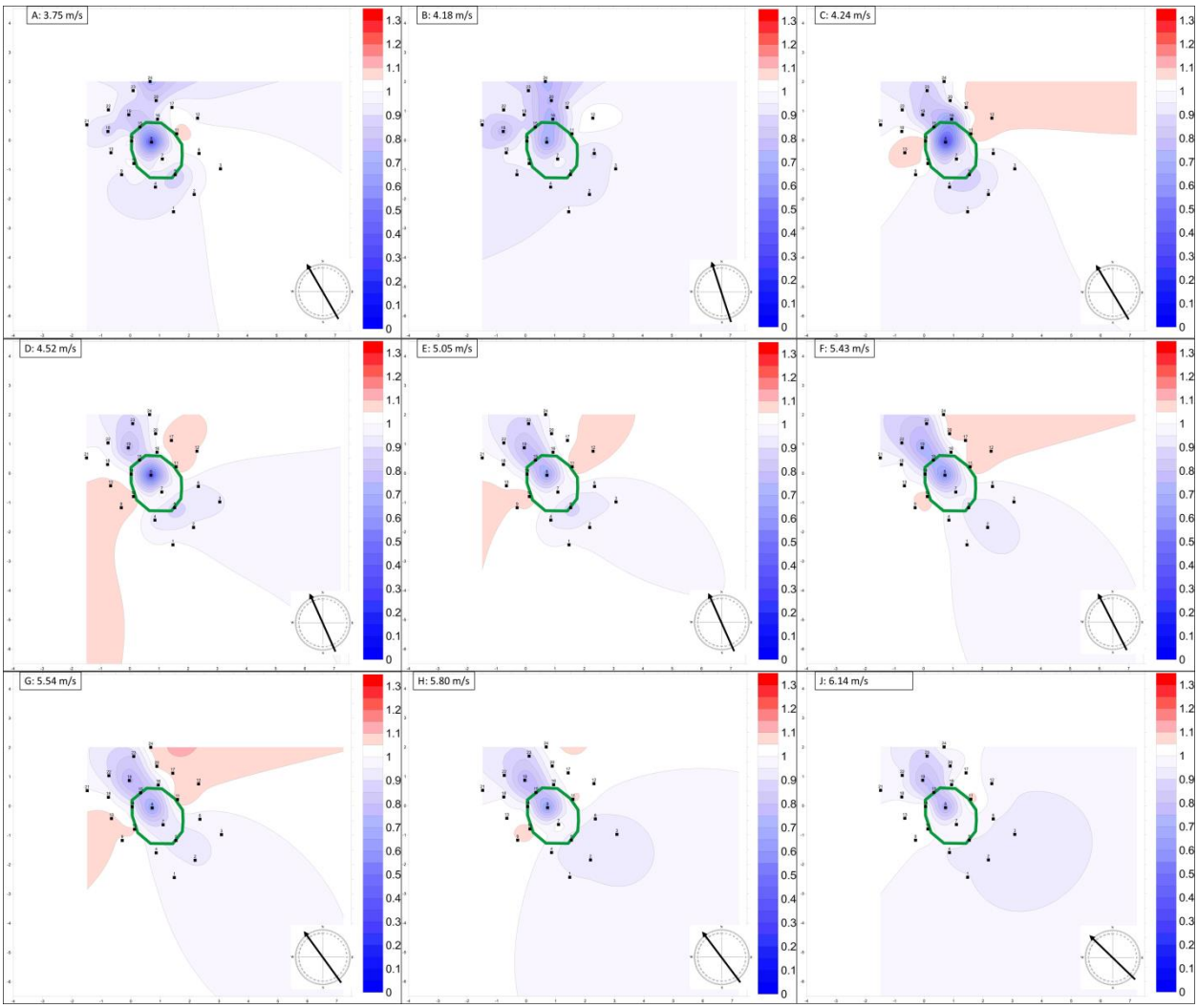

Figure B2. Flow around *Sporobolus virginicus* in 2013.

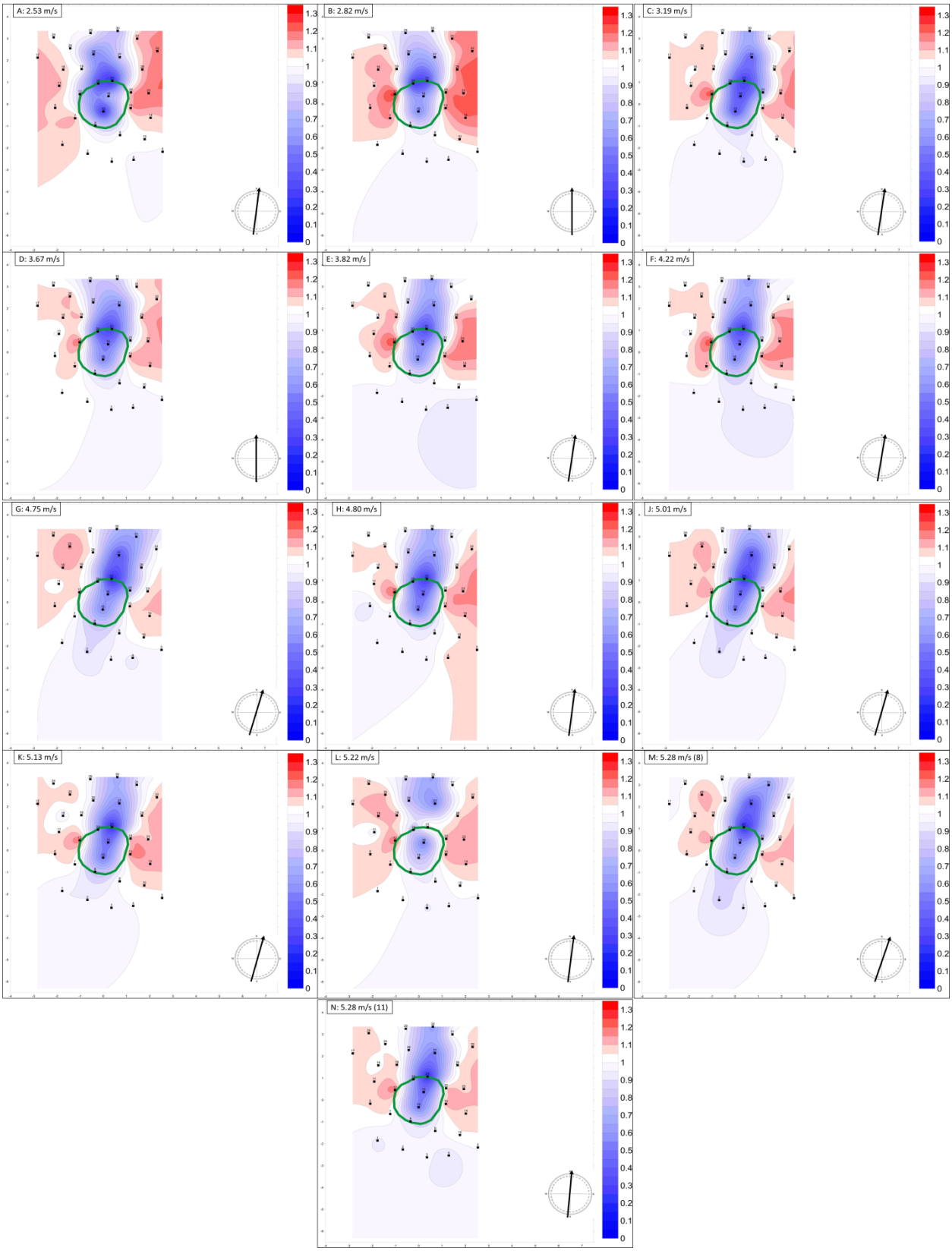

Figure B3. Flow around *Sporobolus virginicus* in 2014.

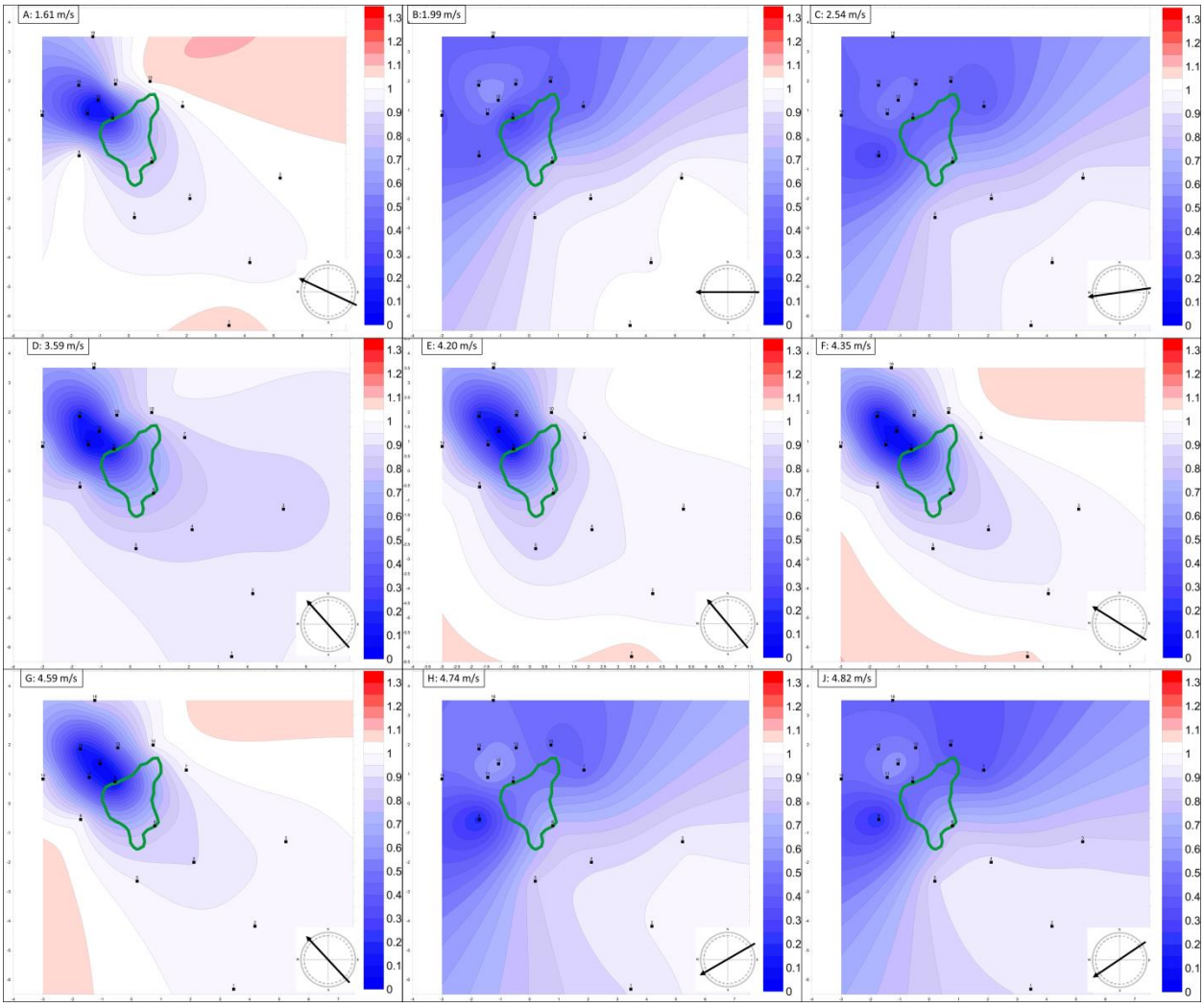

Figure B4. Flow around *Uniola paniculata* in 2012.

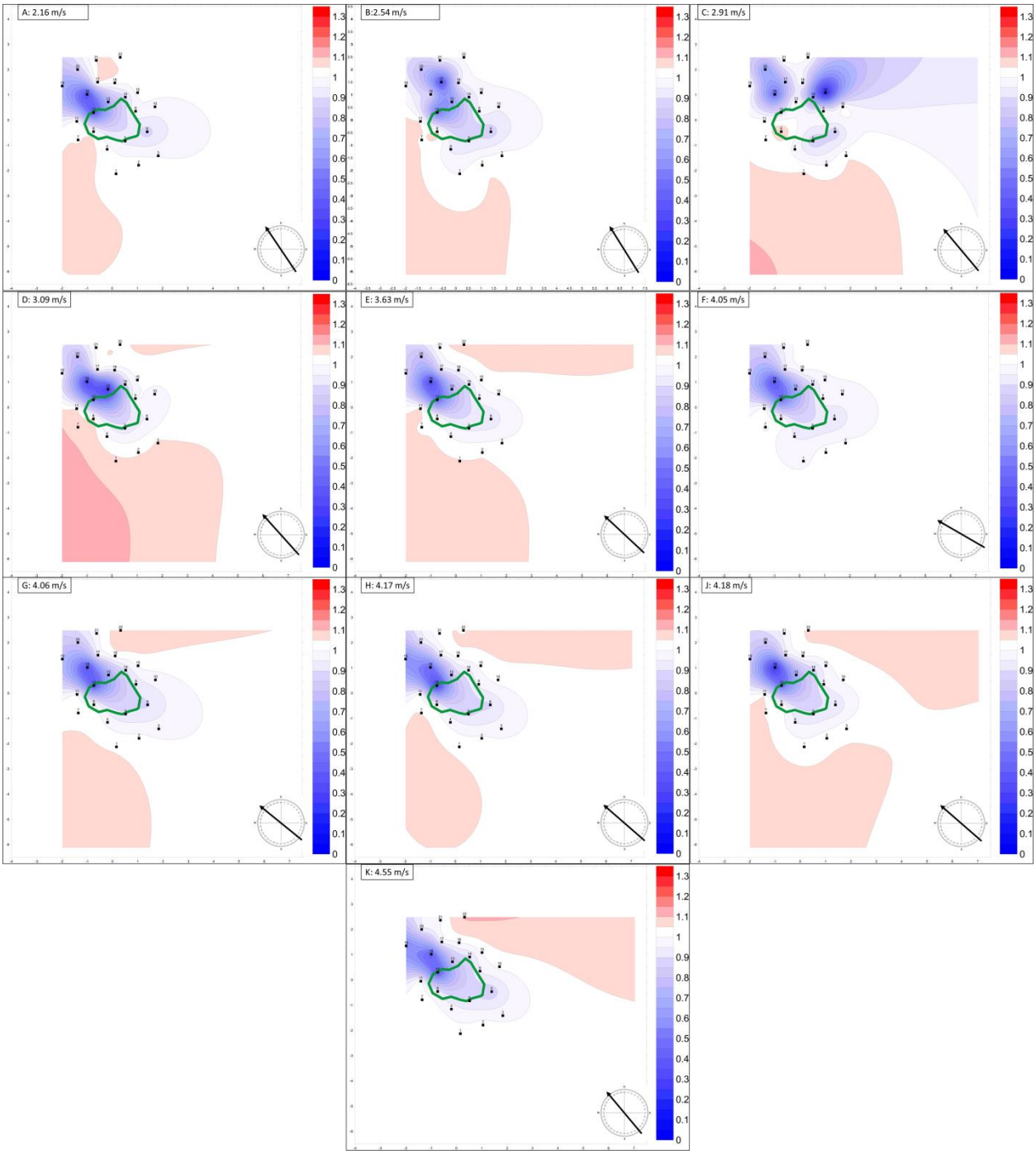

Figure B5. Flow around *Uniola paniculata* in 2013.

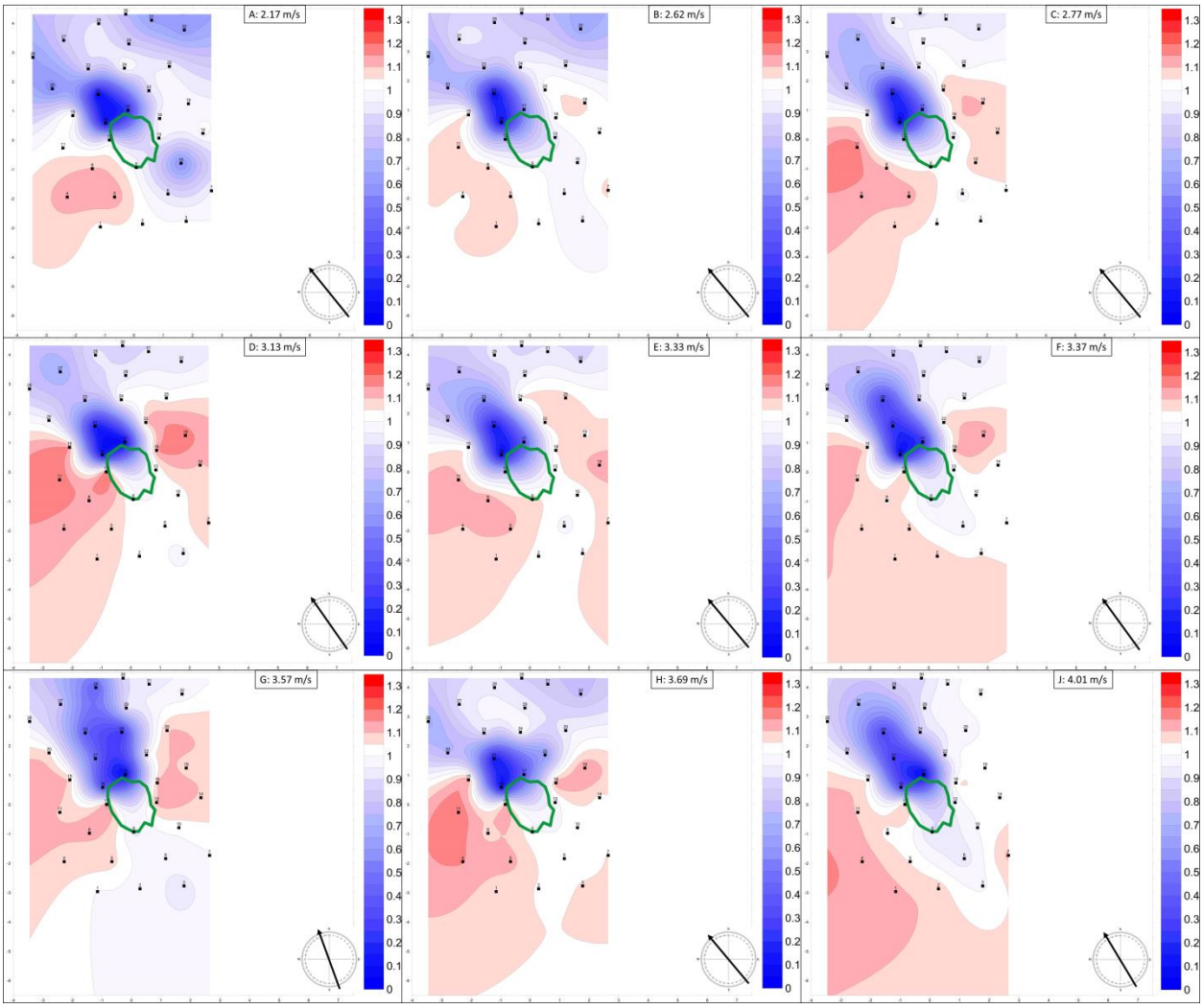

Figure B6. Flow around *Uniola paniculata* 1 for lowest 9 velocities in 2014.

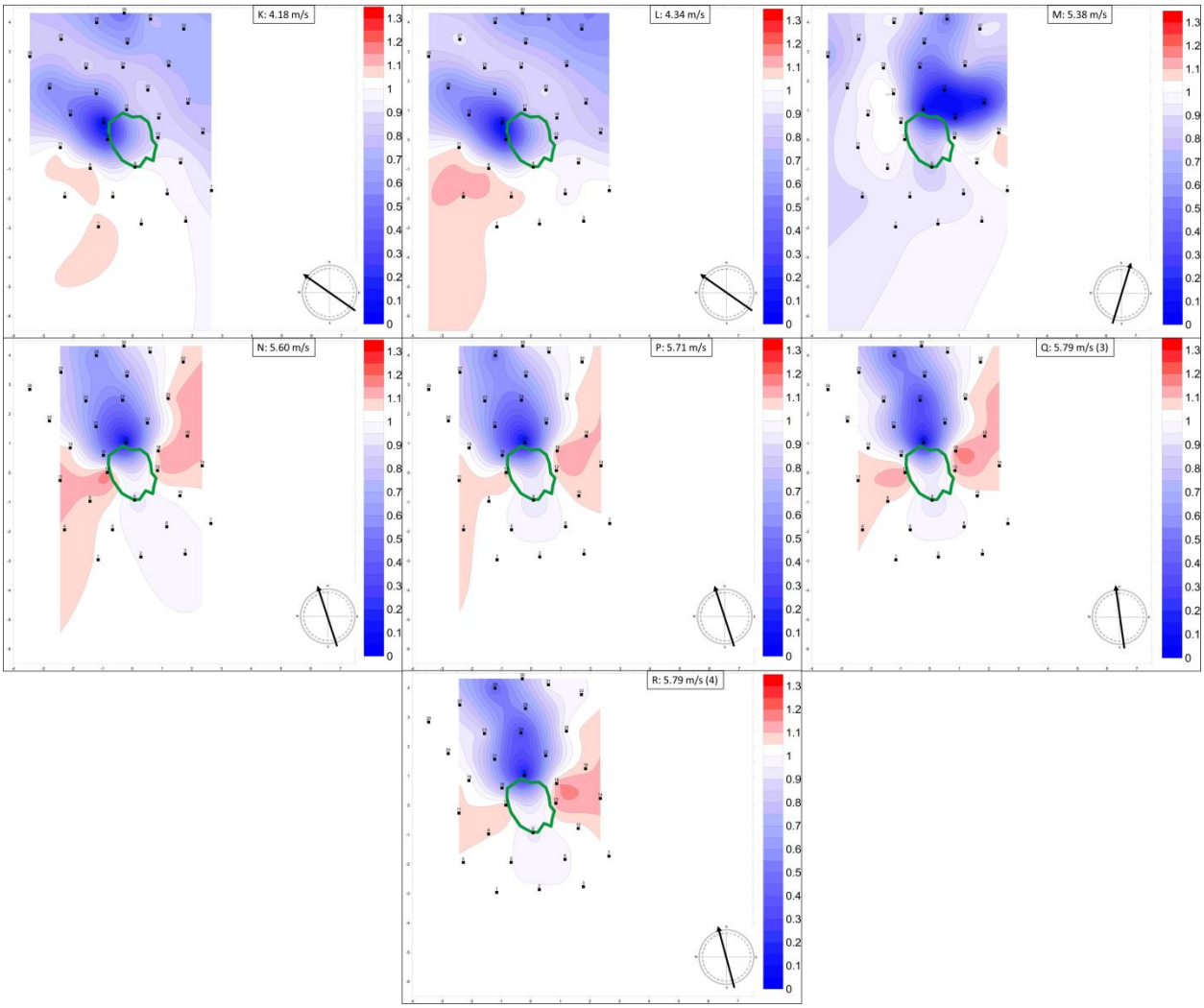

Figure B7. Flow around *Uniola paniculata* 1 for highest 7 velocities in 2014.

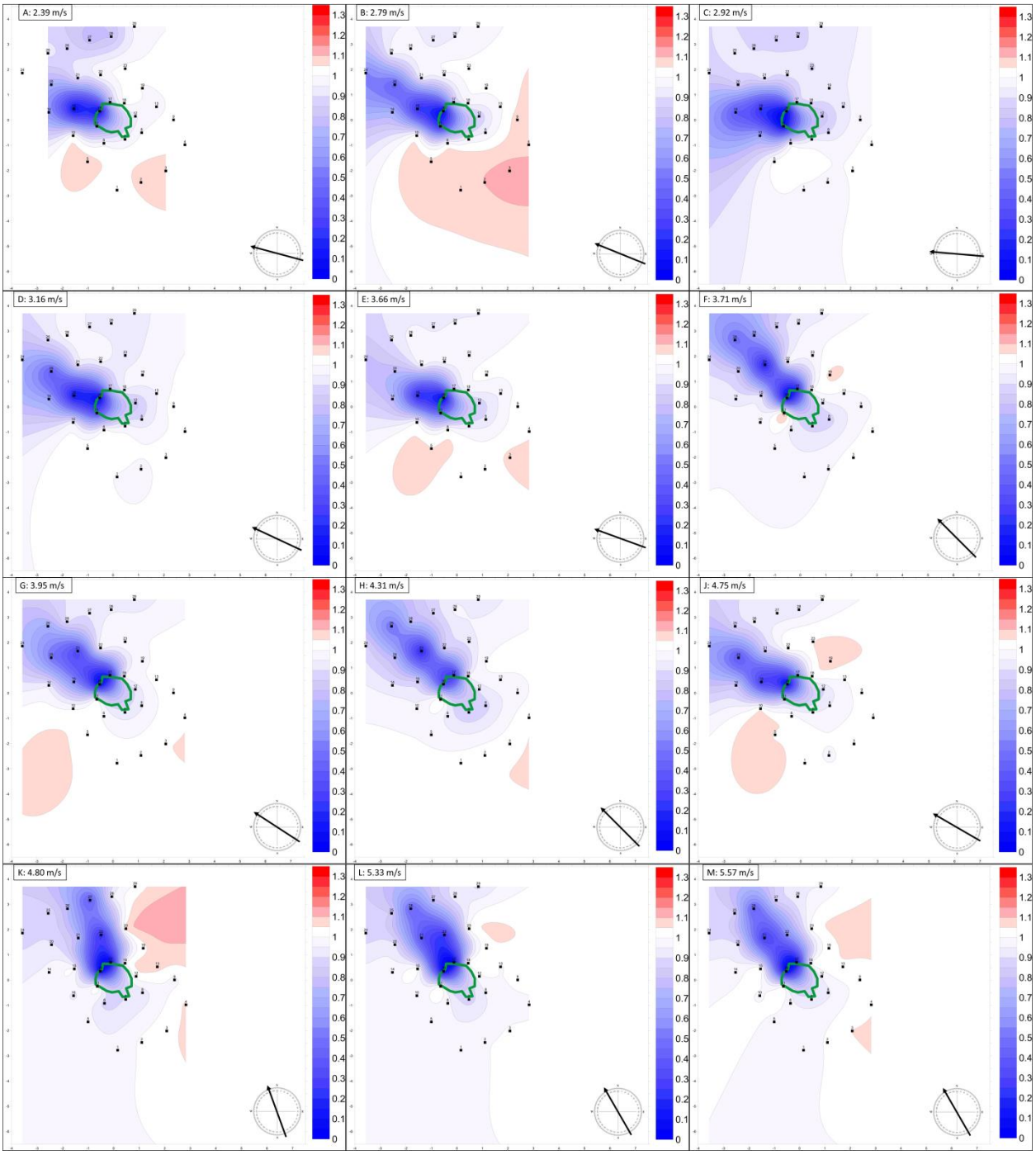

Figure B8. Flow around *Uniola paniculata* 2 in 2014.

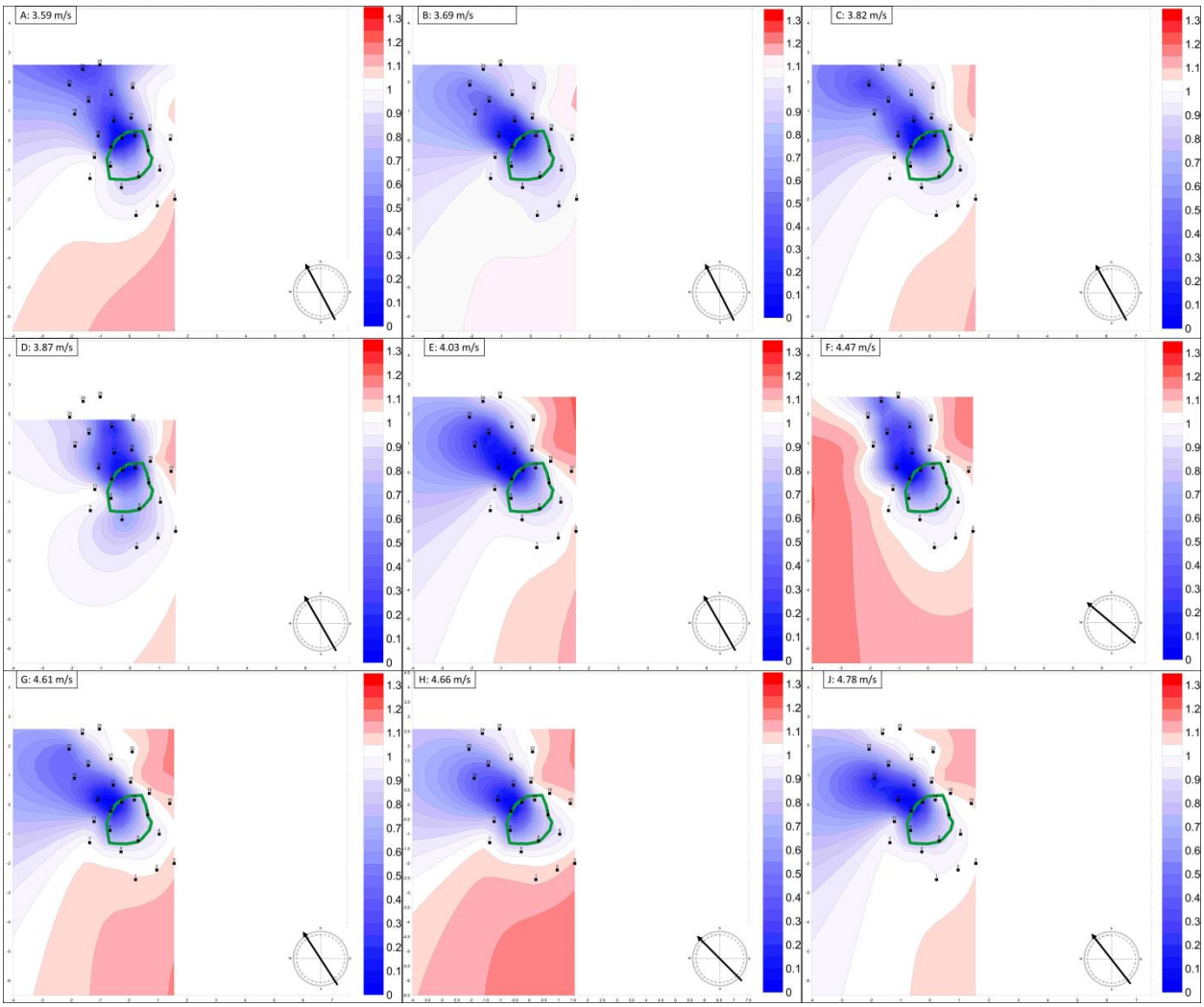

Figure B9. Flow around *Tidestromia lanuginosa* in 2013.

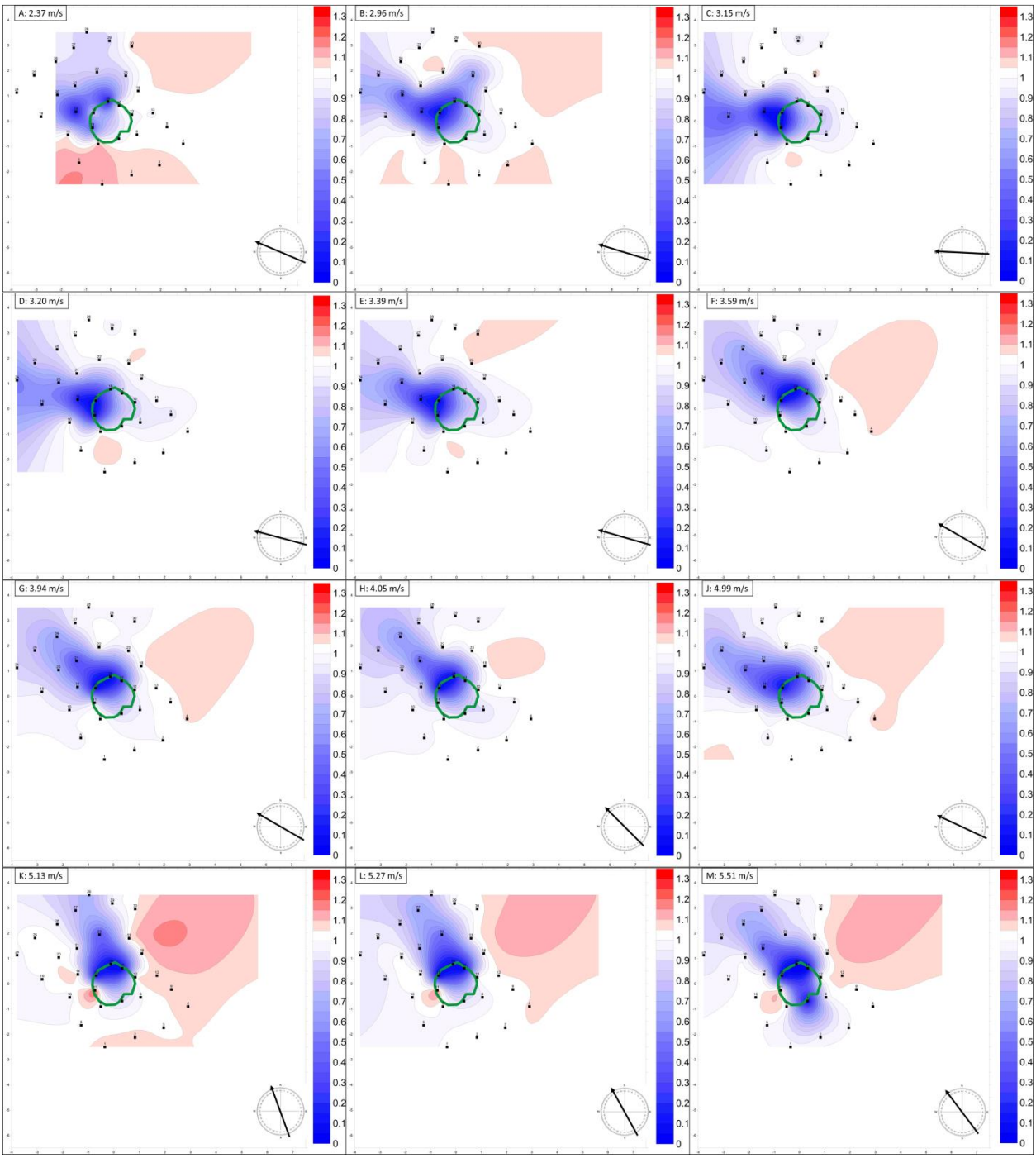

Figure B10. Flow around *Amaranthus greggii* in 2014.

Vita

Katherine Anne Renken was born at Fort Belvoir, Virginia, to Chief Warrant Officer Dennis Renken and Julia Renken. As a daughter of a United States Army Warrant Officer, she lived in Damscus, Syria; Fayetteville, North Carolina; Mönchengladbach, Germany; and Sierra Vista, Arizona. She graduated from Pine Forest High School in Fayetteville, North Carolina, in 2002. She received a Bachelor of Science in Environmental Geology from the University of North Carolina at Chapel Hill in 2006. She received a Master of Arts in Geography from East Carolina University in 2008.